

SYNTHESIS AND EVALUATION OF CARBORANE ANALOGUES OF  
TAMOXIFEN

SYNTHESIS AND EVALUATION OF CARBORANE ANALOGUES OF  
TAMOXIFEN

By

Michael L Beer, B.Sc.

A Thesis

Submitted to the School of Graduate Studies

In Partial Fulfillment of the Requirements

For the Degree

Masters of Science

McMaster University

© Copyright by Michael L Beer, January 2010.

MASTERS OF SCIENCE (2009)  
(Chemistry)

McMASTER UNIVERSITY  
Hamilton, Ontario

TITLE: THE SYNTHESIS AND EVALUATION OF CARBORANE  
SERMS

Author: Michael L Beer, B.Sc. (McMaster University)

Supervisor: Professor John Fitzmaurice Valliant

Number of Pages: xiv, 100

## Abstract

A stereoselective synthesis of *closo* carborane analogues of Tamoxifen was developed where the products represent a new platform for developing metabolically robust Selective Estrogen Receptor Modulators (SERMs). Using an ionic liquid-mediated insertion reaction and a highly conjugated ene-yne prepared stereoselectively, the A-ring in the backbone of Tamoxifen was replaced with an *ortho* carborane cluster. X-ray crystal structures of a key intermediate and the final target along with NMR spectroscopy confirmed that the product was in fact the desired Z isomer, which showed superior chemical stability to Tamoxifen both in solution and the solid state even when exposed to light for extended periods of time. Using microwave heating, it was however possible to convert up to 50% of a sample of the Z isomer to the corresponding E isomer, which was isolated by HPLC and fully characterized. Inhibition assays using both isomers and a simple aryl carborane that is known to target the ER were conducted using estrogen receptor (ER) positive and ER negative human breast cancer cell lines with and without estradiol (E2) present. The Z carborane isomer was able to inhibit cell proliferation better than Tamoxifen in an E2 free environment, while the E isomer was able to inhibit cell growth better than Tamoxifen when E2 is present.

Degradation of the *closo* carborane Tamoxifen analogue to the *nido* species under basic and aqueous conditions, using traditional or microwave



heating, resulted in E-Z isomerization, but it was found that in the presence of aprotic solvents, the *nido* species could be prepared as a single geometric isomer. With the *nido* species in hand the carborane Tamoxifen analogue was metalated (Re/<sup>99m</sup>Tc) and iodinated (<sup>127</sup>I). The technetium analogue was evaluated in a cell uptake assay which showed binding to human breast cancer cells MCF-7.

## **Acknowledgements**

This thesis would not have been possible without the help and support of many people. First, I would like to thank my supervisor Dr. John Valliant for the opportunity to work on such an interesting, challenging project and for the encouragement and guidance he provided.

To Dr. Kirk Green, my committee member, thank you for all the support and interest you have shown during my time as a graduate student. I will miss the many hours spent working with you and all the MRCMS facility staff, past and present.

I also want to express my gratitude to Drs. Jim Britten, Don Hughes and Steve Kornic who have always been generous with their time and expertise.

To my colleagues in the Valliant group both past and present, without your support and friendship this work would not have been possible. I will always have fond memories of our time spent together in and outside of the lab.

Finally I would like to thank my girlfriend Meghan for her encouragement and support throughout this entire process.

## Table of Contents

1.0	Introduction.....	1
1.1	Breast Cancer .....	1
1.2	Selective Estrogen Receptor Modulators (SERMs).....	2
1.3	Tamoxifen.....	4
1.4	Breast Cancer Imaging.....	5
1.4.1	Mammography.....	5
1.4.2	Molecular Imaging.....	7
1.4.3	SPECT.....	8
1.4.4	Radionuclides for SPECT .....	8
1.4.5	PET.....	10
1.5	Organometallic Radiopharmaceuticals.....	11
1.6	Carboranes.....	12
1.7	Carborane-Estrogen Analogues .....	14
1.8	Imaging and the ER.....	15
1.9	Rational and Objectives.....	16
1.10	References.....	17
2.0	The Synthesis and In Vitro Evaluation of a Carborane Analogue of Tamoxifen.....	29
2.1	Introduction.....	29
2.2	Synthesis of Z-1-(1,2-dicarba- <i>c</i> loso-dodecaborane-1-yl)-1-(4- hydroxyphenol)-2-phenyl-but-1-ene (2.7).....	29
2.3	Isomerization of 2.7 and the synthesis of E-1-(1,2-dicarba- <i>c</i> loso- dodecaborane-1-yl)-1-(4-hydroxyphenol)-2-phenyl-but-1-ene (2.8) .....	40

2.4	Cell Inhibition Assay - Biological Evaluation .....	43
2.4.1	Introduction .....	43
2.4.2	Results and Discussion.....	44
2.5	Conclusion.....	47
2.6	Experimental Section.....	47
2.6.1	General .....	47
2.6.2	Crystallographic Details .....	49
2.6.3	Experimental.....	50
2.6.4	Cell Lines and Tissue Culture .....	53
2.6.5	Growth Inhibition Study.....	54
2.7	References .....	56
3.0	Radiolabelling and Evaluation of a Carborane Analogue of Tamoxifen for Imaging Estrogen Receptor Expression .....	61
3.1	Introduction.....	61
3.2	Synthesis of E/Z-1-(1,2-dicarba- <i>nido</i> -undecaborane-1-yl)-1-(4- hydroxyphenyl)-2-phenyl-but-1-ene.....	63
3.3	Synthesis of piperidinium Z-1-(1,2-dicarba- <i>nido</i> -undecaborane-1-yl)-1-(4- phenol)-2-phenyl-but-1-ene.....	66
3.4	Isomerization of piperidinium Z-1-(1,2-dicarba- <i>nido</i> -undecaborane-1-yl)- 1-(4-phenol)-2-phenyl-but-1-ene .....	69
3.4.1	Preparation of the Rhenium Complex 3.10 .....	71
3.4.2	Rhenium Standard – Carborane Isomerization .....	74
3.4.3	Tc – Tamoxifen .....	75
3.5	Cell uptake assay .....	77

3.5.1	Introduction .....	77
3.5.2	Results and Discussion.....	78
3.6	Synthesis of Iodo-Tamoxifen .....	81
3.7	Conclusion.....	89
3.8	Experimental .....	89
3.9	References .....	95
4.0	Future Work.....	99
4.1	Carborane Tamoxifen Analogue for the treatment of Estrogen Receptor Positive Breast Cancer.....	99
4.2	Carborane Tamoxifen Analogue for imaging Estrogen Receptor .....	99
Figure 1.1:	17- $\beta$ -estradiol .....	1
Figure 1.2:	X-Ray Structure of 17- $\beta$ -estradiol-ER Dimer .....	2
Figure 1.3:	Structures of Diethylstilbestrol ( <b>1.2</b> ), Ethamoxytripphetol (MER-25) ( <b>1.3</b> ) and Tamoxifen ( <b>1.4</b> ) The various rings of Tamoxifen are labeled A-C. ....	3
Figure 1.4:	Tamoxifen Analogues: Raloxifen ( <b>1.5</b> ), Idoxifen ( <b>1.6</b> ) and 4-Hydroxy-tamoxifen ( <b>1.7</b> ).....	5
Figure 1.5:	X-ray attenuation coefficients of fat and fibroglandular tissue .....	6
Figure 1.6:	Fraction of fibroglandular tissue in the breast (a) 0, (b) <10%, (c) 10-25%, (d) 26-50%, (e) 51-75%, (f) >75% .....	6
Figure 1.8:	Synthesis of 1.8.....	11
Figure 1.9:	Alkyne insertion reaction .....	12
Figure 1.10:	Degradation of a <i>closo</i> -carborane to form <i>nido</i> -carborane .....	14
Figure 1.11:	Metallation (right) and halogenations (left) of <i>ortho</i> -carborane .....	14
Figure 1.12:	<i>Closo</i> carborane derivatives which bind the estrogen receptor <sup>63</sup> ....	15
Figure 2.1:	<sup>1</sup> H NMR of 2.0 (500 MHz, CDCl <sub>3</sub> ) and proton numbering scheme ...	31

Figure 2.2: Nucleophilic attack on (2.1) - a prochiral carbonyl carbon atom.....	34
Figure 2.3: Conformations leading to the two isomer 2.2 and 2.3.....	35
Figure 2.4: <sup>1</sup> H NMR of 2.4/2.5 following liquid-liquid extraction. Integration of the triplets in the highlighted region show a Z:E ratio of 15:1 (600 MHz, CDCl <sub>3</sub> ).....	36
Figure 2.5: <sup>1</sup> H NMR of 2.6 (600 MHz, CDCl <sub>3</sub> ).....	38
Figure 2.6: Crystal structure and atomic numbering scheme for 2.7 (50% thermal ellipsoids). Hydrogen atoms were omitted for clarity .....	40
Figure 2.7: Thermal E-Z isomerization of 2.7 .....	41
Figure 2.8: HPLC chromatogram of 2.7 following microwave heating at 180°C for 20 min in 95% ethanol (elution conditions: Solvent A = Water, Solvent B = Acetonitrile: Gradient elution 0-10 min, 80→20% A, 10-25 min, 20→0% A; column: Zorbax RX-C18 (4.6x250mm); flow rate:1 mL/min).....	42
Figure 2.9: <sup>1</sup> H NMR spectra of 2.7 (top, 500 MHz, CDCl <sub>3</sub> ) and 2.8 (bottom) (600 MHz, CDCl <sub>3</sub> ) .....	43
Figure 2.10: The results of cell inhibition assays reported a percentage of control for compounds 2.7, 2.8, 2.9 and Tamoxifen at days 1, 4, 7 and 10: A: 1μM, B: 0.001μM, C: 1 μM with E2, D: 0.001μM with E2. ....	46
Figure 3.1: Estrogen receptor imaging agents: 3.1: (Z)-2-(4-(1,2-diphenylbut-1-enyl)-2-iodophenoxy)-N,N-dimethylethanamine, 3.2: (Z)-2-(4-(2-(2-iodophenyl)-1-phenylvinyl)phenoxy)-N,N-dimethylethanamine, 3.3: 2-(4-(3,3-Bis(thioacetamidomethylene)propanamido)phenyl)-1-(4-(2-(N,N-dimethylamino)ethoxy)phenyl)-1-phenyl-1(E/Z)-butene Oxotechnetium-99m, 3.4: FES and 3.5: Z-MIVE. ....	62
Figure 3.2: <sup>1</sup> H NMR of 3.6 and 3.7 (500 MHz, CH <sub>3</sub> OD) .....	65
Figure 3.3: <sup>11</sup> B NMR of 2.9 (500 MHz, CD <sub>3</sub> OD).....	68
Figure 3.4: Compound 3.8 after one week in a solution (methanol) (600 MHz, CD <sub>3</sub> OD) .....	70
Figure 3.5: Crude preparative HPLC trace of the reaction of 3.6 and 3.7 with [Re(CO) <sub>3</sub> (H <sub>2</sub> O) <sub>3</sub> ] <sup>+</sup> in 20% EtOH NaF. The red box indicates the peaks with a m/z	

of 625. (Zorbax SB C18 21x250 mm, 18 mL/min, 50:50 ACN : 5 mM ammonium acetate) .....	72
Figure 3.6: HPLC Trace of the HPLC purified reaction of 3.6 and 3.7 with $[\text{Re}(\text{CO})_3(\text{H}_2\text{O})_3]^+$ in 20% EtOH NaF. (Zorbax SB C18 21x250 mm, 18 mL/min, 50:50 ACN : 5 mM ammonium acetate) .....	73
Figure 3.7: $^1\text{H}$ NMR spectra of 3.10 and 3.11 Showing a E:Z Ratio of 25:1 ( $\text{CD}_3\text{OD}$ , 600MHz) .....	74
Figure 3.8: Possible rhenium carborane Isomers 3.12. (Structures drawn using HyperChem Release 7.5) .....	75
Figure 3.9: HPLC trace of 3.12a/b (Top) and 3.14a/b (Bottom). (Zorbax SB C18, 4.6x250mm, 5 $\mu$ , 60% ACN with 5 mM ammonium acetate). .....	77
Figure 3.10: Cell Uptake Assay Results for 3.14a .....	80
Figure 3.11: Cell Uptake Assay Results for 3.14b .....	80
Figure 3.12: Representation of the top face of <i>nido</i> carborane 3.8 and 3.15 showing two possible iodination sites (the rest of the carborane has been omitted for clarity).....	82
Figure 3.13: HPLC-ESMS (ion-trap) spectrum of 3.15 showing two distinct signals with the same mass (482 m/z) (Zorbax SB C18, 1 mL/min, 70% ACN with 15 mM ammonium acetate) .....	82
Figure 3.14: $^1\text{H}$ NMR Spectrum of the products from the treatment of 3.8 with $\text{I}_2$ (3.15 and 3.16) (Pyridine- $\text{d}_5$ , 700MHz) .....	84
Figure 3.15: Expansions of the aliphatic regions of the $^1\text{H}$ NMR spectrum of ethyl groups of 3.15 / 3.16 (Pyridine- $\text{d}_5$ , 700MHz, Gaussian multiplication) .....	85
Figure 3.16: HPLC trace of: <i>nido</i> carboranes 3.6 and 3.7 (top) and the cold iodine standards 3.15 and 3.16 (bottom). (Zorbax SB-C18, 254nm, 1mL/min, 50% ACN (5 mM ammonium acetate. The early eluting peaks at 5.6 min (top, 3.7) and 9.2 min (bottom, 3.16) corresponds to the E isomer while the late eluting peaks at 6.3 min. (top, 3.6) and 10.7 (bottom, 3.15) correspond to the Z isomer.....	87

Scheme 2.1: Synthesis of 2.7: a) 1. TMS-acetylene, n-BuLi, -78°C, THF; 2. Saturated ammonium chloride b) pyridine, thionyl chloride, -78°C c) 1. NaOMe, MeOH 2. H <sub>2</sub> O d) 1-Butyl-3-methylimidazolium chloride, B <sub>10</sub> H <sub>14</sub> , toluene e) BBr <sub>3</sub> , dichloromethane, -78°C. ....	32
Scheme 3.1: Synthesis of 3.6 and 3.7 .....	65
Scheme 3.2: Synthesis of 3.8.....	66
Scheme 3.3: Proposed mechanism for the isomerization of 3.6 to 3.7.....	66
Scheme 3.4: Stereoselective Formation of 3.8 Using Piperidine .....	67
Scheme 3.5: Possible phenanthrene derivative of 3.8.....	70
Scheme 3.6: Synthesis of rhenium Tamoxifen analogues 3.10 and 3.11 .....	72
Scheme 3.7: Synthesis of 3.14.....	76
Scheme 3.8: Iodination of 3.8 in 95% ethanol .....	81
Scheme 3.9: Iodination of a mixture of 3.6 and 3.7 .....	86
Scheme 4.1: Charge Compensation of Tc Tamoxifen with NO <sup>+</sup> .....	100
Table 1.1: Medically Relevant Radioisotopes of Iodine .....	10
Table 2.1: E/Z Isomerization of 2.7 in 95% ethanol using microwave heating....	41
Table 3.1: E/Z Isomerization of 2.7 In 56% 2-propanol + NaF Using Microwave Heating .....	64
Table 3.2: Microwave Heating of 2.7 in Neat Pyridine .....	67
Table 3.3: Cell Uptake Assay Protocol for 3.12a/b .....	78
Table 3.4: Assignments of the E/Z Isomers of 3.15 and 3.16 .....	85



## List of Abbreviations and Symbols

Å	Angstrom
<sup>11</sup> B NMR	Boron Nuclear Magnetic Resonance Spectroscopy
<sup>13</sup> C NMR	Carbon Nuclear Magnetic Resonance Spectroscopy
Calc.	Calculated
d	Doublet ( <sup>1</sup> H NMR)
DEPT	Distortionless Enhancement by Polarization Transfer
EI	Electron Ionization
equivs.	Equivalents
Et	Ethyl
EtOH	Ethanol
ER	Estrogen receptor
ESMS	Electrospray Mass Spectrometry
FTIR	Fourier Transform Infrared Spectroscopy
h	hour(s)
<sup>1</sup> H NMR	Proton Nuclear Magnetic Resonance Spectroscopy
HPLC	High Pressure Liquid Chromatography
HRMS	High-Resolution Mass Spectrometry
Hz	Hertz

IR	Infrared Spectroscopy
K	Kelvins
m	Multiplet ( $^1\text{H}$ NMR)
Me	Methyl
MER-25	1-(p-2-diethylaminoethoxyphenyl)-1-phenyl-2-p- Methoxyphenylethanol
MHz	Megahertz
min.	Minute(s)
mp	Melting Point
MRI	Magnetic Resonance Imaging
MS	Mass Spectrometry
nBuLi	n-butyl lithium
NMR	Nuclear Magnetic Resonance Spectroscopy
NOE	Nuclear Overhauser Effect
NOESY	Nuclear Overhauser Effect Spectroscopy
OEt	Ethoxy
PET	Positron Emission Tomography
Pet. Ether	Petroleum Ether
pK <sub>a</sub>	log acidity constant (K <sub>a</sub> )
ppm	Parts per million

q	quartet ( $^1\text{H}$ NMR)
$R_f$	Retention Factor (TLC)
RBA	Relative Binding Affinity
s	Singlet ( $^1\text{H}$ NMR)
SPECT	Single Photon Emission Computed Tomography
t	triplet ( $^1\text{H}$ NMR)
TFA	Trifluoroacetic acid
THF	Tetrahydrofuran
TLC	Thin Layer Chromatography
TMS	Trimethylsilyl

## 1.0 Introduction

### 1.1 Breast Cancer

Currently in Ontario, genetic screening is underway for high risk women as a way to detect the presence of the BRCA1 and BRCA2 gene mutations. Women identified with mutations on the BRCA1 and/or BRCA2 genes will be recommended for further screening and preventative therapies. While this screening process is making great strides in the field of cancer prevention, it has been shown that the BRCA1 gene mutation results largely in estrogen receptor (ER) negative breast cancer.<sup>1</sup> To date there is no routine method to screen for hormone dependent breast cancer (ER positive) which accounts for as many as one in three cases.<sup>2</sup>

The ER is a nuclear receptor which binds the natural substrate 17- $\beta$ -estradiol (**Figure 1.1**) with sub-nanomolar affinity.<sup>3</sup> A recent review by Song and Santen has shown that binding of 17- $\beta$ -estradiol to the estrogen receptor initiates a signaling pathway involving multiple kinases which are known to regulate cell growth and apoptosis.<sup>4</sup>

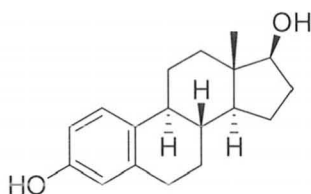


**Figure 1.1:** 17- $\beta$ -estradiol

In healthy tissue, when 17- $\beta$ -estradiol binds to the ER there is stimulation of growth factors which result in the growth of adjacent non-ER positive cells. In contrast, when 17- $\beta$ -estradiol binds to the ER in estrogen positive malignant cells, cell growth is initiated and apoptosis is inhibited.<sup>4</sup> Following binding, the ER and estrogen form an activated dimer that subsequently binds to a specific DNA sequence; (**Figure 1.2**) this binding initiates transcription which causes cell growth.<sup>5</sup>

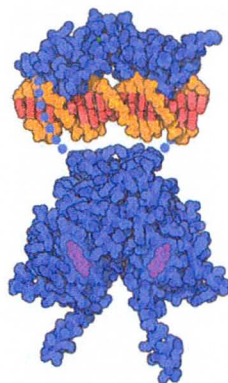


**Figure 1.2:** X-Ray Structure of 17- $\beta$ -estradiol-ER Dimer<sup>6, 7</sup>

## 1.2 Selective Estrogen Receptor Modulators (SERMs)

The ER in either the alpha or beta form is found in many locations within the body, including the uterus<sup>8</sup> and breast<sup>9</sup> and to a lesser extent in bone,<sup>10</sup> prostate,<sup>11</sup> brain,<sup>12</sup> and heart.<sup>13</sup> Given that malignant cells are stimulated to grow *via* binding of 17- $\beta$ -estradiol to the ER, a common cancer treatment involves the use of drugs that can inhibit formation of the hormone-receptor complex.

Originally, drugs that were able to inhibit estradiol binding to the ER were known as anti-estrogens. In recent years, anti-estrogens have come to be referred to as Selective Estrogen Receptor Modulators (SERMs). Examples of potent SERMs that are currently in use, or have been screened as potential therapeutics, are shown in **Figure 1.3**.

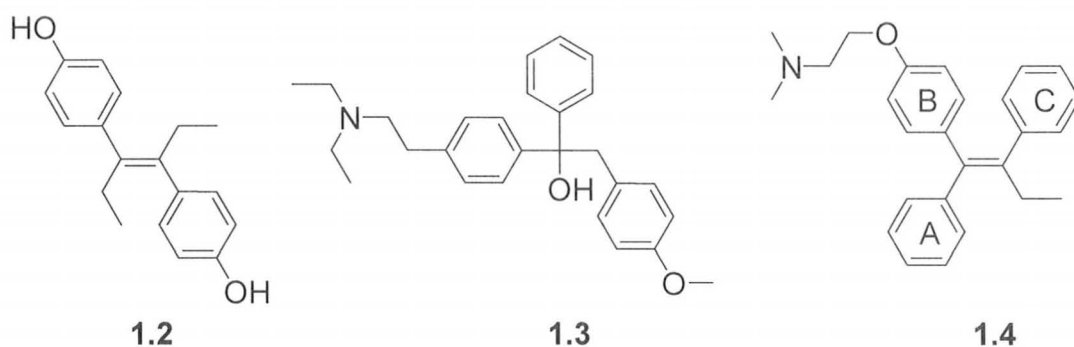


**Figure 1.3:** Structures of Diethylstilbestrol (**1.2**), Ethamoxytriphetol (MER-25) (**1.3**) and Tamoxifen (**1.4**) The various rings of Tamoxifen are labeled A-C.

The search for anti-estrogens began in 1938 with the synthesis of the estrogenic compound diethylstilbestrol (**1.2**).<sup>14, 15</sup> During the next 20 years, other estrogenic compounds were identified, though it was not until 1958 that a true anti-estrogen was synthesized. Ethamoxytriphetol (MER-25, **1.3**) was the first compound found to inhibit estrogen binding<sup>14</sup> and, although encouraging results were obtained in animal studies,<sup>16-18</sup> the human trials were not conducted due to the drug's low potency and high toxicity. Success was realized in 1971 when Tamoxifen (**1.4**) was discovered and reported to be an effective anti-estrogen.

### 1.3 Tamoxifen

Tamoxifen is currently used as a frontline treatment in cases of hormone dependent breast cancer<sup>19</sup> and is described by the World Health Organization (WHO) as an essential drug for the treatment of breast cancer.<sup>20</sup> In addition to cancer treatment, Tamoxifen is used as a preventative treatment<sup>21</sup> for high risk women as well as in long term adjuvant therapy.<sup>22</sup> Furthermore, the National Surgical Adjuvant Breast and Bowel Project P-1 study was able to show a decrease in the rate of invasive breast cancer with an occurrence of 2.48% in women who were taking tamoxifen for 5 years compared to 4.25% in women taking a placebo after a 7 year follow up (N = 13,388).<sup>23</sup>

Several Tamoxifen analogues (**Figure 1.4**) have been produced; some of the more notable ones include: Raloxifen (**1.5**), Idoxifen (**1.6**) and the Tamoxifen metabolite, 4-hydroxy-Tamoxifen (**1.7**). Many of the analogues retain key elements of the Tamoxifen structure that have been shown to aid in binding to the ER. One key element is the pendant amino group which, when modified, can reduce binding of the agent to the ER.<sup>24, 25</sup> It has been found that the addition of certain groups to the *para* position of the A ring (**Figure 1.3**) does not adversely affect binding;<sup>26</sup> in the case of **1.7**, the hydroxyl group has been shown to increase binding to the ER.<sup>27</sup>

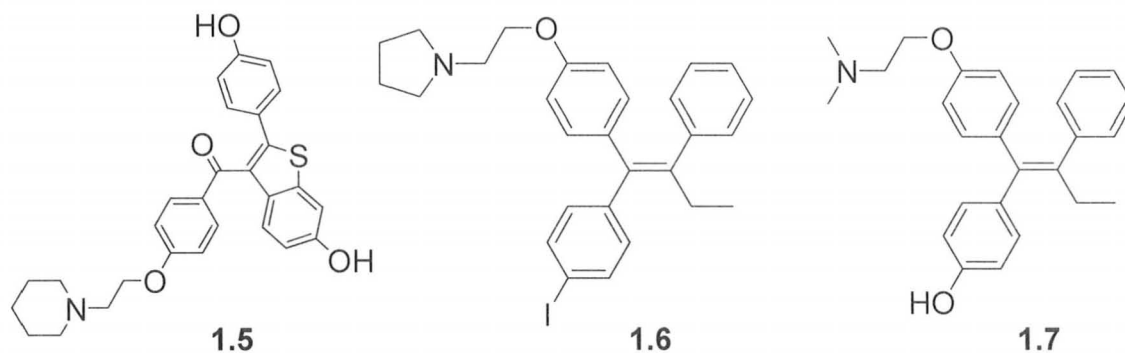


**Figure 1.4:** Tamoxifen Analogues: Raloxifen (1.5), Idoxifen (1.6) and 4-Hydroxytamoxifen (1.7)

## 1.4 Breast Cancer Imaging

### 1.4.1 Mammography

Currently mammography (x-ray) is the standard screening modality used worldwide for the detection of breast cancer. During the last 10 years, there has been doubt about the advantages of screening women routinely in terms of mortality,<sup>28, 29</sup> cost,<sup>30</sup> efficacy<sup>28, 31</sup> and the psychological effects of false positive results and recalls.<sup>32</sup> A specific case where the use of mammography is not favorable is when women have dense breast tissue. The breast contains two major tissue components: fibroglandular tissue and fat; the higher the amount of fibroglandular tissue the denser the breast.<sup>33</sup> When x-rays pass through the fatty portion of the breast a low attenuation to the x-ray beam is observed (**Figure 1.5**), which results in a dark image. The x-ray attenuation coefficient for tumours is much higher than that of fatty tissue and therefore a bright spot is seen on the image. However, fibroglandular tissue has a similar x-ray attenuation coefficient to breast tumours and it is therefore difficult to distinguish between the two.<sup>34</sup>



This can be seen in **Figure 1.6** which shows mammograms of women who range from zero to over 75% fibroglandular tissue.<sup>35</sup>

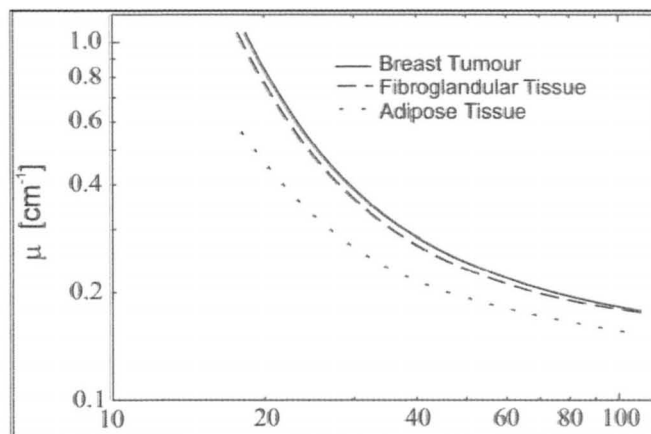


**Figure 1.5:** X-ray attenuation coefficients of fat and fibroglandular tissue<sup>34</sup>

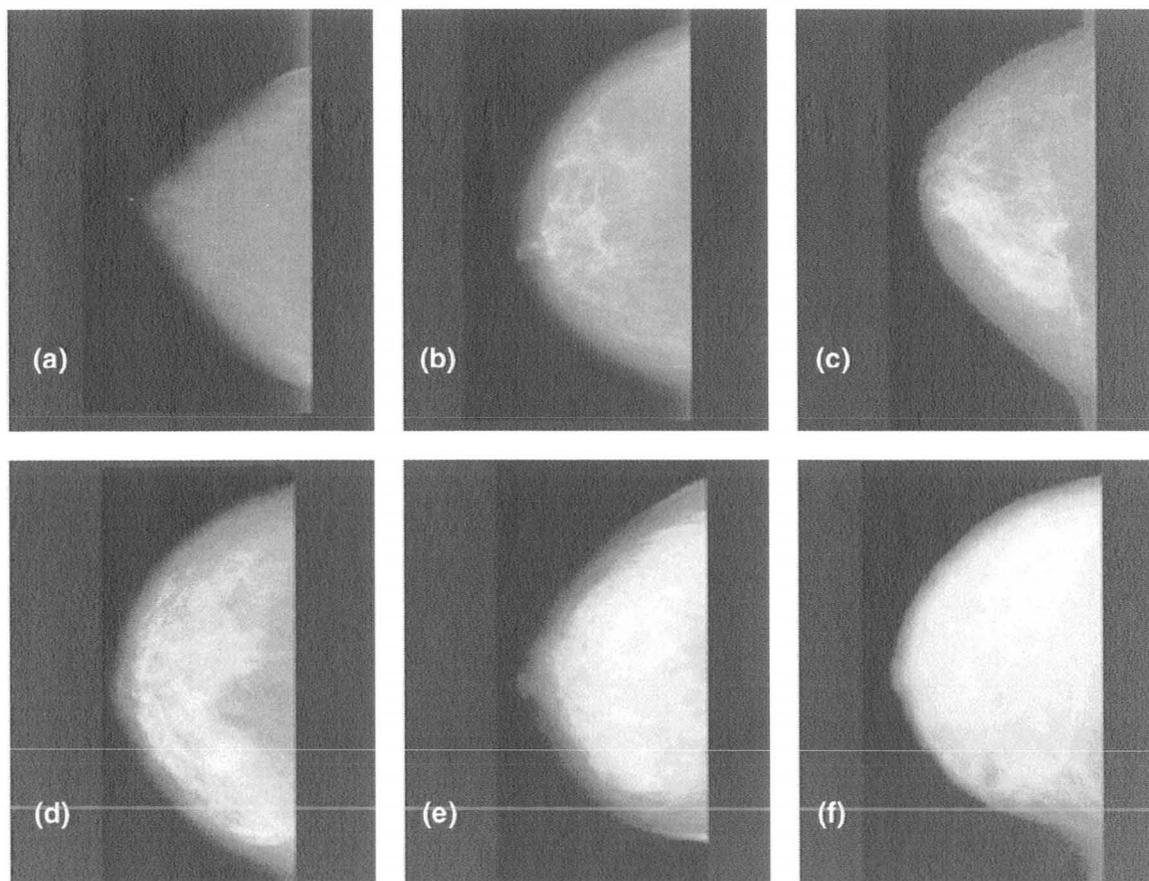


**Figure 1.6:** Fraction of fibroglandular tissue in the breast (a) 0, (b) <10%, (c) 10-25%, (d) 26-50%, (e) 51-75%, (f) >75%<sup>35</sup>

At present the only other method for breast cancer screening is Magnetic Resonance Imaging (MRI). Several large scale trials have shown that MR has significantly higher sensitivity than mammography (71-100% vs 33-40% respectively). Nevertheless, it has been shown that the specificity of MR is lower than that of mammography, and it therefore has a higher false positive rate resulting in unnecessary biopsies.<sup>36-39</sup> In addition to MR's poor specificity it is also cost prohibitive with a bilateral MR procedure costing over \$4,000 (cost of mammogram is approximately \$200).

With this knowledge and because of the key role played by the ER in the growth of breast cancer tumours and the importance of using hormone dependency in designing an effective treatment regime, it is highly desirable to be able to visualize and monitor ER expression non-invasively. More specifically, the use of molecular imaging to detect the ER would aid in the identification of ER positive malignant cells and would avoid sampling errors common to biopsies.<sup>40</sup> The ability to effectively image the ER requires the development of a potent ER probe, which has the potential to facilitate earlier detection of tumours and metastases compared to other screening techniques such as mammography and MRI.

#### **1.4.2 Molecular Imaging**

Molecular imaging (MI) is the process of visualizing or monitoring a specific *in vivo* process with a targeted probe. There are several MI modalities

including optical and ultrasound imaging, Single Photon Emission Computed Tomography (SPECT) and Positron Emission Tomography (PET). In addition to these modalities, many hybrid systems like PET-CT and SPECT-CmT (Computed Mammotomography) have been developed and are able to show the structure and function of the region of interest. The research at hand will focus on radioimaging probes for SPECT.

### **1.4.3 SPECT**

Single Photon Emission Computed Tomography (SPECT) is an imaging technique that is based on the detection of gamma emitting radionuclides having the appropriate energy. SPECT uses a gamma “camera” that is comprised of scintillation crystals and a collimator fitted onto a rotating gantry. To generate tomographic images the camera is rotated around the patient to give a series of two dimensional projections which can be combined to give a three dimensional image of the subject.<sup>41</sup>

### **1.4.4 Radionuclides for SPECT**

#### **1.4.4.1 Meta-Stable Technetium 99 – $^{99m}\text{Tc}$**

Of all the radionuclides used in SPECT, the metastable isotope of technetium-99 ( $^{99m}\text{Tc}$ ) is the most widely employed.<sup>41</sup> This widespread use is a result of the fact that technetium can be obtained in high purity and at low cost using a  $^{99}\text{Mo}/^{99m}\text{Tc}$  generator. The generator contains  $^{99}\text{Mo}$  bound to a solid

support of alumina ( $\text{Al}_2\text{O}_3$ ) in the form of molybdate ( $\text{MoO}_4^{2-}$ ). A saline solution (0.9% NaCl) is passed through the alumina column to selectively elute  $^{99\text{m}}\text{Tc}$  as pertechnetate ( $\text{TcO}_4^-$ ).<sup>41</sup> Not only is this system simple and inexpensive, it is also easily shielded and can be handled effortlessly.  $^{99}\text{Mo}/^{99\text{m}}\text{Tc}$  generators are shipped around the world where they are used for one to two weeks before requiring replacement. This is a significant advantage over other isotopes like  $^{18}\text{F}$  where a cyclotron must be present in close proximity to the clinic in order to efficiently produce sufficient quantities of the isotope and tracer.

In addition to the convenience of the generator,  $^{99\text{m}}\text{Tc}$  has several other favorable properties, the most notable being its 6 hour half-life. This relatively long half-life allows adequate time for preparation of the radioimaging agent and performance of an imaging study. Another favorable nuclear property is that the gamma ray energy emitted from  $^{99\text{m}}\text{Tc}$  is 140 KeV, which is sufficient to escape all depths in a patient and be detected by the camera, but low enough that the dose to the patient is minimal and external shielding can be achieved with small quantities of lead.<sup>41</sup>

#### 1.4.4.2 Radio-Iodine $^{123}\text{I}/^{125}\text{I}/^{131}\text{I}$

Radioactive isotopes of iodine have been used for over 50 years in the field of cancer therapy.<sup>42</sup> **Table 1.1** summarizes the three most widely used of the thirty radioisotopes of iodine. Iodine-125 is an ideal radionuclide for method

development and small animal imaging<sup>43</sup> due to its low cost (reactor produced), although it does not have significant energy to be used for clinical studies. In its place iodine-123 can be employed as a result of its half life and gamma energy of 159 KeV (similar to <sup>99m</sup>Tc).<sup>44</sup> <sup>124</sup>I can be used for PET imaging while <sup>131</sup>I can be used for imaging and therapy. The ability to select the appropriate isotope to fit the desired application (imaging and therapy) is a real benefit to developing agents based on iodine.

**Table 1-1: Medically Relevant Radioisotopes of Iodine**

Isotope	Half Life <sup>44</sup>	Decay Mode <sup>44</sup>	Application
<sup>125</sup> I	59.4 d	x-ray	Therapy, <sup>42</sup> Small animal SPECT <sup>45</sup>
<sup>123</sup> I	13.3 h	Gamma	SPECT <sup>46</sup>
<sup>131</sup> I	8.0 d	Beta (-), gamma	Therapy <sup>44</sup>

#### 1.4.5 PET

Positron Emission Tomography (PET) is an imaging technique that utilizes the annihilation radiation that is produced from positron emitting radionuclides. When a positron is emitted from the nucleus, it combines with an electron to undergo an annihilation process that results in two 511 KeV photons that are expelled from the tissue at 180 degrees from each other. The photons are detected by a ring of detectors that sense coincidence interactions and can use the information to generate an image of the tracers location.

## 1.5 Organometallic Radiopharmaceuticals

The majority of technetium radiopharmaceuticals are based on classical Werner coordination compounds.<sup>55</sup> Progress has been made recently on developing organometallic radiopharmaceuticals.<sup>56</sup> This is a particularly challenging field because reactions done at the tracer level are performed in aqueous reaction media, under highly dilute reaction conditions; which are not usually amenable to organometallic chemistry. A further challenge is that, reactions must be high yielding and complete within one half-life to be clinically useful.

Alberto *et al.*<sup>57</sup> developed a convenient starting material to prepare organometallic radiopharmaceuticals derived from  $^{99m}\text{Tc}$ .  $[\text{Tc}(\text{CO})_3(\text{OH}_2)_3]^+$  (**1.8**) can be prepared in water at the tracer level by heating pertechnetate in the presence of CO and a reducing agent in a saline solution (**Figure 1.8**). The three labile water molecules in **1.8** can then be displaced by a variety of tridentate ligands to form very stable Tc(I) complexes.

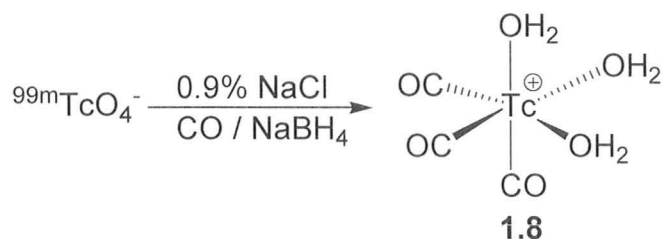


**Figure 1.7:** Synthesis of **1.8**<sup>57</sup>

Given the availability of **1.8**, Katzenellenbogen *et al.*<sup>58</sup> began designing and testing  $\text{CpRe}(\text{CO})_3$  (Cp = cyclopentadienyl) derivatives as novel antiestrogens in the hopes of discovering a potent ligand whose Tc analogue could be used to image the ER. Compounds containing up to 4 aryl substituents on the Cp ring were prepared and in select cases Re complexes having relative binding affinities of 20% compared to estradiol were reported. One of the limitations of this approach is that it is extremely difficult to prepare the Tc analogues of the compounds as Cp derivatives are not soluble in water and the ligand has a tendency to oligomerize rather than form the desired metal complex.<sup>58</sup> A new class of organometallic ligands could reduce these limitations.

## 1.6 Carboranes

The Valliant group has been investigating the use of carboranes as an alternative to Cp as an organometallic ligand for technetium. Carboranes are polyhedral clusters of boron and carbon atoms that can be prepared using an alkyne insertion reaction (**Figure 1.9**). Here a *closo*-carborane is formed by combining an alkyne with the bisacetonitrile adduct of **1.9**.

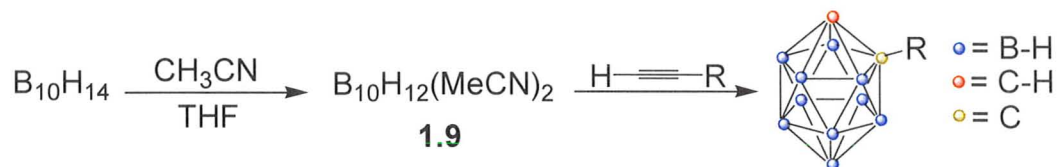


**Figure 1.8:** Alkyne insertion reaction



Carboranes have been investigated previously in medicinal chemistry as boron neutron capture therapy (BNCT) agents as a result of their high boron content. Beyond being boron rich, carboranes are promising synthons in medicinal chemistry due to their high thermal stability as well as their resistance to catabolism *in vivo*.<sup>59</sup> It should be pointed out that carboranes can be obtained in three isomeric forms: *ortho*, *meta* and *para*. The latter two are formed by heating *ortho* carborane to high temperatures under an inert atmosphere. In the work described here, only the *ortho* isomer was used.

*Ortho*-carboranes can be degraded under mild conditions to give the corresponding *nido*-carboranes (**Figure 1.9**). Removal of the bridging hydrogen atom generates the dicarbollide dianion which binds to metals in a similar fashion as Cp. The Valliant group has demonstrated that it is possible to produce Tc-carborane complexes at the tracer level using **1.8** as well as *nido*-carborane complexes that are stable indefinitely. In this way, carboranes can be used as surrogates for Cp to produce organometallic molecular imaging agents.

In addition to being able to metallate a carborane in an aqueous environment, carboranes can also be radiohalogenated<sup>60</sup> (**Figure 1.10**). This makes carboranes one of the most versatile synthons available in that they can be used to generate SPECT, PET and therapeutic agents using radiometals (Tc and Re) and radiohalogens.



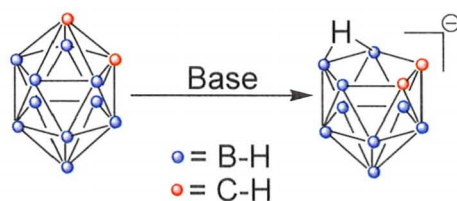


**Figure 1.9:** Degradation of a *closo*-carborane to form *nido*-carborane

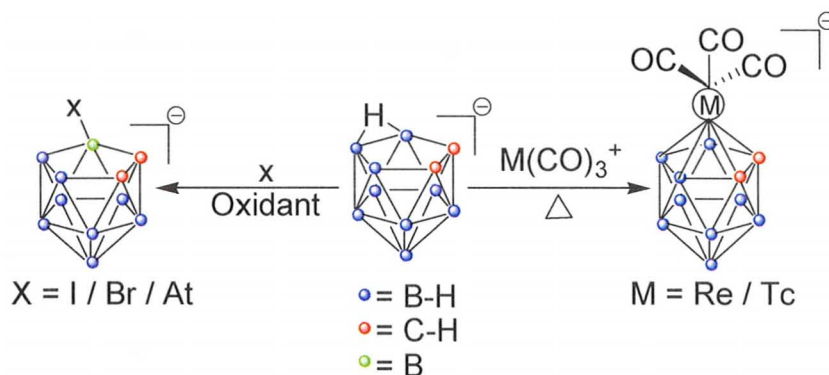


**Figure 1.10:** Metallation (right) and halogenations (left) of *ortho*-carborane

## 1.7 Carborane-Estrogen Analogues

Endo *et al.* have produced several carborane estrogen analogues that have been shown to bind the estrogen receptor (**Figure 1.11**),<sup>61-63</sup> where the key structural components needed for binding are a phenol ring and a *closo* carborane unit.

What is less commonly known is that carboranes are interesting hydrophobic structural motifs for use in medicinal chemistry due to their unique 3-D structures, ease of synthesis and functionalization, and low toxicity. Recently, work published in the Valliant group has showed promising results when compounds similar to those synthesized by Endo were metallated in an attempt to produce an ER imaging agent.<sup>64</sup>

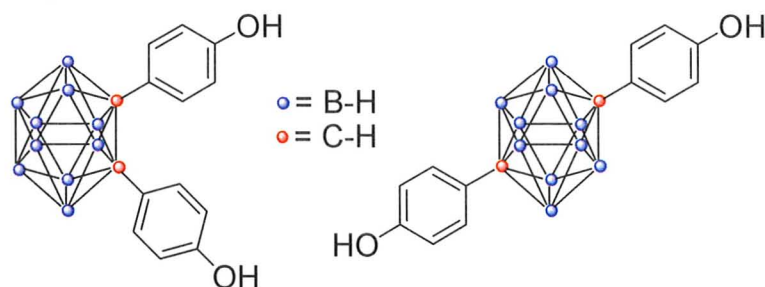


**Figure 1.11:** Closo carborane derivatives which bind the estrogen receptor<sup>63</sup>

## 1.8 Imaging and the ER

There are a limited number of examples of radioimaging agents that have been developed to target the ER. These include iodo-vinylestradiol,<sup>65</sup> <sup>18</sup>F-fluorotamoxifen,<sup>66-68</sup> <sup>123</sup>I-iodomethyl-*N,N*-diethyltamoxifen,<sup>69</sup> <sup>123</sup>I-4-hydroxy-Tamoxifen,<sup>70</sup> <sup>99m</sup>Tc-Tamoxifen conjugates<sup>71</sup> and <sup>18</sup>F-fluoroestradiol (FES).<sup>72, 73</sup> FES is the only probe to have been used regularly in the clinic, however, the high cost of producing the material and questions regarding poor specificity have motivated a search for a superior technetium or iodine ER probe.

One possible approach to addressing the limitations of the existing agents is to design a radiopharmaceutical based on a preexisting antiestrogen like Tamoxifen. Unfortunately it is not possible to directly label Tamoxifen with a widely available radionuclide like Tc, as the resulting complex would not be sufficiently stable *in vivo* and introduction of the metal in this manner would likely destroy the pharmaceutical activity of the complex. Alternatively, it is conceivable that one of the aryl rings of Tamoxifen could be replaced with a carborane. This way the corresponding Tc complex or iodinated carborane

derivative could be prepared using existing strategies. The carborane-Tamoxifen analogue itself would also be of interest if it has retained its affinity for the ER as it would represent a metabolically resistant form of Tamoxifen.

Structure activity data have shown that the A ring of Tamoxifen can be substituted without having a detrimental impact on activity.<sup>74, 75</sup> Carboranes can be used in place of existing aryl rings as they occupy a similar volume as a rotating phenyl ring.<sup>59</sup> In addition, Katzenellenbogen's work shows that the ligand binding domain of the ER has sufficient space to accommodate bulky CpRe(CO)<sub>3</sub> derivatives and in fact, the additional hydrophobicity of the metal-tricarbonyl core increased the RBA compared to the free ligand. This provides additional evidence that a metallocarborane analogue of Tamoxifen with the cluster located in place of the A ring would be a viable ER imaging probe.

## 1.9 Rational and Objectives

Taking advantage of the favorable binding of Tamoxifen to the ER, and the fact that rhenacarboranes derived from arylcarboranes have been shown to have affinity to the ER, the research at hand is designed to develop a means to substitute the phenyl ring A with a *closo ortho* carborane as a platform to create a new class of imaging and therapeutic agents. Carboranes offer versatility, as they can be radio-metallated and halogenated, thus PET and SPECT imaging agents can be synthesized from a single core. By producing an imaging agent that will specifically target the ER with minimal non-specific binding, there is a

potential for an increase in sensitivity and specificity when compared to traditional breast screening methods.

### 1.10 References

1. Foulkes, W. D.; Metcalfe, K.; Sun, P.; Hanna, W. M.; Lynch, H. T.; Ghadirian, P.; Tung, N.; Olopade, O. I.; Weber, B. L.; McLennan, J.; Olivotto, I. A.; Be'gin, L. R.; Narod., S. A., Estrogen Receptor Status in BRCA1- and BRCA2-Related Breast Cancer: The Influence of Age, Grade, and Histological Type. *Clinical Cancer Research* **2004**, 10, 2029-2034.
2. Theobald, A. J., Management of advanced breast cancer with endocrine therapy : The role of the primary healthcare team. *International Journal of Clinical Practice* **2000**, 54, 665.
3. Brzozowski, A. M.; Pike, A. C. W.; Dauter, Z.; Hubbard, R. E.; Bonn, T.; EngstrÅm, O.; Åhman, L.; Greene, G. L.; Gustafsson, J.; Carlquist, M., Molecular basis of agonism and antagonism in the oestrogen receptor. *Nature* **1997**, 389, 753-758
4. Song, R. X. D.; Santen, R. J., Membrane Initiated Estrogen Signaling in Breast Cancer. *Biology of Reproduction* **2006**, 75, 9-16.
5. Klinge, C. M., Estrogen receptor interaction with co-activators and co-repressors. *Steroids* **2000**, 65, 227-251
6. Tanenbaum, D. M.; Wang, Y.; Williams, S. P.; Sigler, P. B., Crystallographic comparison of the estrogen and progesterone receptor's ligand binding

- domains. . *Proceedings of the National Academy of Sciences of the United States of America* **1998**, 95, 5998-6003.
7. Schwabe, J. W.; Chapman, L.; Finch, J. T.; Rhodes, D., The crystal structure of the estrogen receptor DNA-binding domain bound to DNA: how receptors discriminate between their response elements. *Cell* **1993**, 75, 567-578.
  8. Moyano, P.; Rotwein, P., Mini-review: estrogen action in the uterus and insulin-like growth factor-I *Growth Hormone & IGF Research* **2004**, 14, 431-435.
  9. Simpson, E. R.; Misso, M.; Hewitt, K. N.; Hill, R. A.; Boon, W. C.; Jones, M. E.; Kovacic, A.; Zhou, J.; Clyne, C. D., Estrogen—the Good, the Bad, and the Unexpected. *Endocrine Reviews* **2008**, 26, (3), 322-330.
  10. Eriksen, E. F.; Colvard, D. S.; Berg, N. J.; Graham, M. L.; Mann, K. G.; Spelberg, T. C.; Riggs., B. L., Evidence of estrogen receptor in normal human osteoblast-like cells. *Science* **1988**, 84-86.
  11. Prezioso, D.; Denis, L. J.; Klocker, H.; Sciarra, A.; Reis, M.; Naber, K.; Lobel, B.; Pacik, D.; Griffiths, K., Estrogens and aspects of prostate disease. *International Journal of Urology* **2007**, 14, 1-16.
  12. Rissman, E. F., Roles of Oestrogen Receptors a and b in Behavioural Neuroendocrinology: Beyond Yin/Yang. *Journal of Neuroendocrinology* **2008**, 20, 873-879.

13. Vuolteenaho, O.; Ruskoaho, H., Gender matters: estrogen protects from cardiac hypertrophy. *TRENDS in Endocrinology and Metabolism* **2008**, *14*, 52-54.
14. Dodds, E. C.; Lawson, W.; Noble, R. L., *Lancet* **1938**, 1389-1391.
15. Dodds, E. C.; Goldberg, L.; Lawson, W.; Robinson, R., Estrogenic Activity of Certain Synthetic Compounds. *Nature* **1938**, *141*, 247-248.
16. Kistner, R. W.; Smith, O. W., *surgical forum* **1959**, *10*, 725-729.
17. Kistner, R. W.; Smith, O. W., *Fertility and Sterility* **1961**, *12*, 121-141.
18. Kistner, R. W.; Smith, O. W., *J. Am. Reed. Ass.* **1963**, *184*, 122-130.
19. Jordan, V. C., Antitumour activity of the antiestrogen ICI 46,474 (Tamoxifen) in the dimethylbenzanthracene (DMBA)—induced rat mammary carcinoma model. *Journal of Steroid Biochemistry* **1974**, *5*, 354.
20. Jordan, V. C., Tamoxifen: A Most Unlikely Pioneering Medicine. *Nature Drug Review* **2003**, *2*, 205-213.
21. Fisher, B.; Costantino, J. P.; Wickerham, D. L.; Redmond, C. K.; Kavanah, M.; Cronin, W. M.; Vogel, V.; Robidoux, A.; Dimitrov, N.; Atkins, J.; Daly, M.; Wieand, S.; Tan-Chiu, E.; Ford, L.; Wolmark, N., Tamoxifen for Prevention of Breast Cancer: Report of the National Surgical Adjuvant Breast and Bowel Project P-1 Study. *Journal of the National Cancer Institute* **1998**, *90*, (18), 1371-1388.
22. Gelber, R. D.; Cole, B. F.; Goldhirsch, A.; Rose, C.; Fisher, B.; Osborne, C.; Boccardo, F.; Gray, R.; Gordon, N. H.; Bengtsson, N.; Sevela, P.,

- Adjuvant chemotherapy plus tamoxifen compared with tamoxifen alone for postmenopausal breast cancer: meta-analysis of quality adjusted. *Lancet* **1996**, 347, 1066-1071.
23. Fisher, B.; Costantino, J. P.; Wickerham, D. L.; Redmond, C. K.; Kavanah, M.; Cronin, W. M.; Vogel, V.; Robidoux, A.; Dimitrov, N.; Atkins, J.; Daly, M.; Wieand, S.; Tan-Chiu, E.; Ford, L.; Wolmark, N., Tamoxifen for the Prevention of Breast Cancer: Current Status of the National Surgical Adjuvant Breast and Bowel Project P-1 Study. *Journal of the National Cancer Institute* **2005**, 97, (22), 1652-1662.
24. Wakeling, A. E.; Seater, S. R., *Cancer Treatment Reports* **1980**, 64, 741-744.
25. Jordan, V. C.; Chem, C., Metabolites of tamoxifen in animals and man: Identification, pharmacology, and significance *Breast Cancer Research and Treatment* **1982**, 2, 123-138.
26. Allen, K. E.; Clark, E. R.; Jordan, V. C., *J. Pharmac. Chemother.* **1980**, 71, 89-91.
27. Jordan, V. C.; Collins, M. M.; Rowsby, L.; Prestwich, G. J., A Monohydroxylated Metabolite Of Tamoxifen With Potent Antioestrogenic Activity. *Journal of Endocrinology* **1977**, 75, 305-316.
28. Gøtzsche, P. C.; Olsen, O., Is screening for breast cancer with mammography justifiable? *Lancet* **2000**, 355, 129-134.

29. Horton, R., Screening mammography—an overview revisited. *Lancet* **2001**, 358, 1284-1285.
30. Moskowitz, M., Breast Cancer: age-specific growth rates and screening strategies. *Radiology* **1986**, 161, 37-41.
31. Olsen, O.; Gøtzsche, P. C., Cochrane review on screening for breast cancer with mammography. *Lancet* **2001**, 358, 1340-1342.
32. Brewer, N. T.; Salz, T.; Lillie, S. E., Systematic Review: The Long-Term Effects of False-Positive Mammograms. *Annals of Internal Medicine* **2007**, 146, (7), 502-517.
33. Yaffe, M. J., Measurement of mammographic density. *Breast Cancer Research* **2008**, 10, (3).
34. Johns, P. C.; Yaffe, M. J., X-ray Characteristics of Normal and Neoplastic Breast Tissue *Physics in Medicine and Biology* **1987**, 32, 675-695.
35. Boyd, N. F.; Lockwood, G. A.; Byng, J. W.; Tritchler, D. L.; Yaffe, M. J., Mammographic Densities and Breast Cancer Risk *Cancer Epidemiology, Biomarkers & Prevention* **1998**, 7, 1133-1144.
36. Kuhl, C. K., MRI of Breast Tumors. *European Radiology* **2000**, 10, 46-58.
37. Kriege, M.; Brekelmans, C. T. M.; Boetes, C.; Besnard, P. E.; Zonderland, H. M.; Obdeijn, I. M.; Manoliu, R. A.; Kok, T.; Peterse, H.; Tilanus-Linthorst, M. M. A.; Muller, S. H.; Meijer, S.; Oosterwijk, J. C.; Beex, L. V. A. M.; Tollenaar, R. A. E. M.; Koning, H. J. d.; Rutgers, E. J. T.; Klijn, J. G. M., Efficacy of MRI and Mammography for Breast-Cancer Screening in



- Women with a Familial or Genetic Predisposition. *the New England Journal of Medicine* **2004**, 351, (5), 427-437.
38. Lehman, C. D.; Gatsonis, C.; Kuhl, C. K.; Hendrick, R. E.; Pisano, E. D.; Hanna, L.; Peacock, S.; Smazal, S. F.; Maki, D. D.; Julian, T. B.; DePeri, E. R.; Bluemke, D. A.; Schnall, M. D., MRI Evaluation of the Contralateral Breast in Women with Recently Diagnosed Breast Cancer. *The New England Journal of Medicine* **2007**, 356, (13), 1295-1303.
39. Bigenwald, R. Z.; Warner, E.; Gunasekara, A.; Hill, K. A.; Causer, P. A.; Messner, S. J.; Eisen, A.; Plewes, D. B.; Narod, S. A.; Zhang, L.; Yaffe, M. J., Is Mammography Adequate for Screening Women with Inherited BRCA Mutations and Low Breast Density? *Cancer Epidemiology Biomarkers & Prevention* **2008**, 17, (3), 706-711.
40. Shaw, V. I.; Raju, U.; Chitale, D.; Deshpande, V.; Gregory, N.; Strand, V., False-negative core needle biopsies of the breast. *Cancer* **2003**, 97, 1824-1831.
41. Sorenson, J. A.; Phelps, M. E., *Physics in Nuclear Medicine*. Grune and Stratton: New York, 1987.
42. Park, U. J.; Lee, S. J.; Son, K. J.; Han, H. S.; Nam, S. S., The adsorption of  $^{125}\text{I}$  on a  $\text{Ag}+\text{Al}_2\text{O}_3$  rod as a carrier body for a brachytherapy source. *Journal of Radioanalytical and Nuclear Chemistry* **2008**, 277, (2), 429-432.
43. Seevers, R. H.; Counsell, R. E., Radioiodination techniques for small organic molecules. *Chemical Review* **1982**, 82, 575-590.

44. Saha, G. B., *Physics and Radiobiology of Nuclear Medicine*. 2 ed.; Springer-Verlag: New York, 2001.
45. Accorsi, R.; Celentano, L.; Laccetti, P.; Lanza, R. C.; Marotta, M.; Mettivier, G.; Montesi, M. C.; Roberti, G.; Russo, P., High-Resolution 125I Small Animal Imaging With a Coded Aperture and a Hybrid Pixel Detector. *IEEE Transactions On Nuclear Science* **2008**, 55, (1), 481-490.
46. Hahner, S.; Stuermer, A.; Kreissl, M.; Reiner, C.; Fassnacht, M.; Haescheid, H.; Beuschlein, F.; Zink, M.; Lang, K.; Allolio, B.; Schirbel, A., [123I]Iodometomidate for Molecular Imaging of Adrenocortical Cytochrome P450 Family 11B Enzymes. *J. Clin. Endocrinol. Metab.* **2008**, 96, (6), 2358-2365.
47. *Handbook of Radiopharmaceuticals Radiochemistry and Applications*. John Wiley & Sons Ltd.: West Sussex, 2003.
48. Israel, I.; Wolfgang, B.; Farmakis, G.; Samnick, S., Improved synthesis of no-carrier-added p-[124I]iodo-L-phenylalanine and p-[131I]iodo-L-phenylalanine for nuclear medicine applications in malignant gliomas. *Applied Radiation and Isotopes* **2008**, 66, 513-522.
49. Diaz, L. A.; Foss, C. A.; Thornton, K.; Nimmagadda, S.; Endres, C. J.; Uzuner, O.; Seyler, T. M.; Ulrich, S. D.; Conway, J.; Bettgowda, C.; Agrawal, N.; Cheong, I.; Zhang, X.; Ladenson, P. W.; Vogelstein, B. N.; Mont, M. A.; Kinzler, K. W.; Vogelstein, B.; Pomper, M. G., Imaging of

- Musculoskeletal Bacterial Infections by [124I]FIAU-PET/CT. *PLoS ONE* **2007**, 10, 1007.
50. Freudenberg, L. S.; Antoch, G.; Frilling, A.; Jentzen, W.; Rosenbaum, S. J.; Kuhl, H.; Bockisch, A.; Gorges, R., Combined metabolic and morphologic imaging in thyroid carcinoma patients with elevated serum thyroglobulin and negative cervical ultrasonography: role of 124I-PET/CT and FDG-PET. *Eur. J. Nucl. Med. Mol. Imaging* **2008**, 35, 950-957.
51. Bigotta, H. M.; Laforestb, R.; Liub, X.; Ruangmab, A.; Wuestc, F.; Welch, M. J., Advances in the production, processing and microPET image quality of technetium-94m. *Nuclear Medicine and Biology* **2006**, 33, 923-933.
52. Rogers, B. E.; Parry, J. J.; Andrews, R.; Cordopatis, P.; Nock, B. A.; Maina, T., MicroPET Imaging of Gene Transfer with a Somatostatin Receptor-Based Reporter Gene and 94mTc-Demotate 1. *the Journal of Nuclear Medicine* **2005**, 45, (11), 1889-1897.
53. Bigott, H. M.; Parent, E.; Luyt, L. G.; Katzenellenbogen, J. A.; Welch, M. J., Design and Synthesis of Functionalized Cyclopentadienyl Tricarbonylmetal Complexes for Technetium-94m PET Imaging of Estrogen Receptors. *Bioconjugate Chemistry* **2005**, 16, 255-264.
54. Luyt, L. G.; Bigott, H. M.; Welch, M. J.; Katzenellenbogen, J. A., 7 $\alpha$ - and 17 $\alpha$ -Substituted Estrogens Containing Tridentate Tricarbonyl Rhenium/Technetium Complexes: Synthesis of Estrogen Receptor

- Imaging Agents and Evaluation Using MicroPET with Technetium-94m. *Bioorganic and Medicinal Chemistry* **2003**, 11, 4977-4989.
55. Hom, K. R.; Katzenellenbogen, J. A., Technetium-99m-labeled receptor-specific small-molecule radiopharmaceuticals: Recent developments and encouraging results. *Nuclear Medicine and Biology* **1997**, 24, (6), 485-498.
56. Schibli, R.; Schubiger, A. P., Current use and future potential of organometallic radiopharmaceuticals. *European Journal of Nuclear Medicine* **2002**, 29, (11), 1529-1542.
57. Alberto, R.; Schibli, R.; Egli, A.; Schubiger, A. P., A Novel Organometallic Aqua Complex of Technetium for the Labeling of Biomolecules: Synthesis of  $[\text{}^{99\text{m}}\text{Tc}(\text{OH}_2)_3(\text{CO})_3]^+$  from  $[\text{}^{99\text{m}}\text{TcO}_4]^-$  in Aqueous Solution and Its Reaction with a Bifunctional Ligand. *Journal of the American Chemical Society* **1998**, 120, (31), 7987-7988.
58. Mull, E. S.; Sattigeri, V. J.; Rodriguez, A. L.; Katzenellenbogen, J. A., Aryl Cyclopentadienyl Tricarbonyl Rhenium Complexes: Novel Ligands for the Estrogen Receptor with Potential Use as Estrogen Radiopharmaceuticals. *Bioorganic & Medicinal Chemistry* **2002**, 10, 1381-1398.
59. Valliant, J. F.; Guenther, K. J.; King, A. S.; Morel, P.; Schaffer, P.; Sogbein, O. O.; Stephenson, K. A., The medicinal chemistry of carboranes. *Coordination Chemistry Reviews* **2002**, 232, 173-230.

60. Olsen, F. P.; Hawthorne, M. F., Halodicarbaundecaborate (11) Ions. *Inorganic Chemistry* **1965**, 4, (12), 1839.
61. Endo, Y.; Iijima, T.; Yamakoshi, Y.; Yamaguchi, M.; Fukasawa, H.; Shudo, K., Potent Estrogenic Agonists Bearing Dicarba-*closo*-dodecaborane as a Hydrophobic Pharmacophore. *Journal of Medicinal Chemistry* **1999**, 42, 1501-1504.
62. Endo, Y.; Iijima, T.; Yamakoshi, Y.; Fukasawa, H.; Miyaura, C.; Inada, M.; Kubo, A.; Itai, A., Potent estrogen agonists based on carborane as a hydrophobic skeletal structure A new medicinal application of boron clusters. *Chem. Biol.* **2001**, 8, 341-355.
63. Endo, Y.; Yoshimi, T.; Miyaura, C., Boron clusters for medicinal drug design: Selective estrogen receptor modulators bearing carborane. *Pure Appl. Chem.* **2003**, 75, (9), 1197-1205.
64. Causey, P. W.; Besanger, T. R.; Valliant, J. F., Synthesis and Screening of Mono- and Di-Aryl Technetium and Rhenium Metallocarboranes. A New Class of Probes for the Estrogen Receptor. *Journal of Medicinal Chemistry* **2008**, 51, 2833-2844.
65. Hanson, R. N.; Franke, L. A., Preparation and Evaluation of 17{alpha}-<sup>[125]</sup>Iodovinyl-11β-Methoxyestradiol as a Highly Selective Radioligand for Tissues Containing Estrogen Receptors: Concise Communication *Journal of Nuclear Medicine* **1984**, 25, 998-1002.

66. Inoue, T.; Kim, E. E.; Wallace, S., Preliminary study of cardiac accumulation of F-18 fluorotamoxifen in patients with breast cancer. *Clinical Imaging* **1997**, 21, 332-336.
67. Inoue, T.; Kim, E. E.; Wallace, S., Positron Emission Tomography using [<sup>18</sup>F]fluorotamoxifen to Evaluate Therapeutic Responses in Patients with Breast Cancer: Preliminary Study. *Cancer Biotherapy & Radiopharmaceuticals* **1996**, 11, 235-245.
68. Ang, D. J.; Li, C.; Kuang, L. R.; Price, J. E.; Buzdar, A. U.; Tansey, W.; Cherif, A.; Gretzer, M.; Kim, E. E.; Wallace, S., Imaging, biodistribution and therapy potential of Halogenated tamoxifen analogues *Life Sciences* **1994**, 55, (1), 53-67.
69. Wiele, C. V. d.; Vos, F. D.; Sutter, J. D.; Dumont, F.; Slegers, G.; Dierckx; Thierens, H., Biodistribution and dosimetry of (iodine-123)-iodomethyl-N,N-diethyltamoxifen, an (anti)oestrogen receptor radioligand. *European Journal of Nuclear Medicine* **1999**, 26, (10), 1959-1264.
70. Kruijer, P. S.; Klok, R. P.; Koedijk, C. D. M. A. w. d.; Blankenstein, M. A.; Voskuil, J. H.; Verzeijlbergen, J. F.; Ensing, G. J.; Herscheid, J. D. M., Biodistribution of I<sup>125</sup>-Labeled +Hydroxytamoxifen Derivatives in Rats with Dimethylbenzylthiouracil-Induced Mammary Carcinomas. *Nuclear Medicine and Biology* **1997**, 24, 719-722.
71. Hunter, D. H.; Luyt, L. G., Single Isomer Technetium-99m Tamoxifen Conjugates. *Bioconjugate Chemistry* **2000**, 11, 175-181.

72. Linden, H. M.; Stekhova, S. A.; Link, J. M.; Gralow, J. R.; Livingston, R. B.; Ellis, G. K.; Petra, P. H.; Peterson, L. M.; Schubert, E. K.; Dunnwald, L. K.; Krohn, K. A.; Mankoff, D. A., Quantitative Fluoroestradiol Positron Emission Tomography Imaging Predicts Response to Endocrine Treatment in Breast Cancer. *Journal of Clinical Oncology* **2006**, *24*, 2793-2799.
73. Flanagan, F. L.; Dehdashti, F.; Siegel, B. A., PET in breast cancer. *Seminars in Nuclear Medicine* **1998**, *28*, 290-302.
74. Dauer, S. T. B.; Vaissermann, J.; Jaouen, G., Facile route to ferrocifen, 1-[4-(2-dimethylaminoethoxy)]-1-(phenyl-2-ferrocenyl-but-1-ene), first organometallic analogue of tamoxifen, by the McMurry reaction. *Journal of Organometallic Chemistry* **1997**, *541*, 355-361.
75. Hunter, D. H.; Payne, N. C.; Rahman, A.; Richardson, J. F.; Ponce, Y. Z., The iodo-Tamoxifens: molecular structures and syntheses of estrogens for external imaging of carcinoma. *Canadian Journal of Chemistry* **1983**, *61*, 421-426.

## 2.0 The Synthesis and In Vitro Evaluation of a Carborane Analogue of Tamoxifen

### 2.1 Introduction

Tamoxifen is used as a preventative treatment<sup>1</sup> for high risk woman as well as in long term adjuvant therapy.<sup>2</sup> The use of Tamoxifen however has also been associated with increased risk in developing endometrial<sup>3,4</sup> and uterine<sup>5</sup> cancers as well as increased possibility of suffering a pulmonary embolism, stroke or deep vein thrombosis.<sup>6</sup> In light of this, several Tamoxifen analogues (*vide supra*) have been developed in hopes of retaining the benefits of the parent drug while reducing possible side effects.

To date, there have been no reports of a *closo* carborane analogue of Tamoxifen. We previously reported<sup>7</sup> the synthesis of a *nido* carborane analogue but were not able to prepare the complementary *closo* structures or to evaluate the E versus Z isomers. Given the promising results of simple carborane phenol derivatives in binding to the ER,<sup>8-14</sup> a synthetic method to E and Z carborane analogues of Tamoxifen (**Scheme 1**) was developed and the products tested in ER positive and negative cell lines.

### 2.2 Synthesis of Z-1-(1,2-dicarba-*closo*-dodecaborane-1-yl)-1-(4-hydroxyphenol)-2-phenyl-but-1-ene (2.7)

The first step in the synthesis of **2.7** (**Scheme 2.1**) was the preparation of the methoxy ketone (**2.0**) which was performed using a Friedel-Crafts acylation.



The synthetic method was adapted from Smyths and Corby,<sup>15</sup> whose work focused on developing a “green” Friedel-Crafts acylation reaction. The scale up of this reaction facilitated the preparation over 0.5kg of **2.0**. A minor variation from the literature was that hydroxide pellets were used to neutralize the reaction rather than the reported dilute solution in order to reduce the overall reaction volume and amount of waste. In addition, the reaction mixture was cooled using an ice and salt water bath (circa  $-10^{\circ}\text{C}$ ) during this procedure to control the exothermic neutralization reaction.

One possible side reaction in the Friedel-Crafts preparation of **2.0** was the formation of the *ortho*-substituted isomer.  $^1\text{H}$  NMR spectroscopy was employed to verify that the correct isomer had been isolated (**Figure 2.1**). The two doublets at 8.15 and 6.85 ppm are indicative of the sole formation of the *para*-substituted product. Some additional features of the  $^1\text{H}$  NMR spectrum include the multiplets at 1.90 and 2.35 ppm which arise from the methylene protons ( $\text{H}_4$ ). The appearance of the multiplet is consistent with coupling to the ethyl protons ( $\text{H}_5$ ) as well as proton  $\text{H}_3$ .

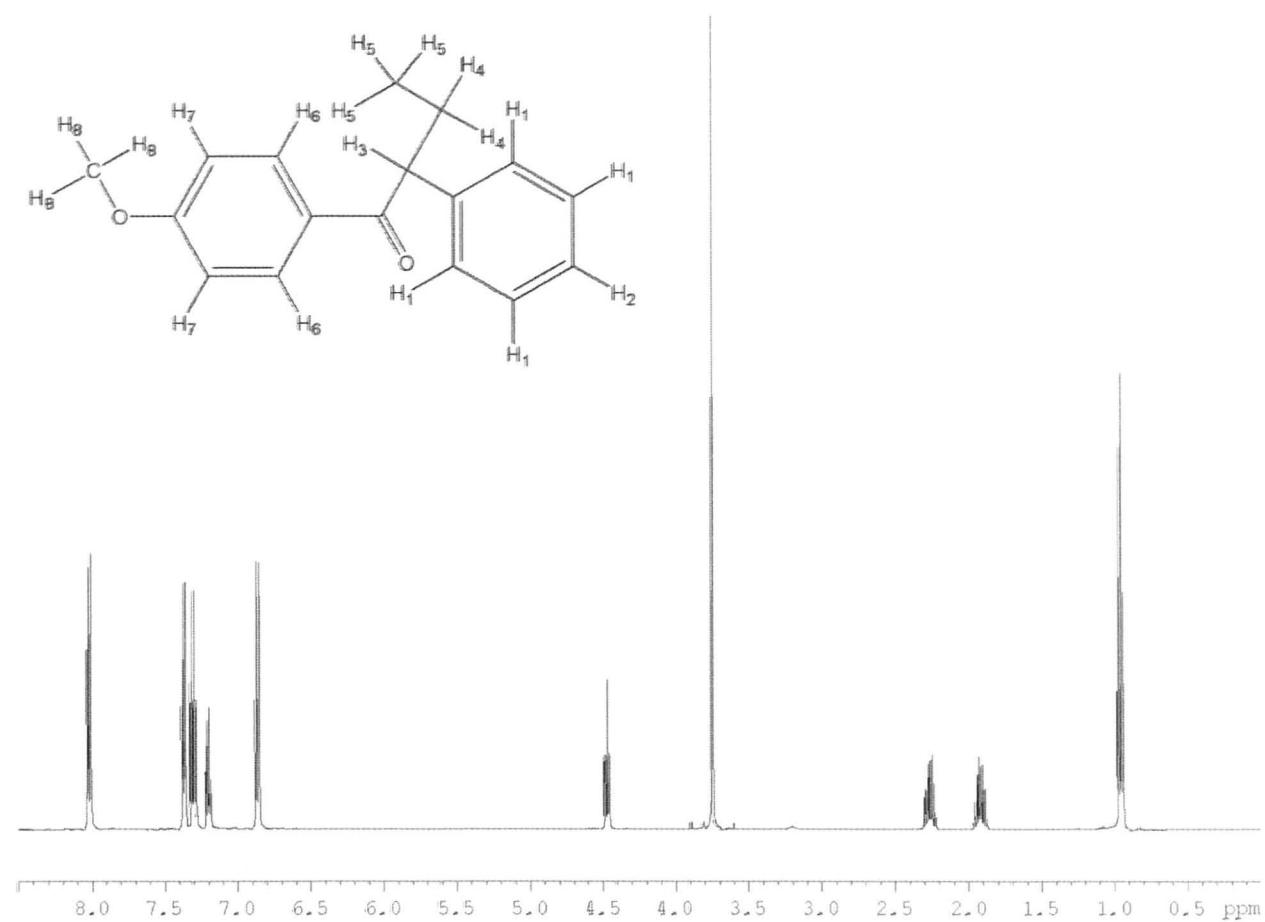
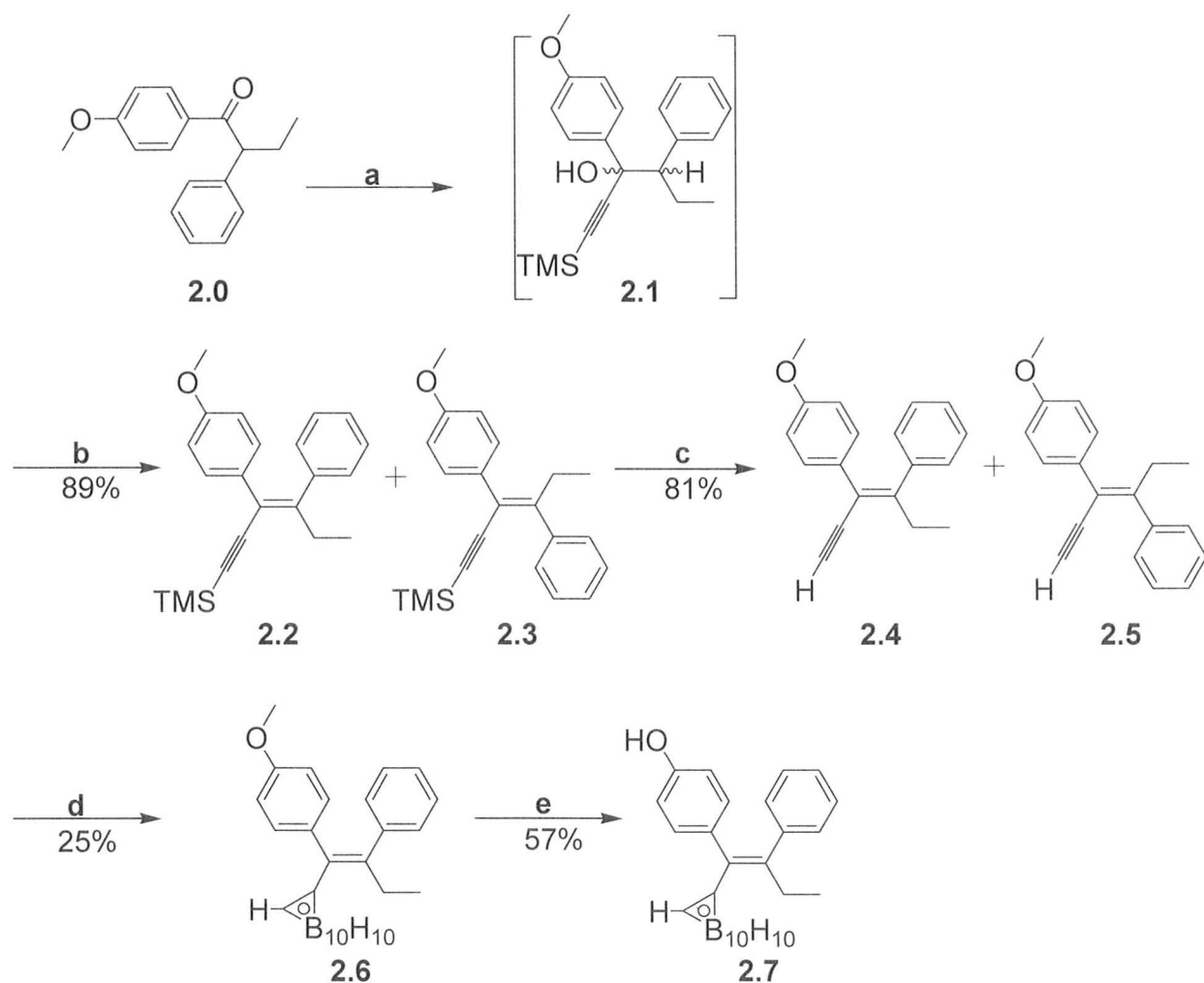


Figure 2.1:  $^1\text{H}$  NMR of 2.0 (500 MHz,  $\text{CDCl}_3$ ) and proton numbering scheme



**Scheme 2.1:** Synthesis of **2.7**: **a**) 1. TMS-acetylene, n-BuLi,  $-78^{\circ}\text{C}$ , THF; 2. Saturated ammonium chloride **b**) pyridine, thionyl chloride,  $-78^{\circ}\text{C}$  **c**) 1. NaOMe, MeOH 2.  $\text{H}_2\text{O}$  **d**) 1-Butyl-3-methylimidazolium chloride,  $\text{B}_{10}\text{H}_{14}$ , toluene **e**)  $\text{BBr}_3$ , dichloromethane,  $-78^{\circ}\text{C}$ .

The methoxy ketone product was combined with TMS-protected lithium acetylide (**Scheme 2.1**), resulting in the tertiary alcohol **2.1**, which was isolated as pale yellow oil and used without further purification. To form the eneynes (**2.2** and **2.3**) an elimination reaction was performed using pyridine and thionyl

chloride at  $-78^{\circ}\text{C}$  to produce the protected ene-yne in an 89 % yield. The  $^1\text{H}$  NMR of **2.2/2.3** showed Z:E ratio of 15:1.

The ratio of the formation of isomers **2.2** and **2.3** is an important consideration because they can have significantly different biological activities *in vivo*.<sup>16</sup> For instance, the Z isomer of Tamoxifen is anti-estrogenic while the E-isomer is estrogenic. The Felkin-Ahn model and mechanism of elimination can be used to rationalize the product ratio.<sup>17</sup> The Felkin-Ahn model is based on the Curtin-Hammet principle which states that the relative energy of the transition state will control selectivity, not the relative energy of the starting materials.<sup>17</sup> Applying the Felkin-Ahn model, nucleophilic attack on the carbonyl group will occur at the Burgi-Dunitz angle of  $107^{\circ}$  on one of the two conformers shown in **Figure 2.2**. Examining the Newman projections (**Figure 2.2**), illustrates that the conformer on the left would be less sterically hindered and the transition state of the conformer on the left would be lower in energy than the conformer on the right.

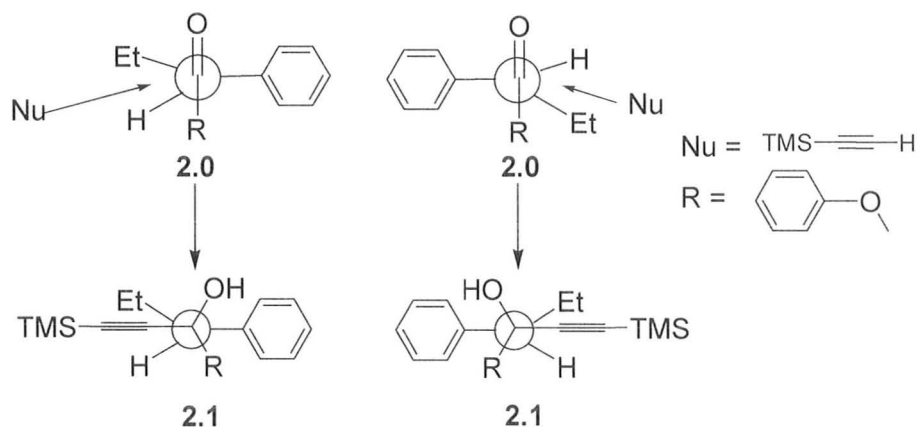


**Figure 2.2:** Nucleophilic attack on (2.1) - a prochiral carbonyl carbon atom

The subsequent elimination reaction occurs via a concerted E2 elimination mechanism which controls the overall ratio of the isomers (**Figure 2.3**). For the E2 elimination to occur, the sigma orbital from the proton that is abstracted (C-H) as well as the sigma antibonding orbital of the leaving group (C-O-SO<sub>2</sub>Cl) need to lie in the same plane. In other words to obtain the required orbital geometry the intermediate needs to adopt an anti-periplanar conformation.<sup>18</sup> Conversely, if this reaction were to proceed via an E1 mechanism, the E isomer would be produced in greater quantities as it is thermodynamically favoured.

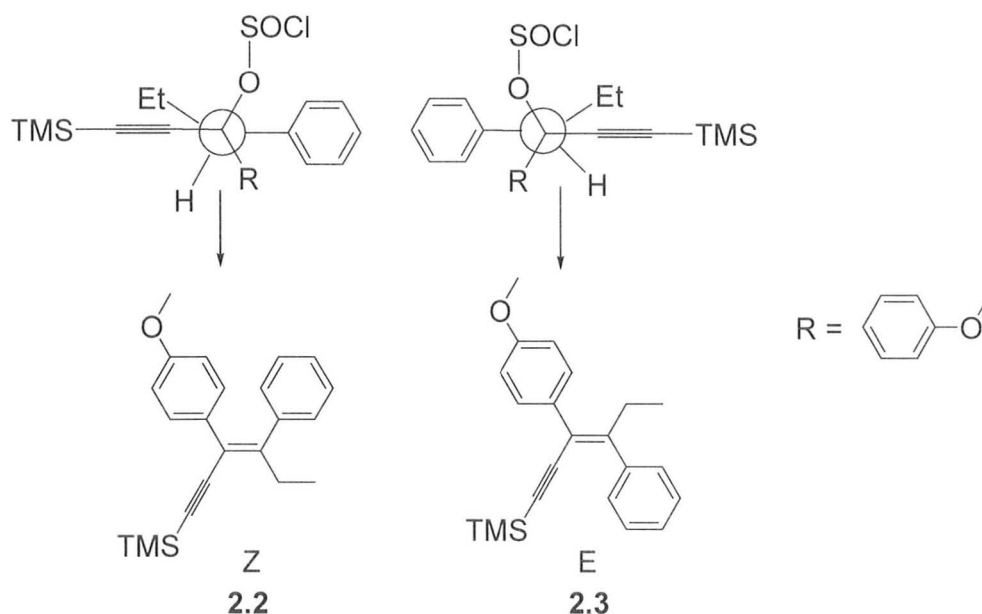


**Figure 2.3:** Conformations leading to the two isomer **2.2** and **2.3**

The TMS protecting group was removed by treating **2.2** and **2.3** with sodium methoxide in methanol (0.30 M). The reaction mixture was stirred for 24 hours whereupon analysis of the mixture by thin layer chromatography (TLC) indicated complete consumption of the starting material. The light sensitive products **2.4** and **2.5** were isolated in 81% yield as a mixture via simple liquid-liquid extraction. Using <sup>1</sup>H nuclear Overhauser effect (nOe) spectroscopy the major product was clearly identified as the Z isomer. Integration of the signals arising from the protons on the ethyl group (**Figure 2.4**) indicated that that the Z:E ratio was 93:7. The residual E isomer was later removed following isolation of the target carborane.

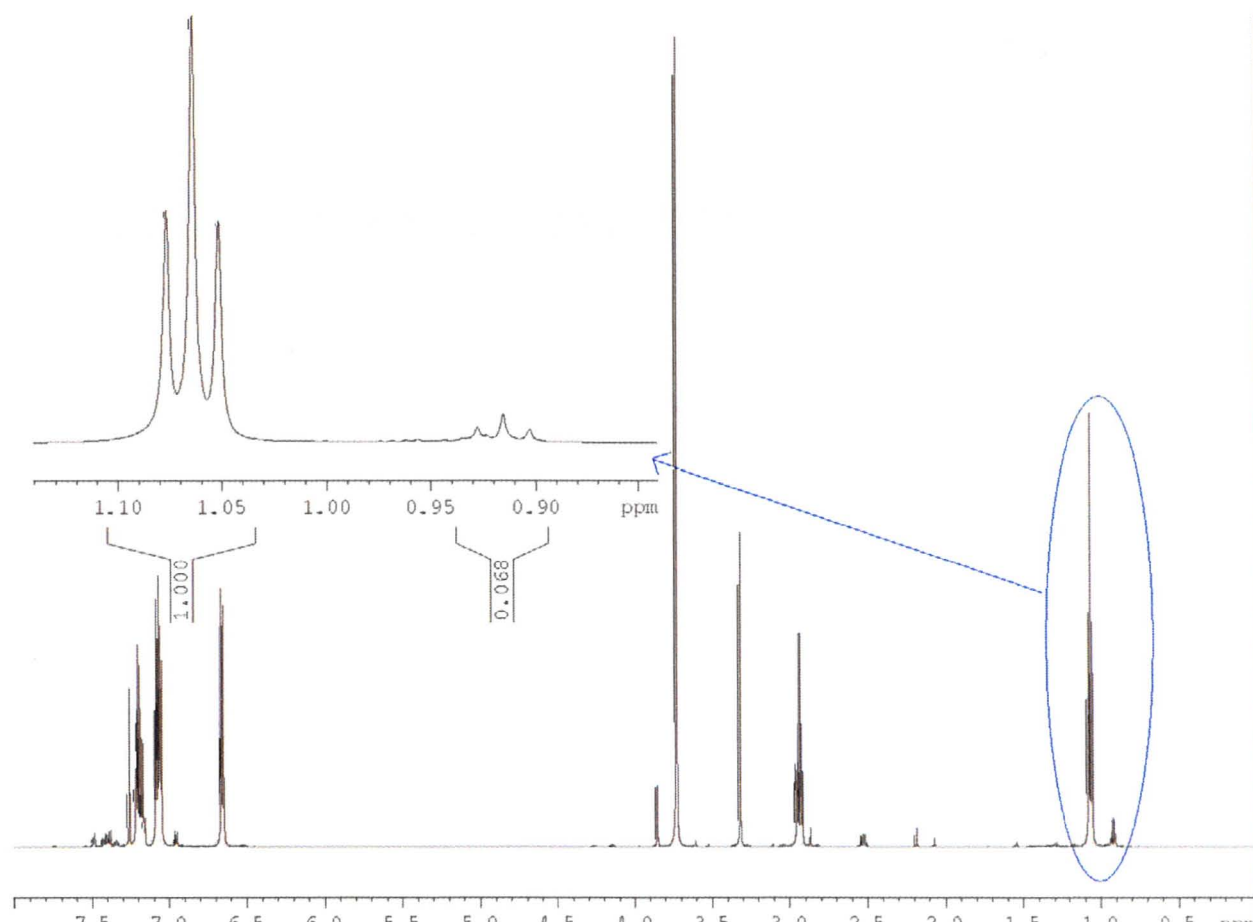


**Figure 2.4:**  $^1\text{H}$  NMR of **2.4/2.5** following liquid-liquid extraction. Integration of the triplets in the highlighted region show a Z:E ratio of 15:1 (600 MHz,  $\text{CDCl}_3$ )

With significant quantities of the acetylene derivative (**2.4**) having the appropriate stereochemistry in hand, the alkyne insertion reaction was performed to generate the desired carborane. Initial attempts to obtain **2.6** utilizing a traditional alkyne insertion reaction failed to yield the target compound. This is likely the result of a combination of the highly conjugated nature of the ene-yne, which would reduce the overall activity of the compound to carborane formation,

and the steric bulk around the reaction centre. The ultimately successful approach involved the use of 1-butyl-3-methylimidazolium chloride (Bmim-Cl), an ionic liquid.<sup>19</sup> Decaborane and catalytic amounts of Bmim-Cl were dissolved in toluene to create a biphasic mixture to which **2.4** and **2.5** were added, the mixture was heated at reflux for 12 hours under argon. The removal of the reaction solvent yielded a dark solid that was purified via silica gel chromatography and recrystallization gave the product as a white solid in 25% yield.

The <sup>1</sup>H NMR of **2.6** (**Figure 2.5**) was similar to that of the deprotected acetylene derivative with the exception that purification lead to the isolation of a single Z isomer. This was evident looking at the triplet at 0.92 ppm which lacks the corresponding signal from the E isomer (see **Figure 2.4**). A broad peak was observed at 3.15 ppm that is attributable to the C-H of the carborane cage while the B-H groups of the carborane form another broad signal spanning from 1-4 ppm.<sup>20</sup> The peaks in the <sup>11</sup>B NMR spectrum and the MS isotope pattern were consistent with the presence of a *closo* carborane cage while the IR spectrum showed B-H stretches at 2605 cm<sup>-1</sup>.



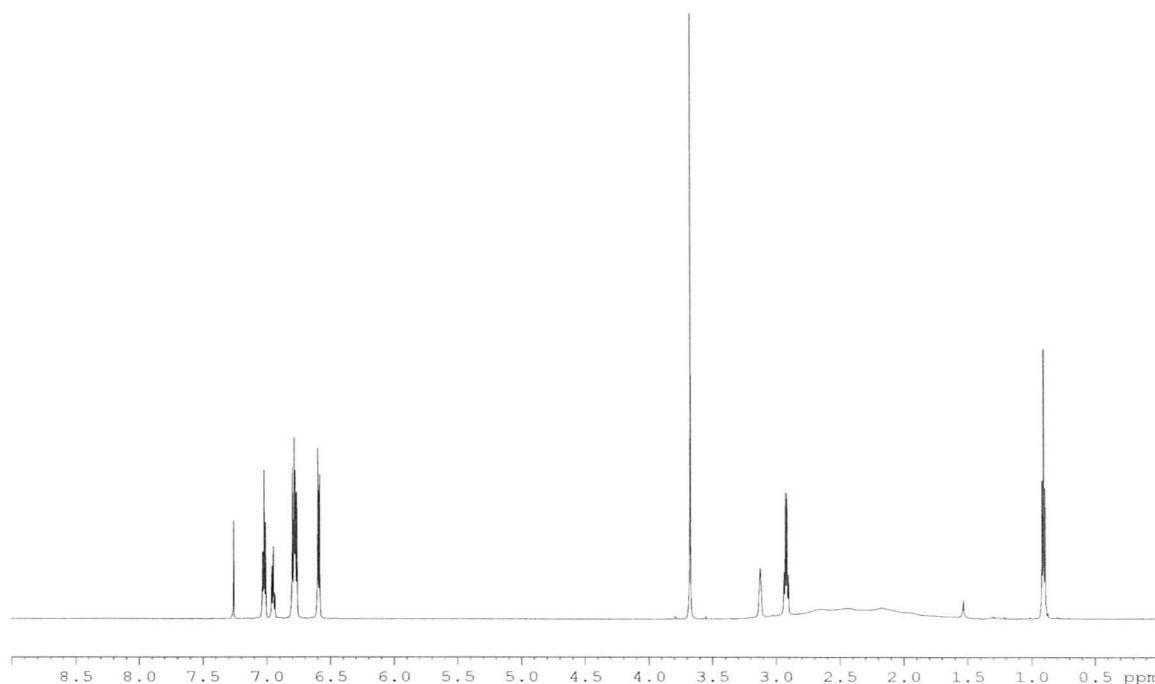


**Figure 2.5:**  $^1\text{H}$  NMR of **2.6** (600 MHz,  $\text{CDCl}_3$ )

X-ray quality single crystals of **2.6** were obtained by dissolving the white solid in boiling petroleum ether, followed by slow evaporation over nine days. The crystal structure of the *closo* carborane was consistent with the results of the nOe experiments and confirmed that the product was in fact the *Z*-isomer. The average C-C bond length of the carborane was 1.600(2) while the average B-B and C-B bond lengths were 1.782(3) and 1.719(2) respectively which was similar to the values reported for simple aryl-carboranes.<sup>14</sup>

Removal of the methoxy protecting group in **2.6** was carried out using  $\text{BBr}_3$  in dichloromethane to produce the phenol *closo* carborane **2.7** in 57% yield after recrystallization. The removal of the methoxy protecting group proved to be difficult and required a longer reaction time than generally described in the

literature.<sup>26</sup> This may be a result of the extended conjugation in **2.6** which would reduce the electron density on the methoxy oxygen, thereby slowing the rate of reaction. Despite the poor reactivity, the <sup>1</sup>H NMR spectrum of **2.7** clearly indicated the formation of the phenol through the loss of the signal associated with the methoxy group and appearance of signal associated with the phenol proton ( $\delta$ 4.47 ppm). The IR spectrum further confirmed the formation of the phenol group ( $\nu = 3566 \text{ cm}^{-1}$ ).

Single crystals of **2.7** were obtained by slow evaporation of a methanol solution and the crystal structure (**Figure 2.6**) confirmed that **2.7** remained as the Z-isomer. The crystallographic data allowed for comparison of the structural backbone where the introduction of the carborane seemed to have a negligible effect on the structure of the Tamoxifen backbone in the solid state. For instance the C1'-C9' as well as the C1'-C2' and C9'-C10' bond lengths were found to be 1.348(2), 1.504(2) and 1.502(2) Å respectively. The corresponding bond lengths in Tamoxifen were found to be: 1.34, 1.49 and 1.50 Å.<sup>21</sup> The torsion angles for the aromatic rings for **2.6** and **2.7** were found to be 90.47° and 78.59° and 79.24° and 80.95° respectively (defined by the C2, C7 and C1, C9 planes and C10, C15 and C1 and C9 planes). This is a noteworthy difference from Tamoxifen which exhibits corresponding torsion angles of 133.98 and 126.59.<sup>21</sup>

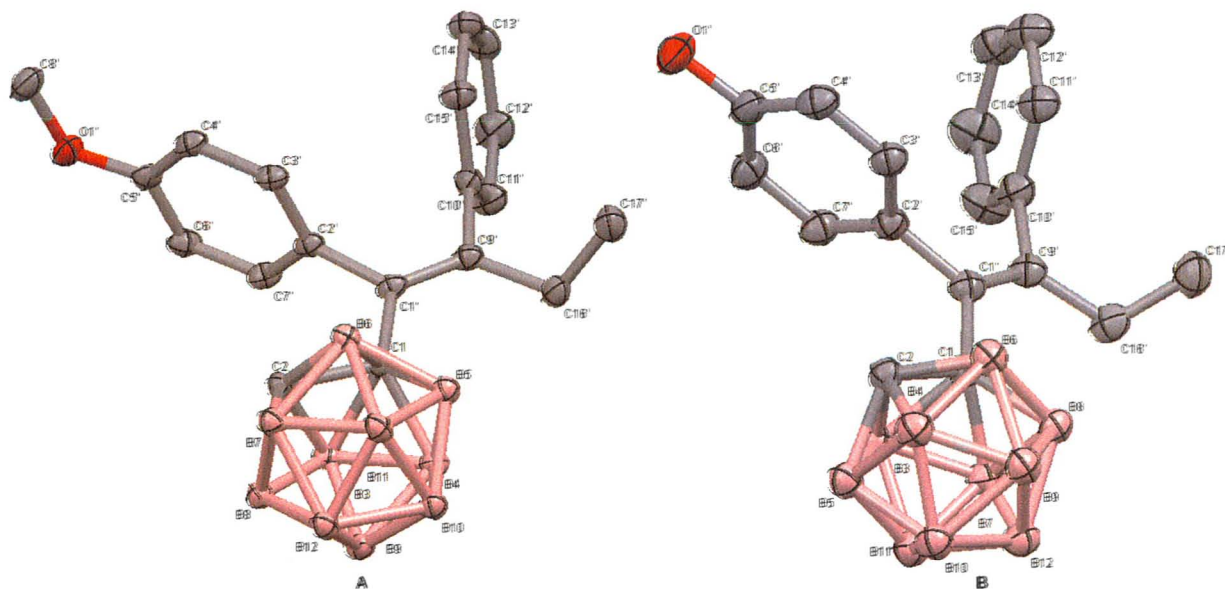


**Figure 2.6:** Crystal structures and atomic numbering schemes for **2.6** and **2.7** (50% thermal ellipsoids). Hydrogen atoms were omitted for clarity.

### 2.3 Isomerization of **2.7** and the synthesis of E-1-(1,2-dicarba-closo-dodecaborane-1-yl)-1-(4-hydroxyphenol)-2-phenyl-but-1-ene (**2.8**)

When compounds **2.2-2.5** are dissolved in a solvent and exposed to light they isomerize and degrade to form a mixture of compounds. In contrast, compound **2.7** can be stored for several months as a solid in an open container and as a methanol solution exposed to sunlight without any evidence of degradation. To further investigate the stability of **2.7**, a temperature course study was conducted (**Table 2.1**) by dissolving the compound in 95% ethanol and heating in a Biotage initiator 60 microwave.  $^1\text{H}$  NMR of the reaction mixture

showed that the compound did not degrade but in fact isomerized to form a mixture of Z and E isomers (**Figure 2.7**). The relative amount of each isomer present was determined by LC-MS.

**Table 2.1:** E/Z Isomerization of **2.7** in 95% ethanol using microwave heating

Temperature (°C)	Time (min)	Z (%) ( <b>2.7</b> )	E (%) ( <b>2.8</b> )
80	20	100	0
100	20	100	0
120	20	100	0
140	20	99	1
160	20	85	15
180	20	56	44

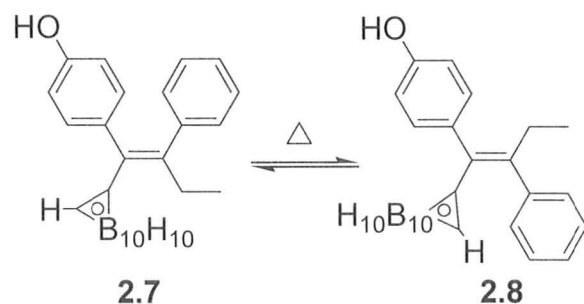


**Figure 2.7:** Thermal E-Z isomerization of **2.7**

In order to determine the identities of the two signals observed in the HPLC of **2.7** (**Figure 2.8**) following heating, the peak eluting at 20.8 minutes was isolated and the product fully characterized. The  $^1\text{H}$  NMR spectrum showed that the product were the E-isomer **2.8** as opposed to the starting Z-isomer (**Figure**

**2.9).** The most notable differences in the NMR was that the upfield shift of the signals associated with the methylene group from 2.80 ppm in **2.7** to 1.89 ppm in **2.8** and the significant (0.5 ppm) downfield shift of the aromatic protons of **2.8** relative to those in **2.7**.

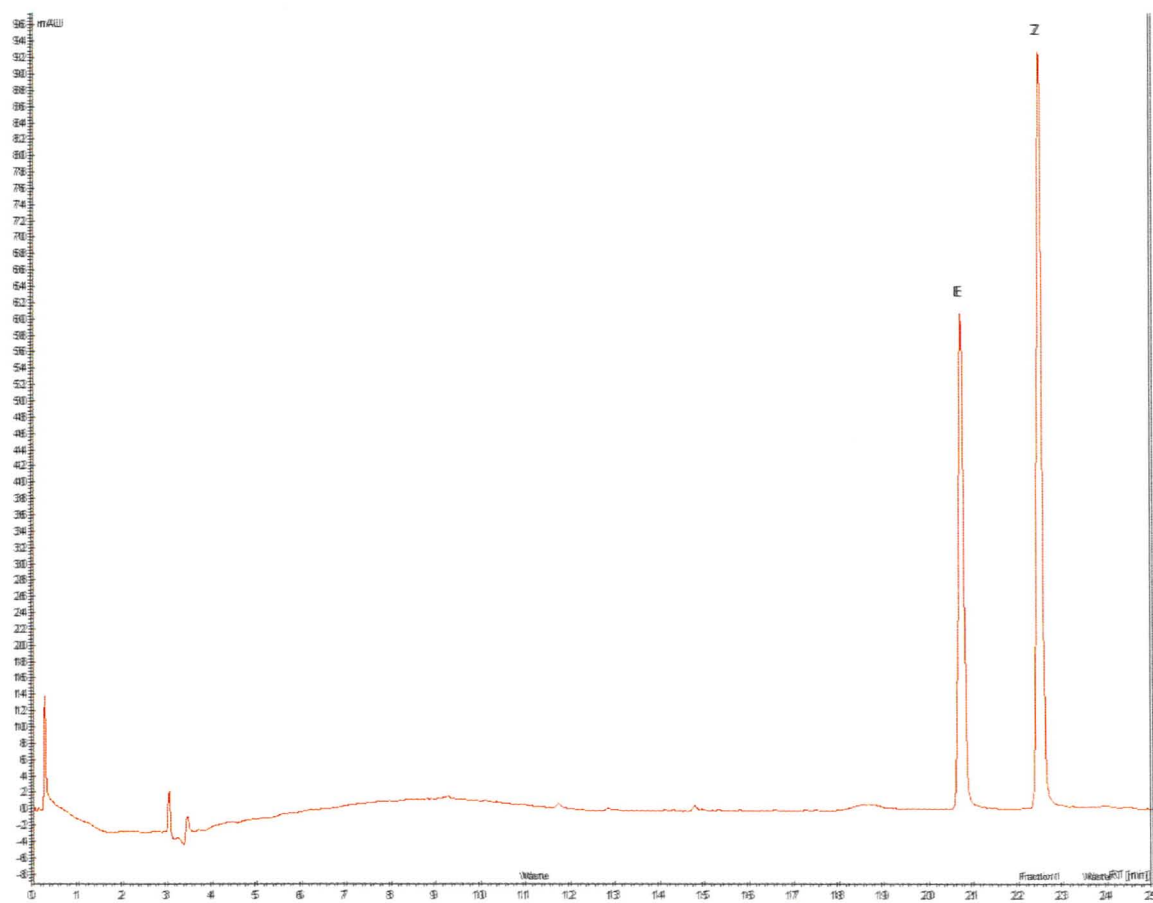


**Figure 2.8:** HPLC chromatogram of **2.7** following microwave heating at 180°C for 20 min in 95% ethanol (elution conditions: Solvent A = Water, Solvent B = Acetonitrile: Gradient elution 0-10 min, 80→20% A, 10-25 min, 20→0% A; column: Zorbax RX-C18 (4.6x250mm); flow rate:1 mL/min)

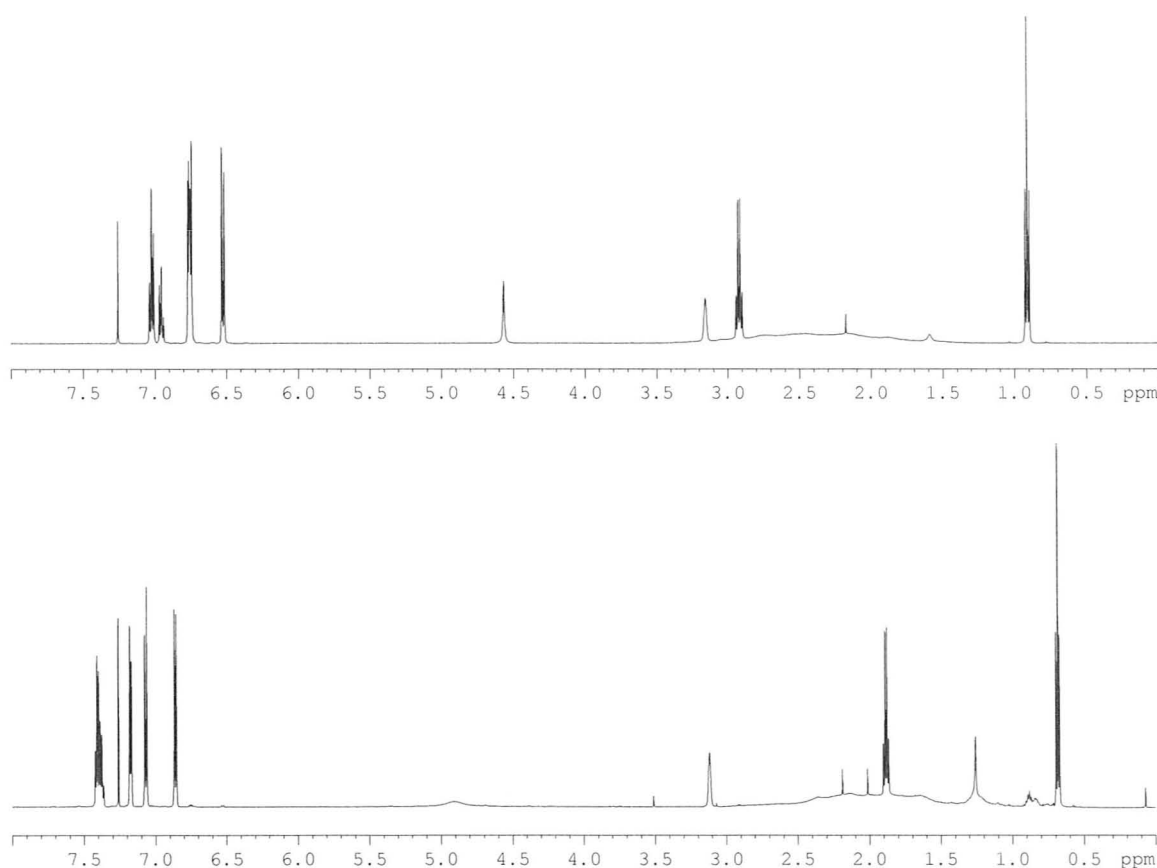


**Figure 2.9:** <sup>1</sup>H NMR spectra of **2.7** (top, 500 MHz, CDCl<sub>3</sub>) and **2.8** (bottom) (600 MHz, CDCl<sub>3</sub>)

## 2.4 Cell Inhibition Assay - Biological Evaluation

### 2.4.1 Introduction

Prior to screening, the purities of **2.7**, **2.8** and 1-(4-hydroxyphenyl)-1,2-dicarba-*c*-*closo*-dodecaborane (**2.9**) were determined by reversed phase HPLC and found to be 98, 97 and 99% respectively. Their ability to inhibit cell growth was evaluated using MCF-7 cells which are known to over-express the estrogen receptor (ER)<sup>22</sup> as well as the MDA MB 231 cells that are known to have low

endogenous ER expression.<sup>23</sup> Assays were done in comparison to **2.9**, a compound that has been previously been prepared by our group<sup>24</sup> and Endo *et al.*<sup>25</sup> that has shown the ability to bind the ER. Compounds were evaluated at five different concentrations (0.001, 0.01, 0.1, 1 and 10  $\mu\text{M}$ ) in the presence and absence of estradiol (E2) at four time points (1, 4, 7 and 10 days). Inhibition assays using MDA MB 231 cells showed no appreciable difference between the control wells and the wells containing compounds **2.7**, **2.8** and **2.9** which is expected given the cells low ER expression.

#### 2.4.2 Results and Discussion

In the MCF-7 cells, at the highest concentration, **2.7** without E2 present (**Figure 2.10A**), showed nearly identical results to Tamoxifen with an average percent inhibition of  $15.3 \pm 2.1\%$  and  $16.6 \pm 5.1\%$ , respectively. At  $0.001\mu\text{M}$  Tamoxifen performed approximately 20% better than **2.7**, showing an average of  $51.0 \pm 3.0\%$  viable cells compared to  $60.8 \pm 0.3\%$  for **2.7** (**Figure 2.10B**). In the presence of  $1\mu\text{M}$  E2 (**Figure 2.10C**) the impact of Tamoxifen changed significantly over time with percent of control ranging from  $69.7 \pm 6.7\%$  on day one to  $14.4 \pm 1.3\%$  on day ten, which differs considerably from that for **2.7** ( $20.0 \pm 8.8\%$  to  $18.4 \pm 1.7\%$ ) under the same conditions. This result indicates that the onset of inhibitory action of **2.7** is faster than Tamoxifen, which could in the future be potentially advantageous. From **Figure 2.10C** it is evident that Tamoxifen

starts to inhibit proliferation slightly better than **2.7** ( $14.4 \pm 1.3$  vs.  $18.40 \pm 1.7$ ) between days seven to ten. The plot also illustrates that **2.8** exhibits inhibitory action similar to Tamoxifen, in that is most effective at the later time points, although its ability to inhibit cell growth better than **2.7** occurs after day four. The E Tamoxifen analogue (**2.8**) also exhibits superior inhibition to Tamoxifen on days four, seven and ten, showing an inhibition of  $23.6 \pm 7.5\%$ ,  $13.4 \pm 2.1\%$  and  $8.6 \pm 6.4\%$  in comparison to  $35.2 \pm 3.5\%$ ,  $23.3 \pm 2.3\%$  and  $14.4 \pm 1.3\%$ . At  $1\mu\text{M}$  in the presence of E2 **2.8** is able to inhibit proliferation better than **Tamoxifen**, **2.7** and **2.9**, however as the concentration of each drug was decreased with the level of E2 remaining constant, proliferation increased, which was expected as E2 stimulates cell growth in MCF7 cells. At the lowest concentration in the presence of E2 (**Figure 2.10D**) **2.9** showed the fewest number of viable cells ( $45.48 \pm 1.8\%$ ).



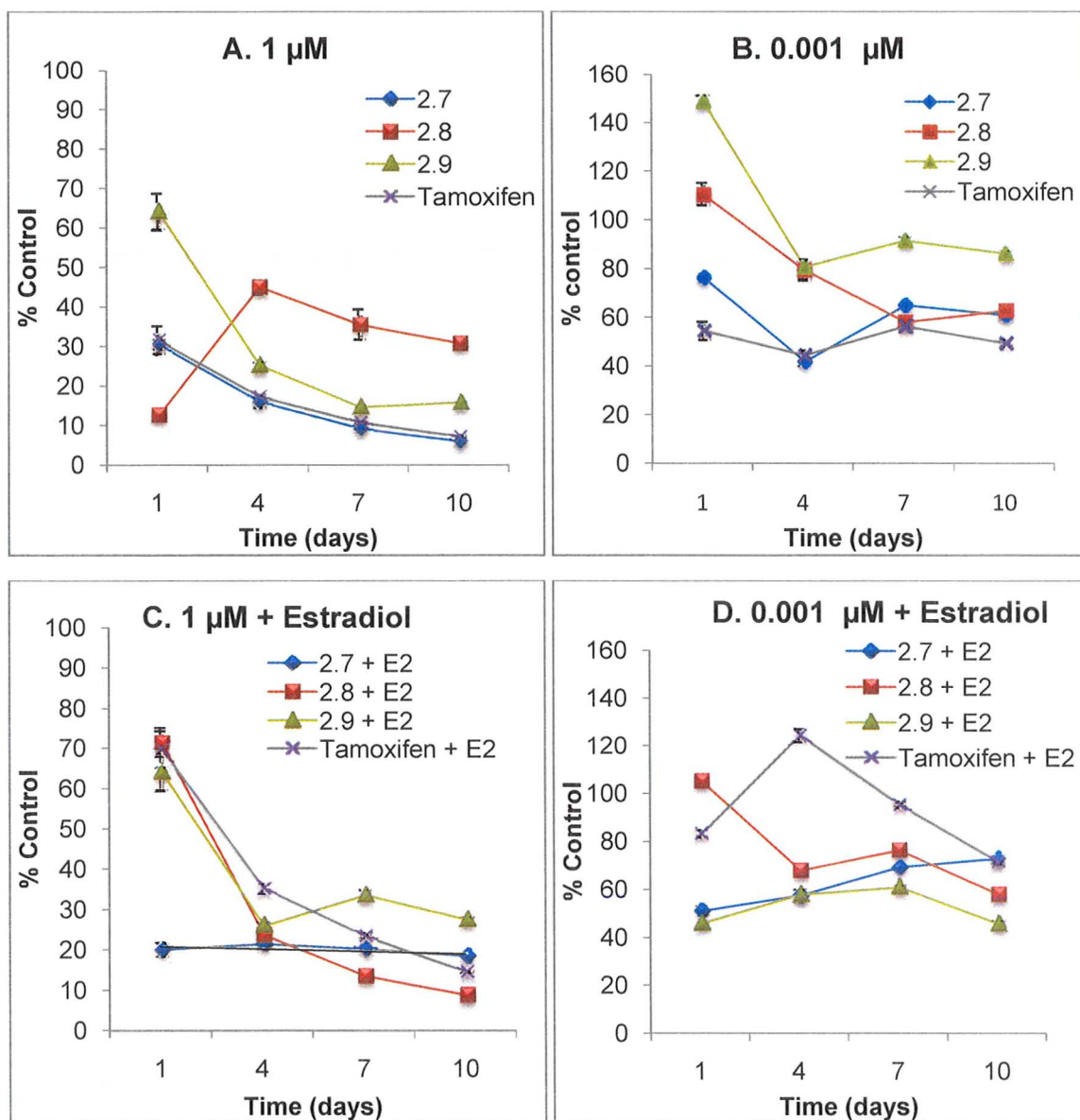


**Figure 2.10:** The results of cell inhibition assays reported a percentage of control for compounds **2.7**, **2.8**, **2.9** and Tamoxifen at days 1, 4, 7 and 10: **A:** 1  $\mu\text{M}$ , **B:** 0.001  $\mu\text{M}$ , **C:** 1  $\mu\text{M}$  with E2, **D:** 0.001  $\mu\text{M}$  with E2.

## 2.5 Conclusion

The stereoselective synthesis of a *closo* carborane Tamoxifen analogue was achieved in reasonable overall yield. It was demonstrated that the *closo* (Z-) carborane Tamoxifen analogue has greater stability towards degradation than Tamoxifen itself. It was also determined that isomerization could be carried out using microwave heating to obtain a mixture of the E and Z *closo* carborane isomers which could be separated in sufficient quantity for characterizing and screening. The results of the inhibition assay indicate that the Z carborane Tamoxifen analogue (**14**) shows similar inhibition to Tamoxifen in an E2 free environment, while in the presence of E2 the E carborane Tamoxifen analogue (**15**) showed the lowest number of viable cells remaining after four days. These results illustrate the potential of the carborane analogues of Tamoxifen as a new class of inorganic SERMs.

## 2.6 Experimental Section

### 2.6.1 General

All reactions were carried out under argon that had been passed through drierite, using commercial grade solvents dried using a Pure Solv MD-6 solvent purification system (Innovative Technology Inc.). Chemicals were purchased from Sigma-Aldrich or SGF chemicals and used without further purification.

Decaborane was purchased from Katchem. Reactions requiring microwave heating were performed using a Biotage Initiator 60 instrument. Compound **7** was prepared following literature procedure.<sup>26</sup>  $^1\text{H}$ ,  $^{13}\text{C}$  and  $^{11}\text{B}$  NMR spectra were recorded on a Bruker AV600, Bruker DRX500, or Bruker AV200 spectrometers with probe temperatures of 30, 25 and 25°C, respectively.  $^1\text{H}$  NMR chemical shifts are reported in ppm relative to the residual proton signal of the NMR solvent. Coupling constants ( $J$ ) are reported in Hertz (Hz).  $^{13}\text{C}$  chemical shifts are reported in ppm relative to the carbon signal of the solvent while  $^{11}\text{B}$  chemical shifts are reported in ppm relative to an external standard of  $\text{BF}_3\cdot\text{Et}_2\text{O}$ . Thin layer chromatography plates (Merck F254 silica gel on aluminum plates) were visualized using 0.1%  $\text{PdCl}_2$  in 3 M  $\text{HCl}(\text{aq})$  and/or UV light. Infrared spectra were acquired using a BioRad FTS-40 FT-IR or Nicolet 510 FTIR spectrometer. High resolution mass spectra were obtained on a Waters/micromass Q-ToF Ultima Global spectrometer. Low resolution LCMS were obtained on a Waters 2695 LC with a Quattro Ultima triple quadrupole mass spectrometer. Analytical and semi preparative HPLC were performed using a Varian Pro Star model 330 PDA detector, model 410 auto sampler, model 230 solvent delivery system and model 710 fraction collector. Analysis was conducted using Agilent Zorbax SB-C18 (2a. 4.6x250mm and 2b. 9.8x250mm) columns. Analytical HPLC experiments were monitored at 254nm using a flow rate of  $1.0\text{mLmin}^{-1}$  at 30°C. Semi preparative HPLC experiments were monitored at 254nm using a flow rate of  $4.0\text{mLmin}^{-1}$  at room temperature. The elution protocol used was as follows:

HPLC **Method A**: Solvent A = Water, Solvent B = Acetonitrile: Gradient elution 0-10 min, 80→20% A, 10-25 min, 20→0% A.

### 2.6.2 Crystallographic Details

X-ray crystallographic data for **2.6** was collected from a single crystal frozen in paratone oil. Data was collected at 173 K on a Bruker Smart<sup>27</sup> Apex2 Mo diffractometer using an Apex2 detector (512x512 mode) at 5cm from the sample, 3-circle D8 goniometer, 50kV/30mA fine focused sealed tube with graphite monochromator and 0.50 mm pinhole collimator. Data was collected with omega and phi scans. Data for **2.7** was collected on a 3-circle D8 Bruker diffractometer equipped with a Bruker SMART 6000 CCD area detector and a rotating anode utilizing cross-coupled parallel focusing mirrors to provide monochromated Cu K $\alpha$  radiation ( $\lambda = 1.54178 \text{ \AA}$ ). Data processing for both compounds was carried out by use of the program SAINT,<sup>28</sup> while the program SADABS<sup>29</sup> was utilized for the scaling of diffraction data, the application of a decay correction and an empirical absorption correction based on redundant reflections. The structures were solved by using the direct-methods procedure in the Bruker SHELXTL program library<sup>30</sup> and refined by full-matrix least-squares methods on  $F^2$ . All non-hydrogen atoms were refined using anisotropic thermal parameters and hydrogen atoms were located using the difference map and refined using isotropic thermal parameters.

### 2.6.3 Experimental

#### **(Z/E)-(3-(4-Methoxyphenyl)-4-phenylhex-3-en-1-ynyl)trimethylsilane (2.2/2.3)**

Trimethylsilyl acetylene (35 mL, 250 mmol) was added to dry THF (750 mL) that had been cooled to  $-78^{\circ}\text{C}$ . To this, *n*-BuLi (100 mL, 250 mmol) was added dropwise to form a clear colourless solution. Compound **2.0**, (63.5 g, 250 mmol) dissolved in dry THF (500 mL) was added over 30 minutes whereupon the reaction turned bright pink. The reaction mixture was allowed to warm to room temperature over 12 hours. To the pale yellow solution chilled to  $0^{\circ}\text{C}$ , saturated ammonium chloride solution (400 mL) was added followed by water (800 mL). The mixture was separated into two fractions and each was extracted with diethyl ether (3×500 mL) which was pooled and dried over anhydrous sodium sulfate and evaporated giving yellow oil. The oil (**2.1**) was dissolved in 40 mL of anhydrous pyridine and THF (500 mL), the solution cooled to  $-78^{\circ}\text{C}$ , and thionyl chloride (16 mL, 185 mmol) added dropwise over 30 minutes. The reaction mixture was allowed to warm to room temperature over a 12 hour period. Water (200 mL) was added to the pale yellow solution, followed by 2M HCl (100 mL). The organic and aqueous layers were separated and the organic fraction washed with 2M HCl (2×600 mL). The aqueous fractions were washed with diethyl ether (3×500 mL) and all organic fractions combined, dried over anhydrous sodium sulfate and evaporated to give brown oil (75g, 89%). TLC (7.5:1 hexanes : ethyl acetate)  $R_f = 0.78$ ;  $^1\text{H NMR}$  (200 MHz,  $\text{CDCl}_3$ ):  $\delta$  7.13 (m, 2H, aryl), 7.06 (m, 3H,

aryl), 6.64 (d, 4H, aryl), 3.73 (s, 3H, OCH<sub>3</sub>), 2.89 (q, J=7.5Hz, 2H, CH<sub>3</sub>), 1.05 (t, J=7.5Hz, 3H, CH<sub>2</sub>), 0.25 (s, 9H, -Si-(CH<sub>3</sub>)<sub>3</sub>); <sup>13</sup>C NMR (50 MHz, CDCl<sub>3</sub>): δ 158.1, 151.8, 140.8, 131.0, 129.0, 128.0, 126.8, 119.4, 113.0, 105.9, 98.3, 55.1, 31.4, 12.3, 0.1; m/z calculated for [M+H]<sup>+</sup> C<sub>22</sub>H<sub>27</sub>OSi: 335.1831, HRMS EI<sup>+</sup> [M+H]<sup>+</sup> 335.1847; FTIR (NaCl, cm<sup>-1</sup>) ν: 1608, 2138, 2962.

### **(Z/E)-1-Methoxy-4-(4-phenylhex-3-en-1-yn-3-yl)benzene (2.4/2.5)**

Compounds **2.2** and **2.3** (75 g, 225 mmol) were dissolved in a solution of sodium methoxide (16 g, 306 mmol) in methanol (1 L). The reaction was stirred for 24 hours at room temperature. Water (500 mL) was added, and the mixture extracted with dichloromethane (3×600 mL), which in turn was extracted with water (3×600 mL). The organic layer was evaporated to give yellow oil. Yield (53g, 81%). TLC (7.5:1 hexanes : ethyl acetate): R<sub>f</sub> = 0.46; <sup>1</sup>H NMR (600 MHz, CDCl<sub>3</sub>): (major isomer, **11**) δ 7.18 (m, 4H, aryl), 7.07 (m, 3H, aryl), 6.66 (d, 2H, aryl) 3.73 (s, 3H, OCH<sub>3</sub>), 3.32 (s, 1H, CH), 2.93 (q, J=7.5Hz, 2H, CH<sub>2</sub>), 1.05 (t, J=7.5Hz, 3H, CH<sub>3</sub>); (minor isomer, **12**) δ 7.49 (d, 3H, aryl), 7.38 (m, 2H, aryl), 6.96 (d, 4H, aryl) 3.85 (s, 3H, OCH<sub>3</sub>), 2.29 (s, 1H, CH), 2.52 (q, J=7.5Hz, 2H, CH<sub>2</sub>), 0.90 (t, J=7.5Hz, 3H, CH<sub>3</sub>); <sup>13</sup>C NMR (150 MHz, CDCl<sub>3</sub>): (major isomer **11**) δ 158.1, 152.2, 140.5, 130.4, 128.6, 127.6, 126.4, 118.3, 112.6, 84.3, 80.8, 54.6, 30.8, 12.0; m/z calculated for [M+H]<sup>+</sup> C<sub>19</sub>H<sub>19</sub>O: 263.1436, HRMS [M+H]<sup>+</sup> EI<sup>+</sup> 263.1430; FTIR (NaCl, cm<sup>-1</sup>): ν: 1608, 2088, 2969, 3288.

**Z-1-(1,2-Dicarba-closo-dodecaborane-1-yl)-1-(4-methoxyphenyl)-2-phenyl-but-1-ene (2.6)**

1-Butyl-3-methylimidazolium chloride (2.8 g, 89 mmol) and decaborane (12 g, 99 mmol) were dissolved in dry toluene (500 mL) forming a biphasic solution. A solution containing the mixture of **2.4** and **2.5** (22 g, 84 mmol) dissolved in dry toluene was added dropwise and the resulting solution heated to reflux for 12 hours. The mixture was filtered and subsequently evaporated to yield a dark solid which was purified by silica gel column chromatography (100% hexanes  $\rightarrow$  7.5:1 hexane: ethyl acetate) to yield a pale yellow liquid, which upon cooling yielded a white solid. The white solid was recrystallized from low boiling petroleum ether to yield white crystals (8.0g, 25%); mp: 120-121°C ; TLC (7.5:1 hexanes : ethyl acetate):  $R_f$  = 0.55;  $^1\text{H}$  NMR (600 MHz,  $\text{CDCl}_3$ ):  $\delta$  6.99 (m, 2H, aryl), 6.78 (m, 3H, aryl), 6.59 (d, 4H, aryl), 3.67 (s, 3H,  $\text{OCH}_3$ ), 3.15 (s, 1H,  $\text{C}_{\text{carborane-H}}$ ), 2.93 (q,  $J=7.0\text{Hz}$ , 2H,  $\text{CH}_2$ ), 0.91 (t,  $J=7.0\text{Hz}$ , 3H,  $\text{CH}_3$ );  $^{11}\text{B}\{^1\text{H}\}$  (160 MHz,  $\text{CDCl}_3$ ):  $\delta$  -3.7, -8.9, -10.0, -12.3, -14.2;  $^{13}\text{C}$  NMR (150 MHz,  $\text{CDCl}_3$ ):  $\delta$  158.6, 151.1, 142.6, 131.8, 131.4, 129.4, 129.3, 128.5, 127.5, 126.1, 113.7, 63.2, 55.2, 27.7, 12.8; m/z calculated for  $\text{C}_{19}\text{H}_{28}\text{B}_{10}\text{O}$ :  $[\text{M}+\text{formate}]^-$  and  $[\text{M}+\text{acetate}]^-$  425.3129 and 439.3286, HRMS TOF  $\text{EI}^-$   $[\text{M}+\text{formate}]^-$  and  $[\text{M}+\text{acetate}]^-$  425.3120 and 439.3281; FTIR (NaCl,  $\text{cm}^{-1}$ ):  $\nu$ : 1605, 2605, 3071.

**Z-1-(1,2-Dicarba-closo-dodecaborane-1-yl)-1-(4-phenol)-2-phenyl-but-1-ene (2.7)**

Compound **2.6** (1.0g, 2.6 mmol) was dissolved in dry dichloromethane and cooled to  $-78^\circ\text{C}$ .  $\text{BBr}_3$  (4.0 mL, 4.0 mmol) was added over 5 minutes and the

reaction was allowed to warm to room temperature over 12 hours and stirred for an additional 36 hours. The reaction was evaporated to dryness and the residue redissolved in methanol and evaporated. The brown solid was recrystallized from low boiling petroleum ether yielding **2.7** as a colourless solid (0.5g, 57%); mp: 179-181°C ; TLC (7.5:1 hexanes : ethyl acetate):  $R_f = 0.27$ ;  $^1\text{H NMR}$  (500 MHz,  $\text{CDCl}_3$ ):  $\delta$  7.02 (m, 2H, aryl), 6.77 (m, 2H, aryl), 6.66 (m, 3H, aryl), 6.43 (m, 2H, aryl), 4.47 (s, 1H, OH), 3.06 (s, 1H,  $\text{C}_{\text{carborane-H}}$ ), 2.80 (q,  $J=7.5\text{Hz}$ , 2H,  $\text{CH}_2$ ), 0.81 (t,  $J=7.5\text{Hz}$ , 3H,  $\text{CH}_3$ ).  $^{13}\text{C NMR}$  (125 MHz,  $\text{CDCl}_3$ )  $\delta$  154.5, 151.2, 142.5, 131.9, 131.6, 128.3, 127.4, 126.0, 115.1, 63.0, 27.5, 12.6;  $^{11}\text{B}\{^1\text{H}\}$  (160 MHz,  $\text{C}_3\text{D}_6\text{O}$ ):  $\delta$  -3.1, -8.4, -9.2, -11.1, -13.2;  $m/z$  calculated for  $[\text{M-H}]^- \text{C}_{18}\text{H}_{25}\text{B}_{10}\text{O}^-$ : 365.2918, HRMS TOF  $\text{EI}^- [\text{M-H}]^-$  365.2910; FTIR (NaCl,  $\text{cm}^{-1}$ ):  $\nu$ : 1603, 2518, 2974, 3566.

### **E-1-(1,2-Dicarba-closo-dodecaborane-1-yl)-1-(4-phenol)-2-phenyl-but-1-ene (2.8)**

Compound **2.7** (1.0g, 2.6 mmol) was dissolved in dry dichloromethane and cooled to  $-78^\circ\text{C}$ .  $\text{BBr}_3$  (4.0 mL, 4.0 mmol) was added over 5 minutes and the reaction was allowed to warm to room temperature over 12 hours and stirred for an additional 36 hours. The reaction was evaporated to dryness and the residue redissolved in methanol and evaporated. The brown solid was recrystallized from low boiling petroleum ether yielding **2.8** as a colourless solid (0.5g, 57%); mp: 179-181°C ; TLC (7.5:1 hexanes : ethyl acetate):  $R_f = 0.27$ ;  $^1\text{H NMR}$  (500 MHz,  $\text{CDCl}_3$ ):  $\delta$  7.02 (m, 2H, aryl), 6.77 (m, 2H, aryl), 6.66 (m, 3H, aryl), 6.43 (m, 2H,



aryl), 4.47 (s, 1H, OH), 3.06 (s, 1H, C<sub>carborane</sub>-H), 2.80 (q, J=7.5Hz, 2H, CH<sub>2</sub>), 0.81 (t, J=7.5Hz, 3H, CH<sub>3</sub>). <sup>13</sup>C NMR (125 MHz, CDCl<sub>3</sub>) δ 154.5, 151.2, 142.5, 131.9, 131.6, 128.3, 127.4, 126.0, 115.1, 63.0, 27.5, 12.6; <sup>11</sup>B{<sup>1</sup>H} (160 MHz, C<sub>3</sub>D<sub>6</sub>O): δ -3.1, -8.4, -9.2, -11.1, -13.2; m/z calculated for [M-H]<sup>-</sup> C<sub>18</sub>H<sub>25</sub>B<sub>10</sub>O<sup>-</sup>: 365.2918, HRMS TOF EI<sup>-</sup> [M-H]<sup>-</sup> 365.2910; FTIR (NaCl, cm<sup>-1</sup>): ν: 1603, 2518, 2974, 3566.

#### 2.6.4 Cell Lines and Tissue Culture

MCF-7 and MDA MB 231 human breast adenocarcinoma cells lines were obtained from ATCC (Manassas, VA). Both cell lines were cultured in DMEM without Phenol red (CA12001-630; VWR International, Mississauga ON) supplemented with 10% charcoal-stripped fetal bovine serum (CA95039-622; VWR International), 1% L-Glutamine (25030-081; Invitrogen, Mississauga ON) and 1% antibiotic/antimycotic (AB/AM) (15240-062; Invitrogen). All cells were maintained at 37°C in 5% CO<sub>2</sub>.

#### 2.6.5 Growth Inhibition Study

MCF-7, and MDA-MB-231 cell lines were used to assess whether **2.7**, **2.8** and **2.9** were effective inhibitors of cell proliferation in ER positive and ER negative expressing cells. Both cell lines were plated (5.0 x 10<sup>4</sup> cells) in each well of 6-well plates (9.51cm<sup>2</sup> growth surface) in 2 mL medium 24 hours prior to the start of the experiment to allow for cell adhesion to growth surface and repopulation of cell surface receptors. Each cell line had 46 treatment groups (3

replicate wells per group) which included: control (no treatment), 0.001, 0.01, 0.1, 1 and 10  $\mu\text{M}$  of estradiol, Tamoxifen, **2.7**, **2.8** or **2.9** alone, or in conjunction with 10 nM estradiol (excluding the estradiol group). At the start of the experiment (Day 0), the media was removed from each culture and replaced with 2 mL supplemented media containing the appropriate concentration of the experimental compound. The compound levels were maintained by replacing the culture media with fresh compound containing media every 3 days.

Triplicate wells of each treatment group were harvested on Day 1, 4, 7 and 10 to determine total cell number/well. Media was removed from each well and discarded, the cells were gently rinsed with 1 mL phosphate buffered solution (PBS). Cells were released from the growth surface by the addition of 500  $\mu\text{l}$  0.05% trypsin/EDTA to each well, followed by the addition of 1ml media to inactivate the trypsin. The growth surface was flushed three times to ensure the removal of all cells. An aliquot (50  $\mu\text{L}$ ) of the resulting cell suspension was placed in a microcentrifuge tube for counting. An equivalent volume of the viability dye Trypan Blue was added to the cell suspension and mixed well and 10  $\mu\text{l}$  of the resulting solution was pipetted onto a hemocytometer. The cells within 4 grids were counted and averaged to obtain a count of the total cells in each well. A Leitz Dialux light microscope was used for the analysis.

## 2.7 References

1. Fisher, B.; Costantino, J. P.; Wickerham, D. L.; Redmond, C. K.; Kavanah, M.; Cronin, W. M.; Vogel, V.; Robidoux, A.; Dimitrov, N.; Atkins, J.; Daly, M.; Wieand, S.; Tan-Chiu, E.; Ford, L.; Wolmark, N., Tamoxifen for Prevention of Breast Cancer: Report of the National Surgical Adjuvant Breast and Bowel Project P-1 Study. *Journal of the National Cancer Institute* **1998**, 90, 1371-1388.
2. Gelber, R. D.; Cole, B. F.; Goldhirsch, A.; Rose, C.; Fisher, B.; Osborne, C. K.; Boccardo, F.; Gray, R.; Gordon, N. H.; Bengtsson, N.; Sevela, P., Adjuvant chemotherapy plus tamoxifen compared with tamoxifen alone for postmenopausal breast cancer: meta-analysis of quality adjusted survival. *Lancet* **1996**, 347, 1066-1071.
3. Bland, A. E.; Calingaert, B.; Secord, A. A.; Lee, P. S.; Valea, F. A.; Berchuck, A.; Soper, J. T.; Havrilesky, L., Relationship between tamoxifen use and high risk endometrial cancer histologic types. *Gynecological Oncology* **2009**, 112, 150-154.
4. Yuvaraj, S.; Premkumar, V. G.; Shanthi, P.; Vijayasathy, K.; Gangadaran, S. G. D.; Sachdanandam, P., Effect of Coenzyme Q10, Riboflavin and Niacin on Tamoxifen treated postmenopausal breast cancer women with special reference to blood chemistry profiles. *Breast Cancer Research and Treatment* **2009**, 114, 377-384.

4. Hoogendoorn, W. E.; Hollema, H.; Boven, H. H. v.; Bergman, E.; Leeuw-Mantel, G. d.; Platteel, I.; Fles, R.; Nederlof, P. M.; Mourits, M. J. E.; Leeuwen, F. E. v.; Prognosis of uterine corpus cancer after tamoxifen treatment for breast cancer. *Breast Cancer Research and Treatment* **2008**, 112, 99-108.
6. Dobryднева, Y.; Weatherman, R. V.; Trebley, J. P.; Morrell, M. M.; Fitzgerald, M. C.; Fichandler, C. E.; Chatterjee, N.; Blackmore, P. F., Tamoxifen Stimulates Calcium Entry Into Human Platelets. *Journal of Cardiovascular Pharmaceuticals* **2007**, 50, 380-390.
7. Valliant, J. F.; Schaffer, P.; Stephenson, K. A.; Britten, J. F., Synthesis of Boroxifen, A Nido-Carborane Analogue of Tamoxifen. *Journal of Organic Chemistry* **2002**, 67, 383-387.
8. Endo, Y.; Iijima, T.; Yamakoshi, Y.; Fukasawa, H.; Miyaura, C.; Inada, M.; Kubo, A.; Itai, A., Potent estrogen agonists based on carborane as a hydrophobic skeletal structure A new medicinal application of boron clusters. *Chemistry and Biology* **2001**, 8, 341-355.
9. Endo, Y.; Iijima, T.; Yamakoshi, Y.; Kubo, A.; Itai, A., Structure-Activity Study of Estrogenic Agonists Bearing Dicarba-Closo-Dodecaborane. Effect of Geometry and Separation Distance of Hydroxyl Groups at the Ends of Molecules. *Bioorganic & Medicinal Chemistry Letters*. **1999**, 9, 3313-3318.

10. Endo, Y.; Iijima, T.; Yamakoshi, Y.; Yamaguchi, M.; Fukasawa, H.; Shudo, K., Potent Estrogenic Agonists Bearing Dicarba-*closo*-dodecaborane as a Hydrophobic Pharmacophore. *Journal of Medicinal Chemistry* **1999**, *42*, 1501-1504.
11. Endo, Y.; Iijima, Y.; Yamakoshi, Y.; Fukasawa, H.; Miyaura, C.; Inada, M.; Kubo, A.; Itai, A., Potent estrogen agonists based on carborane as a hydrophobic skeletal structure A new medicinal application of boron clusters. *Chemical Biology* **2001**, *8*, 341-355.
12. Endo, Y.; Yamamoto, K.; Kagechika, H., Utility of boron clusters for drug design. Relation between estrogen receptor binding affinity and hydrophobicity of phenols bearing various types of carboranyl groups. *Bioorganic & Medicinal Chemistry Letters* **2003**, *13*, (4089-4092).
13. Endo, Y.; Yoshimi, T.; Miyaura, C., Boron clusters for medicinal drug design: Selective estrogen receptor modulators bearing carborane. *Pure and Applied Chemistry* **2003**, *75*, (9), 1197-1205.
14. Causey, P. W.; Besanger, T. R.; Valliant, J. F., Synthesis and Screening of Mono- and Di-Aryl Technetium and Rhenium Metallocarboranes. A New Class of Probes for the Estrogen Receptor. *Journal of Medicinal Chemistry*. **2008**, *51*, 2833-2844.
15. Smyth, T. P.; Corby, B. W., *Journal of Organic Chemistry* **1998**, *63*, 8946-8951.

16. Harper, M. J. K.; Walpole, A. L., Contrasting Endocrine Activities of cis and trans Isomers in a Series of Substituted Triphenylethylenes. *Nature* **1966**, 212, (5057), 87-87.
17. Ahn, N., Topics in Current Chemistry. **1980**, 88, 145.
18. Clayden, J.; Greeves, N.; Warren, S.; Wothers, P., *Organic Chemistry*. Oxford: New York, 2001.
19. Kursari, U.; Li, Y.; Bradley, M. G.; Sneddon, L. G., Polyborane Reactions in Ionic Liquids: New Efficient Routes to Functionalized Decaborane and o-Carborane Clusters. *Journal of the American Chemical Society* **2004**, 126, 8662-8663.
20. Hegstrom, R. A.; Newton, M. D.; Potenza, J. A.; Lipscomb, W. N., Chemical Shifts of Boron-11 in Icosahedral Carboranes. *Journal of the American Chemical Society* **1966**, 88, 5340-5342.
21. Weeks, C. M.; Griffin, J. F.; Duax, W. L., *American Crystallography Association, Ser. 2* **1977**, 5, 69.
22. Dickson, R. B.; Bates, S. E.; McManaway, M. E.; Lippman, M. E., Characterization of Estrogen Responsive Transforming Activity in Human Breast Cancer Cell Lines. *Cancer Research* **1986**, 46, 1707-1713.
23. Rochefort, H.; Glondu, M.; Sahla, M. E.; Platet, N.; Garcia, M., How to target estrogen receptor-negative breast cancer? *Endocrine-Related Cancer* **2003**, 10, 261-266.

24. Causey, P. W.; Besanger, T. R.; Valliant, J. F., Synthesis and Screening of Mono- and Di-Aryl Technetium and Rhenium Metallocarboranes. A New Class of Probes for the Estrogen Receptor. *Journal of Medicinal Chemistry* **2008**, 51, 2833-2844.
25. Endo, Y.; Yamamoto, K.; Kagechika, H., Utility of boron clusters for drug design. Relation between estrogen receptor binding affinity and hydrophobicity of phenols bearing various types of carboranyl groups. *Bioorganic Medicinal Chemistry Letters* **2003**, 13, (4089-4092).
26. Smyth, T. P.; Corby, B. W., Toward a Clean Alternative to Friedel-Crafts Acylation: In Situ Formation, Observation, and Reaction of an Acyl Bis(trifluoroacetyl)phosphate and Related Structures. *Journal of Organic Chemistry* **1998**, 63, 8946-8951.
27. *SMART: Area-Detector Software*, Siemens Industrial Automation, Inc: Madison, WI, 1993.
28. *SAINT: Area-Detector Integration*, Siemens Industrial Automation, Inc: Madison, WI, 1995.
29. *SADABS: Area-Detector Absorption*, Siemens Industrial Automation, Inc: Madison, WI, 1996.
30. Sheldrick, G. M. *SHELXTL [Includes SHELXS97, SHELXL97, CIFTAB ] Programs for Crystal Structure Analysis*, Institut für Anorganische Chemie der Universität: Tammanstrasse 4, D-3400 Göttingen, Germany, 1998.

### 3.0 Radiolabelling and Evaluation of a Carborane Analogue of Tamoxifen for Imaging Estrogen Receptor Expression

#### 3.1 *Introduction*

The effectiveness of a particular cancer treatment depends largely on the specific biology of the tumours present in a patient. Endocrine therapy, for example, is effective at treating only 6-10% of ER- breast cancers, while ER+ cancers are found to have a positive response 50-60% of the time.<sup>1, 2</sup> The ability to image expression of the ER would be advantageous in determining primary and metastatic ER+ tumours, and assist in providing the most effective treatment. To date several ER imaging agents have been developed with varying levels of success; the majority of these have been based on either estradiol or Tamoxifen (**Figure 3.1**).<sup>3-8</sup>



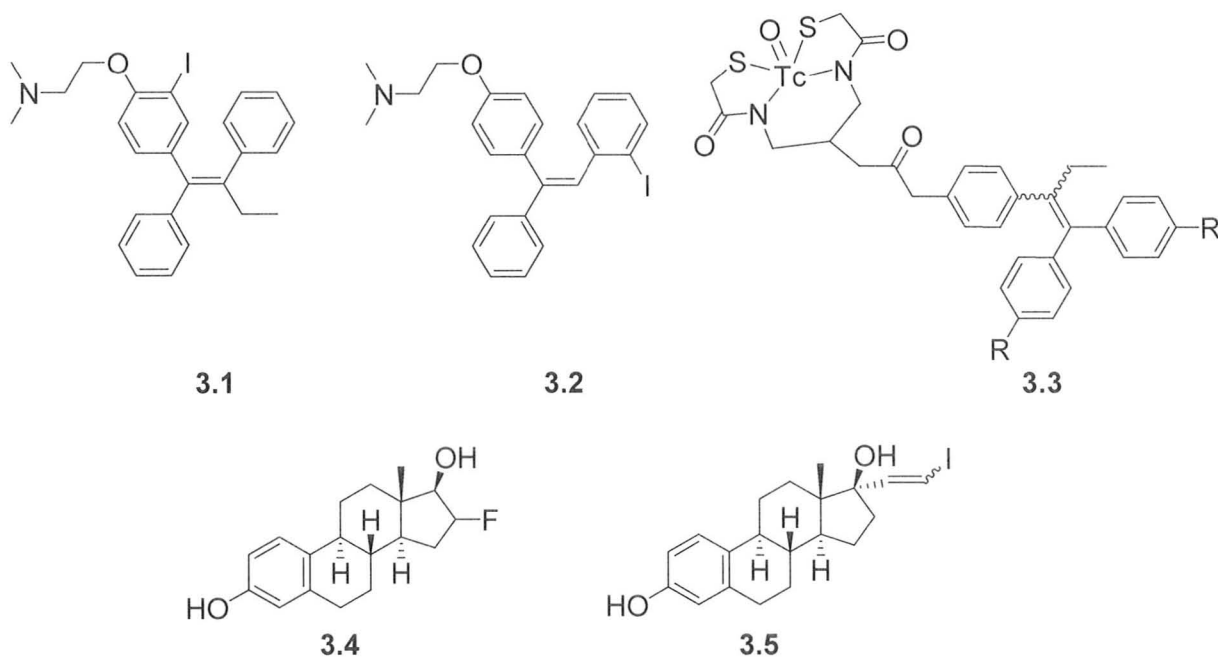


**Figure 3.1:** Estrogen receptor imaging agents: **3.1:** (Z)-2-(4-(1,2-diphenylbut-1-enyl)-2-iodophenoxy)-N,N-dimethylethanamine,<sup>8</sup> **3.2:** (Z)-2-(4-(2-(2-iodophenyl)-1-phenylvinyl)phenoxy)-N,N-dimethylethanamine,<sup>6</sup> **3.3:** 2-(4-(3,3-Bis(thioacetamidomethylene)propanamido)phenyl)-1-(4-(2-(N,N-dimethylamino)ethoxy)phenyl)-1-phenyl-1-(E/Z)-butene Oxotechnetium-99m,<sup>7</sup> **3.4:** FES<sup>3</sup> and **3.5:** Z-MIVE.<sup>9</sup>

Both FES and Z-MIVE are currently being investigated in humans. To date, high FES uptake has been shown to correlate well with the effective response of endocrine therapy; however, FES exhibits poor target to background ratios.<sup>10, 11</sup> Initial trials with Z-MIVE (24 participants) have shown potential for use in predicting antiestrogen effectiveness within weeks of the start of treatment; however, the compound is susceptible to de-iodination *in vivo*.<sup>12</sup>

To date there have been no reports of Tc analogues of Tamoxifen capable of both binding the estrogen receptor with high affinity or being easily synthesized in an aqueous environment, nor has there been an iodo-Tamoxifen analogue that does not suffer from de-iodination *in vivo*. Utilizing the carboranes unique properties, Tc-Tamoxifen and I-Tamoxifen analogues were successfully synthesized and evaluated.

### 3.2 Synthesis of E/Z-1-(1,2-dicarba-*nido*-undecaborane-1-yl)-1-(4-hydroxyphenyl)-2-phenyl-but-1-ene

With the *closo* Carborane Tamoxifen analogue (**2.7**) prepared, it was possible to create labeled analogues by converting the carborane cluster to the corresponding *nido* carborane. Conversion of a *closo* carborane to a *nido* carborane can be achieved by heating the cluster to reflux in the presence of aqueous sodium fluoride. The data in **Table 2.1** suggested that the *closo* to *nido* conversion using fluoride was feasible so long as the reaction was performed at a temperature lower than 120°C, in order to minimize E/Z isomerization. A more detailed temperature course study was completed with temperatures ranging between 60 and 185°C (microwave heating) in 56% 2-propanol and sodium fluoride (**Table 3.1**).

Table 3.1: E/Z Isomerization of 2.7 In 56% 2-propanol + NaF Using Microwave Heating			
Temperature (°C)	Time (min)	<i>Nido</i> formation	Isomerization
60	10	No	No
70	10	Yes	Yes
80	10	Yes	Yes
90	10	Yes	Yes
100	10	Yes	Yes
120	10	Yes	Yes
130	10	Yes	Yes
140	10	Yes	Yes
150	10	Yes	Yes
185	10	Yes	Yes

From **Table 3.1** it can be seen that all temperatures that were evaluated resulted in an isomerized product except for 60°C. Unfortunately at this temperature no *nido* carborane product formed; which was verified by <sup>1</sup>H NMR (**Figure 3.2**). Even at this low temperature, the <sup>1</sup>H NMR (**Figure 3.2**) of the reaction showed the formation of both the E and Z isomers **3.6** and **3.7** (**Scheme 3.1**). The isomerization of **2.7** can occur thermally and via deprotonation of the phenol as the data from **Table 3.1** suggests. To test this, **2.7** was dissolved in a solution of ethanol with hydroxide and heated to 60°C (conventional heating), which resulted in a 50:50 mixture of the E and Z isomers suggesting that formation of the phenolic anion reduces the barrier to isomerization.

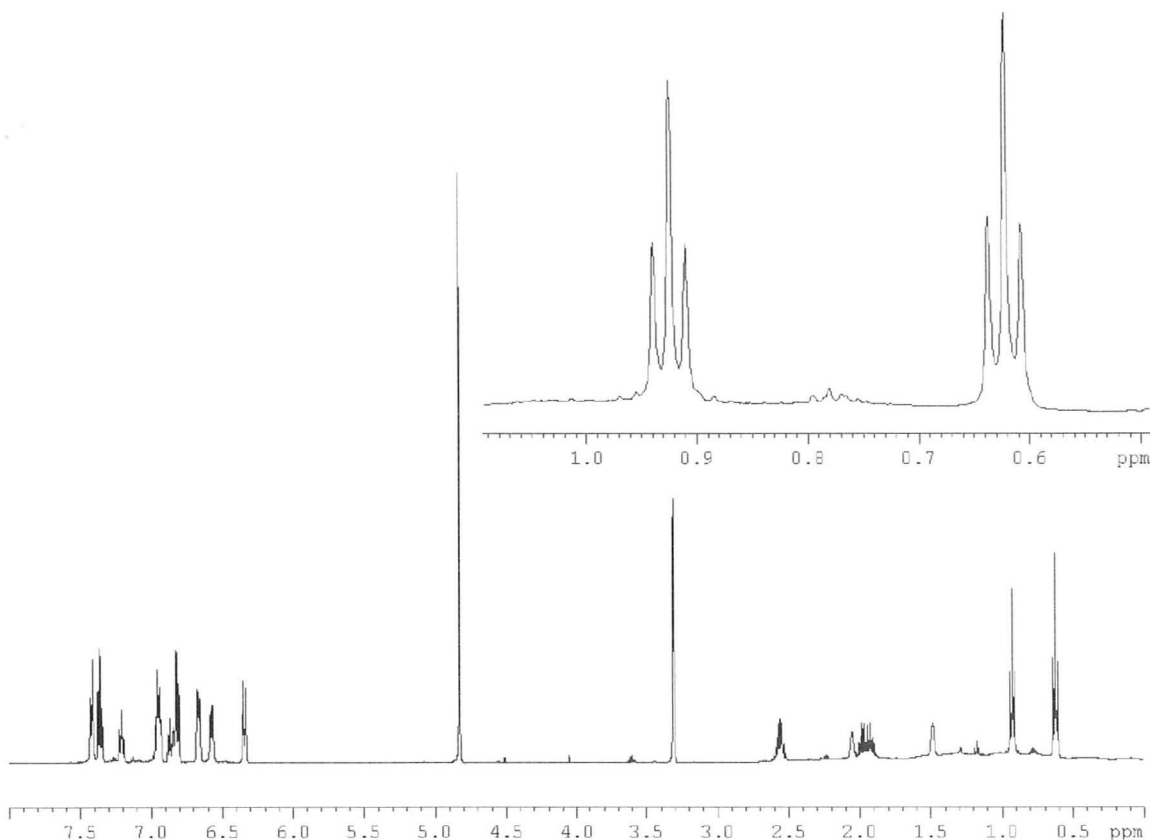
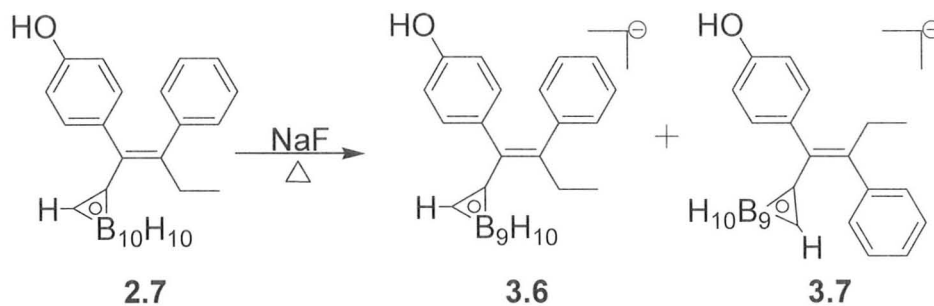
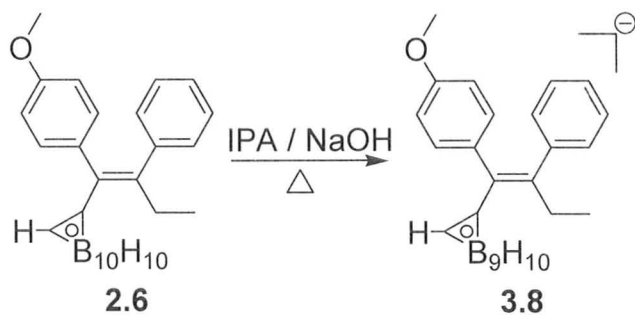


Figure 3.2:  $^1\text{H}$  NMR of **3.6** and **3.7** (500 MHz,  $\text{CH}_3\text{OD}$ )

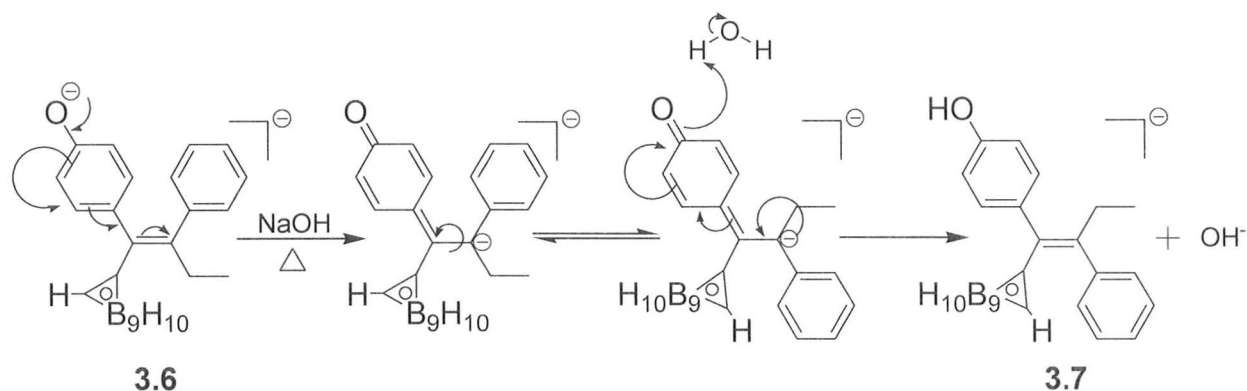


Scheme 3.1: Synthesis of **3.6** and **3.7**

To show that the isomerization was due to the phenolate anion, **2.6** was dissolved in aqueous ethanol with sodium hydroxide (4 days,  $70^\circ\text{C}$ ). The product was obtained as a single isomer (*Z*) as the *nido* carborane **3.8** (Scheme 3.2).



**Scheme 3.2:** Synthesis of **3.8**



**Scheme 3.3:** Proposed mechanism for the isomerization of **3.6** to **3.7**

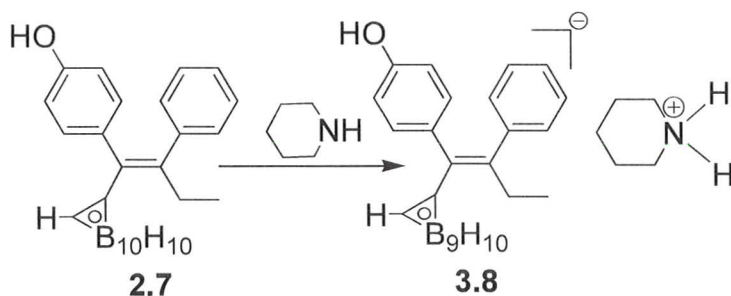
### 3.3 Synthesis of piperidinium Z-1-(1,2-dicarba-*nido*-undecaborane-1-yl)-1-(4-phenol)-2-phenyl-but-1-ene

While attempting alkylation reactions on the phenol group in anhydrous pyridine it was found that **2.7** did not isomerize even when heated. A temperature course study was performed (**Table 3.2**) where **2.7** was dissolved in anhydrous pyridine and heated with microwave radiation for 20 minutes. The relative yield of each isomer was determined using HPLC-ESMS. Even at elevated temperatures, little isomerization was observed. It is also interesting to note that no *nido* formation (to give **3.6**) was observed. These results clearly

indicate that the isomerization process is also solvent dependent, suggesting that formation of the *nido* carborane as a single isomer should be feasible.

Temperature (°C)	Time (min)	Z (%)	E (%)
80	20	100	0
100	20	100	0
120	20	100	0
140	20	100	0
160	20	100	0
180	20	99	1

Having shown that **2.7** can be heated to high temperatures in anhydrous pyridine without isomerizing, the next step was to select a more basic amine to promote formation of the *nido* species **3.8** as a single isomer. It was found that **2.7** dissolved in neat piperidine ( $pK_b = 2.8$ ) at room temperature for 10 minutes resulted in the quantitative formation of **3.8** (**Scheme 3.4**). In addition to the formation of a single isomer, the purification of the compound with a piperidinium cation was found to be far simpler since the organic cation product was not water soluble and thus could be purified via C18 solid phase extraction (SPE). Compound **3.8** was isolated in a 85% yield as an orange coloured semi-solid.



**Scheme 3.4:** Stereoselective Formation of **3.8** Using Piperidine

The MS data of the isolated product was consistent with the expected mass while the  $^1\text{H}$  NMR spectrum clearly showed a single isomer; additionally, the FTIR spectrum exhibited B-H stretches ( $2515\text{ cm}^{-1}$ ). The  $^{11}\text{B}$  NMR spectrum further confirmed the product was *nido* in that two peaks appeared at  $-35.1\text{ ppm}$  and  $-31.4\text{ ppm}$  (**Figure 3.3**) which are indicative of the two boron atoms connected to the bridging proton.

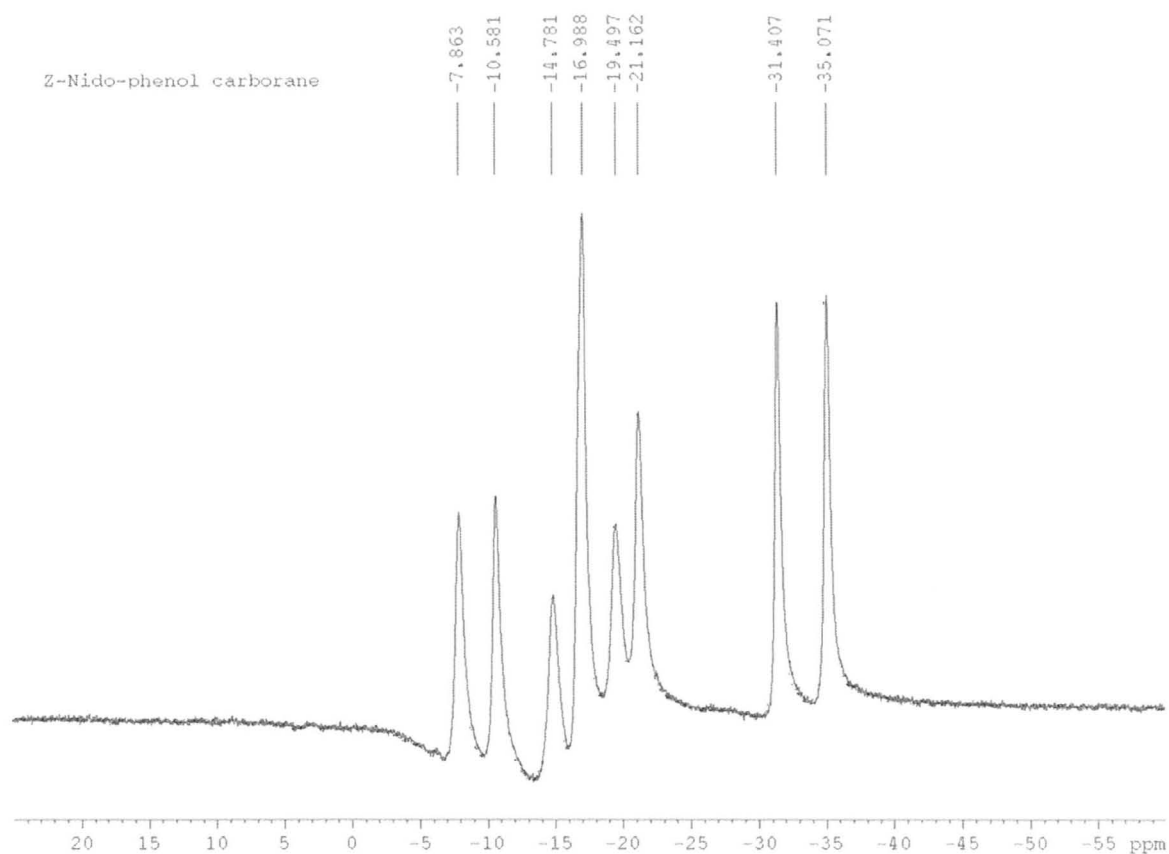


**Figure 3.3:**  $^{11}\text{B}\{^1\text{H}\}$  NMR of **2.9** (160 MHz,  $\text{CD}_3\text{OD}$ )

### 3.4 Isomerization of piperidinium Z-1-(1,2-dicarba-*nido*-undecaborane-1-yl)-1-(4-phenol)-2-phenyl-but-1-ene

While attempting to grow X-ray quality crystals of **3.8** by the slow evaporation of a methanol solution of the carborane, it was found that **3.8** undergoes E/Z isomerization and degradation. The isomerization of Tamoxifen is well established<sup>13</sup> and it has been shown that in solution under UV light the Z isomer of Tamoxifen will convert to both the E isomer and phenanthrenes.<sup>14</sup> **Figure 3.4** shows the proton NMR of compound **3.8** after one week in a solution of methanol at room temperature. The triplets observed at 0.65 and 0.95 ppm can be attributed to **3.7** and **3.8**, respectively, while the third triplet displayed at 1.2 ppm could be due to the formation of a phenanthrene derivative (**3.9**) of **2.9** (**Scheme 3.5**).



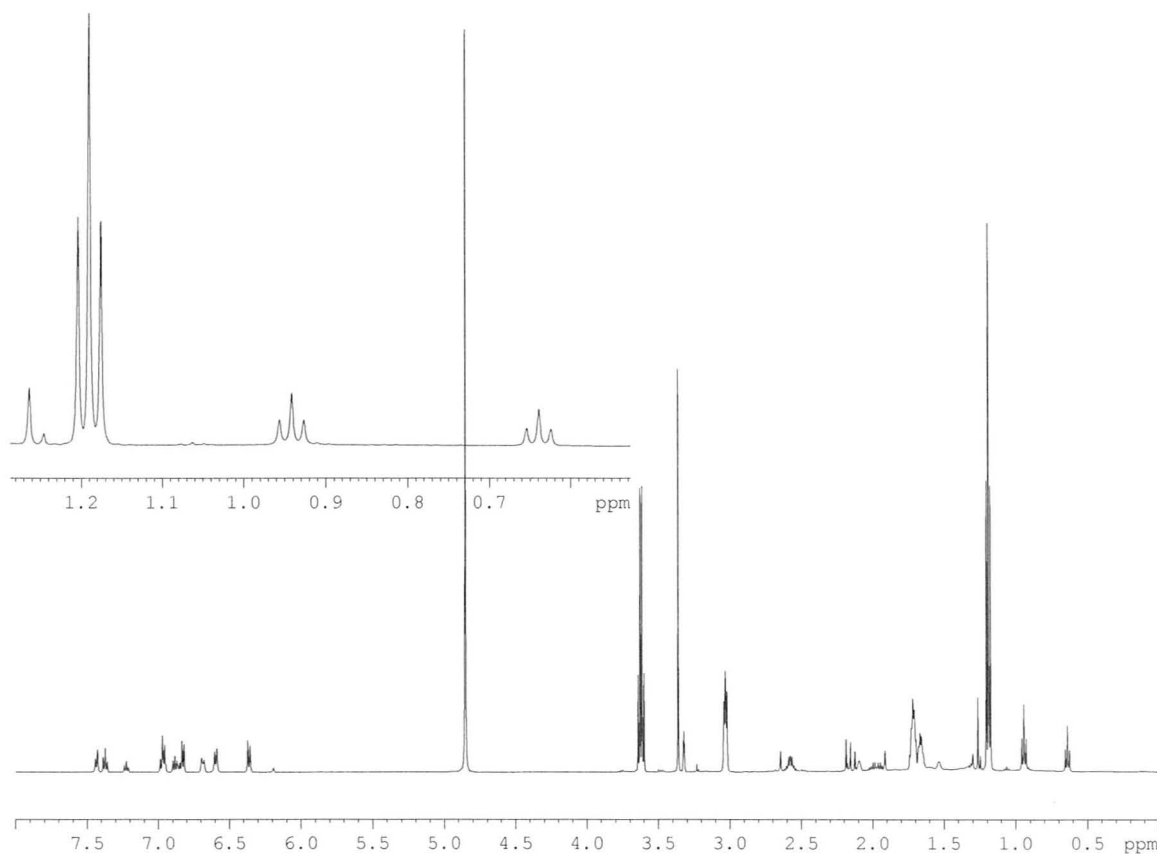
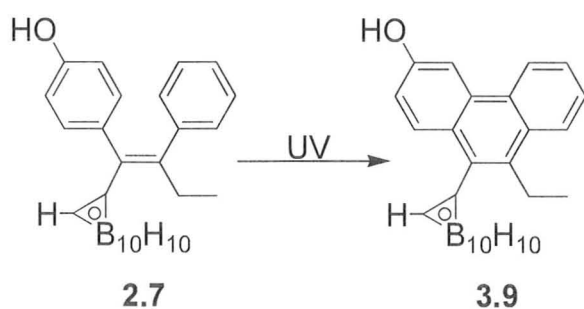


**Figure 3.4:** Compound **3.8** after one week in a solution (methanol) (600 MHz, CD<sub>3</sub>OD)



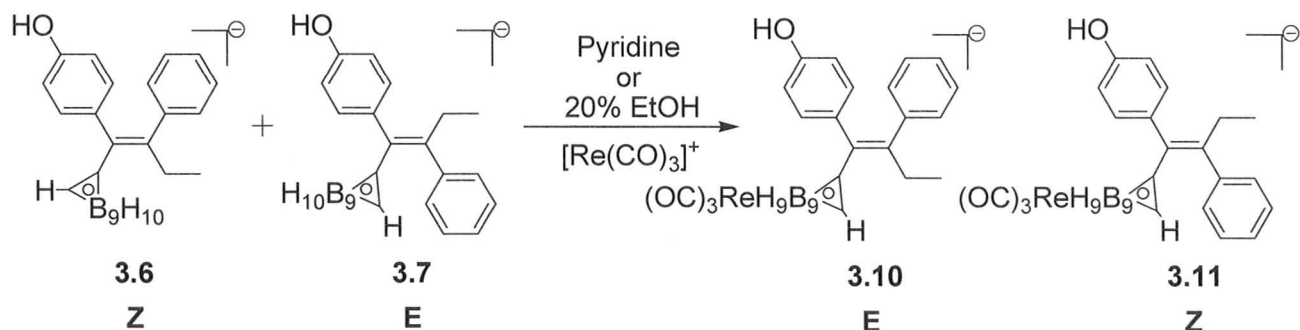
**Scheme 3.5:** Possible phenanthrene derivative of **3.8**

There are many possible ways to rationalize the isomerization of **2.7** and **3.8**. The most widely accepted mechanism for *cis-trans* isomerization involves

the concept of the triplet excited region.<sup>15</sup> It has been shown that for polyenes, electrons in the middle of a conjugated molecule can be excited into a triplet state and thus become single bond-like, allowing for free rotation.<sup>16</sup> The solvent that is used in a reaction can also potentially stabilize or destabilize certain transition states thus promoting or hindering *cis-trans* isomerization.

### 3.4.1 Preparation of the Rhenium Complex 3.10

In the past, the first step in synthesizing a rhenium carborane standard, which is needed to fully characterize the <sup>99m</sup>Tc analogue, involves formation of the *nido* species. This is followed by microwave heating the cluster in aqueous alcohol at high temperature and pressure (200°C, 20 bar) with [Re(CO)<sub>3</sub>(H<sub>2</sub>O)<sub>3</sub>]Br (**Scheme 3.6**). With the knowledge that **2.7** can be heated to high temperatures in an amine base, the metallation reaction was attempted using dry piperidine in the presence of [Re(CO)<sub>3</sub>(H<sub>2</sub>O)<sub>3</sub>]Br. After twice heating the reaction in a microwave at 180°C for 15 minutes HPLC was employed to isolate the desired rhenium Tamoxifen analogue. <sup>1</sup>H NMR indicated the isomeric purity, which was determined to be 6:1 (E:Z) (E:**3.10**, Z:**3.11**, **Scheme 3.6**).



**Scheme 3.6:** Synthesis of rhenium Tamoxifen analogues **3.10** and **3.11**

Since the metalation reaction in anhydrous amine resulted in both the E and Z isomer and not a single E isomer as expected the reaction was repeated in water in the presence of sodium fluoride using a mixture of **3.6** and **3.7**. The crude sample was purified via preparative HPLC collecting all peaks that corresponded to the mass of the target compound (**Figure 3.5:**  $m/z=625$ ,  $T_r= 4.9$ - $6.0$  minutes)

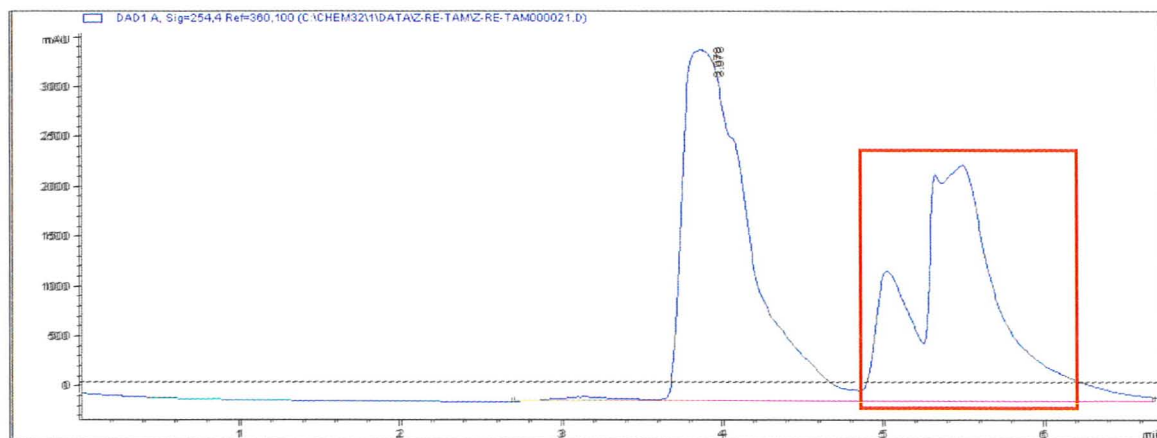


**Figure 3.5:** Crude preparative HPLC trace of the reaction of **3.6** and **3.7** with  $[\text{Re}(\text{CO})_3(\text{H}_2\text{O})_3]^+$  in 20% EtOH NaF. The red box indicates the peaks with a  $m/z$  of 625. (Zorbax SB C18 21x250 mm, 18 mL/min, 50:50 ACN : 5 mM ammonium acetate)

The HPLC was successful at removing unreacted starting materials consequently the next step was to separate the E and Z isomers **3.10** and **3.11**. This was achieved using the same HPLC method employed to purify the bulk sample employing a smaller injection volume (**Figure 3.6**). Following HPLC purification, samples were lyophilized and  $^1\text{H}$  NMR was utilized to identify the purity of the fractions. The NMR spectra obtained from the two HPLC peaks were identical, showing a E:Z ratio of 25:1 based on the integration of the ethyl signals (**Figure 3.7**). The data also suggests that the Z *nido* isomer (**3.6**) is more reactive than the E *nido* isomer (**3.7**) and that the two peaks observed in the HPLC trace were not geometric isomers of the Tamoxifen backbone but possible carborane isomers (**Figure 3.8**).

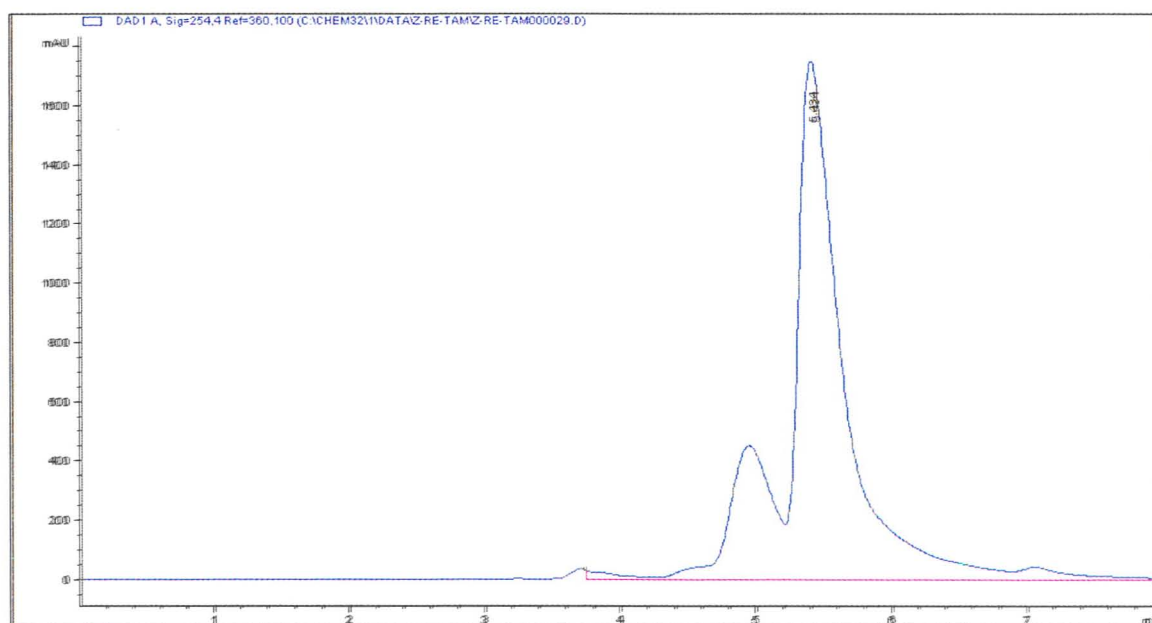


**Figure 3.6:** HPLC Trace of the HPLC purified reaction of **3.6** and **3.7** with  $[\text{Re}(\text{CO})_3(\text{H}_2\text{O})_3]^+$  in 20% EtOH NaF. (Zorbax SB C18 21x250 mm, 18 mL/min, 50:50 ACN : 5 mM ammonium acetate)

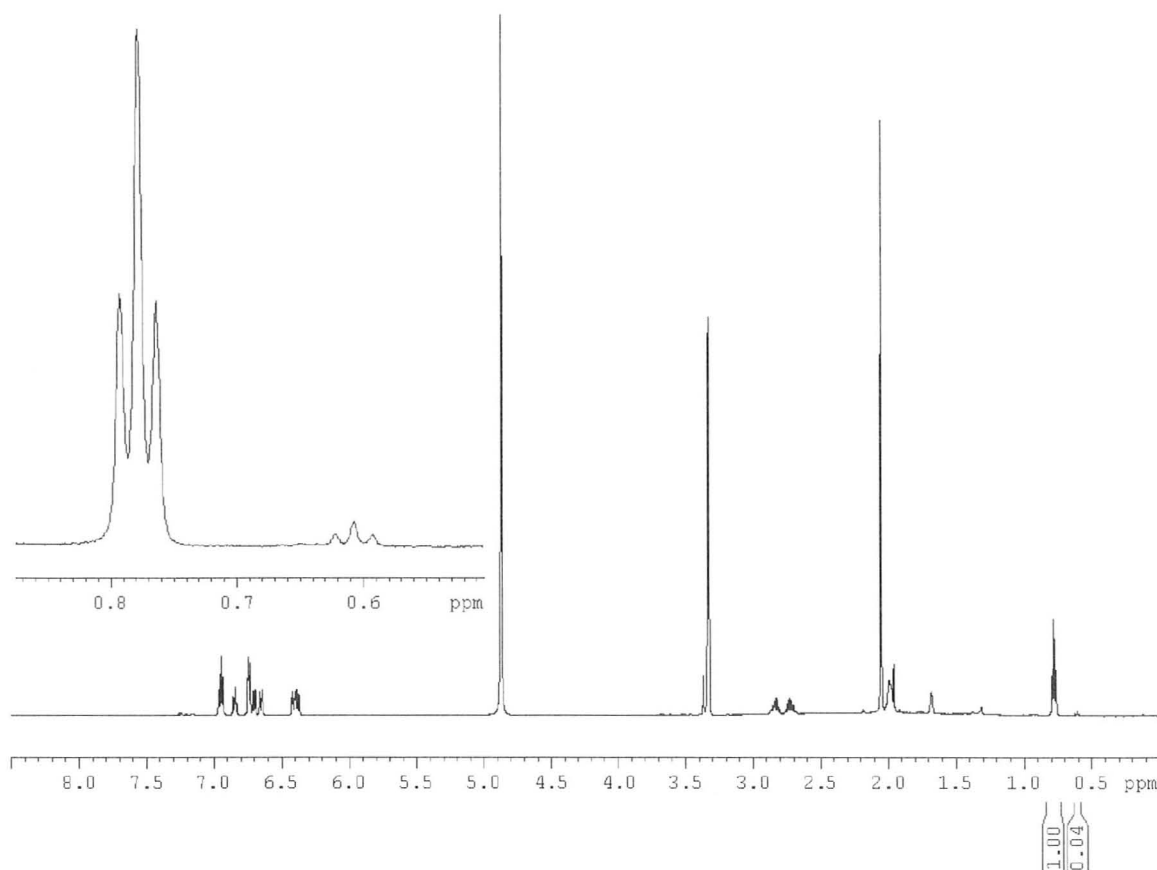


**Figure 3.7:** <sup>1</sup>H NMR spectra of **3.10** and **3.11** Showing a E:Z Ratio of 25:1 (CD<sub>3</sub>OD, 600MHz)

### 3.4.2 Rhenium Standard – Carborane Isomerization

A recent publication from our group<sup>17</sup> has outlined the role that sterics and electronics play in the isomerization of the carborane group upon reaction with Re(CO)<sub>3</sub><sup>+</sup>. There are three possible carborane isomers that can form when the open faced *nido* ligand is recapped with the rhenium tricarbonyl species; these include the 3,1,2 (**3.12a**), 2,1,8 (**3.12b**) and 2,1,8 (**3.12c**) isomers (**Figure 3.8**).

The steric bulk of the Tamoxifen backbone would favour isomerization to the 2,1,8 species **3.12b**, followed by **3.12c**, which is also a 2,1,8 species. Several pieces of evidence support that the rhenium Tamoxifen analogue was in fact a mixture of the two 2,1,8 isomers. First, a large change in chemical shift for the carborane C-H is observed; for the *closo* carborane analogue (**2.7**) which is known to have a 3,1,2 configuration the carborane C-H signal is at at 3.5 ppm, while **3.12b/c** has a C-H signal at 1.6 ppm. In addition to the carborane C-H shift, a 2D NOESY spectrum was obtained in which no enhancement of any of the Tamoxifen backbone protons was seen when the carborane C-H was irradiated; which is consistent with studies on other 2,1,8 isomers.

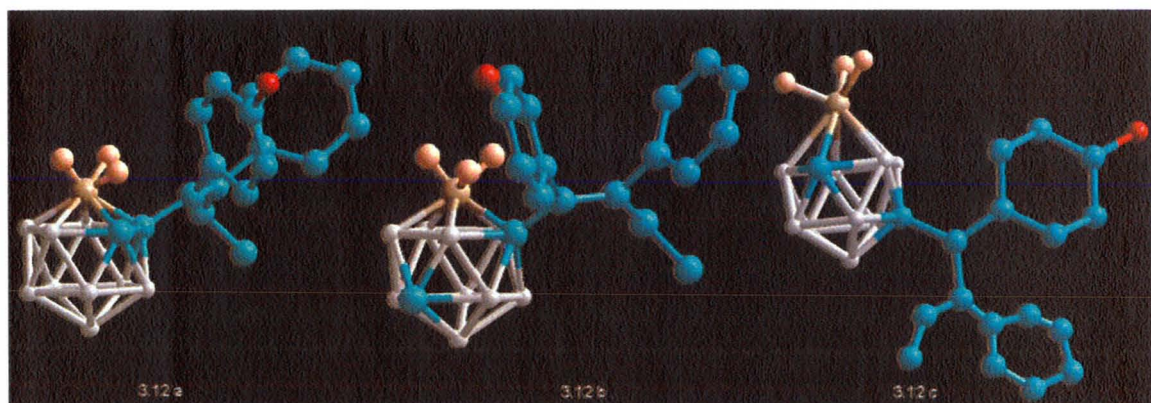


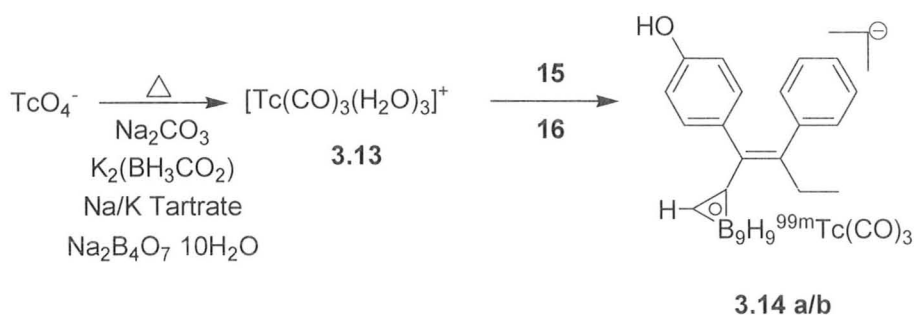
**Figure 3.8:** Possible rhenium carborane Isomers **3.12**. (Structures drawn using HyperChem Release 7.5)

### 3.4.3 Tc – Tamoxifen

With the rhenium standard fully characterized, the next step was to perform the metallation reaction using  $[\text{}^{99\text{m}}\text{Tc}(\text{CO})_3(\text{H}_2\text{O})_3]^+$  (**3.13**, **Schemes**



**3.14).** Starting with 1.2 GBq (32 mCi) of **3.13**, 6 mg of the mixed E/Z *nido* carboranes (**3.6** and **3.7**) in 20% ethanol was added and the reaction was subjected to microwave heating (30 min, 200°C). The mixture was purified using SPE to remove unreacted  $[\text{}^{99\text{m}}\text{Tc}(\text{CO})_3(\text{H}_2\text{O})_3]^+$ , followed by HPLC purification to remove excess starting material. The HPLC fractions were again passed through a SPE cartridge to remove the ammonium acetate buffer from the HPLC eluent and the solution was evaporated using a V10 evaporation system. The purified Tc Tamoxifen analogue (**3.14a/b**) was injected on an analytical HPLC column and the retention time was compared with the rhenium standard (**Figure 3.9**). From **Figure 3.9** it can be seen that the Tc Tamoxifen analogue HPLC trace has two signals that correspond to the two 2,1,8 rhenium isomers (**3.14 a** and **b**). The overall uncorrected yield for the 6 hour synthesis was  $5.9 \pm 1.5\%$  ( $n=3$ ). The low yield of the radiolabeling reaction is most likely due to the steric crowding of the open face of the *nido* carborane. While by no means suitable for clinical use, the yield is sufficient for running in vitro assays and it represents the most sterically crowded carborane labeled to date.



**Scheme 3.7:** Synthesis of **3.14**

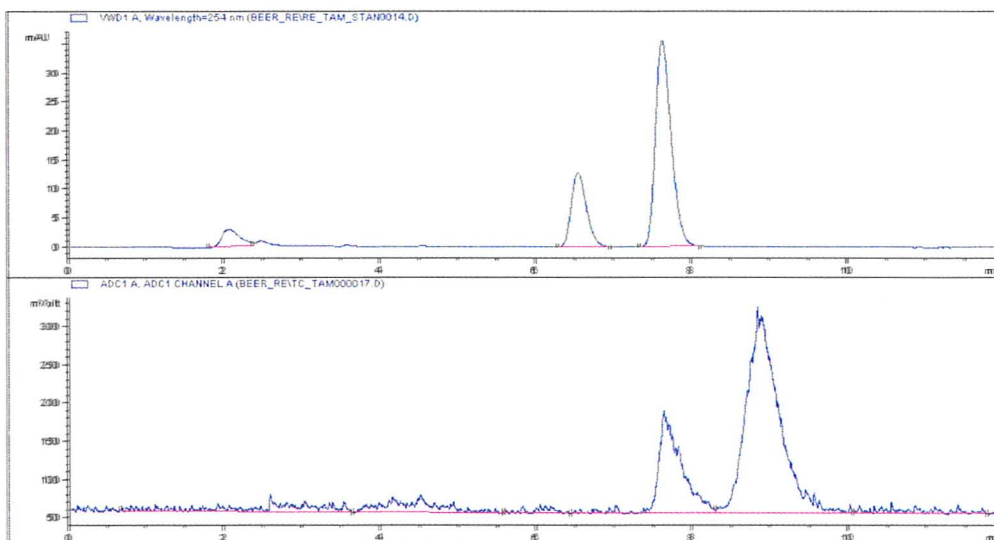


**Figure 3.9:** HPLC trace of **3.12b/c** (Top) and **3.14a/b** (Bottom). (Zorbax SB C18, 4.6x250mm, 60% ACN with 5 mM ammonium acetate).

## 3.5 Cell uptake assay

### 3.5.1 Introduction

Once compounds **3.14a** and **3.14b** had been synthesized with radiochemical purity >98% the next step was to determine if either compound would bind the ER specifically and if there was a difference between the two carborane isomers. The uptake assay consisted of four treatment groups outlined in Table 3.3 and the human MCF-7 cell line was used as it is known to over express the ER.<sup>18</sup> Each isomer was evaluated at five time points (15 min, 30 min, 1 hr, 2 hr, 4hr) at 37°C.



**Table 3.3:** Cell Uptake Assay Protocol for **3.14a/b**

Treatment Group	
<b>A – Control</b>	9.5 ml media + 0.5% BSA, 0.5 ml Tc-Tamoxifen ( <b>3.14a</b> or <b>3.14b</b> )
<b>B – 3.14 + 10nM 3.12</b>	9.5 ml media+0.5% BSA, 0.5 ml Tc-Tamoxifen ( <b>3.14a</b> or <b>3.14b</b> ), 10 $\mu$ l 20 $\mu$ M Re-Tamoxifen ( <b>3.12</b> )
<b>C – 3.14 + 10<math>\mu</math>M 3.12</b>	9.3 ml media+0.5% BSA, 0.5 ml Tc-Tamoxifen ( <b>3.14a</b> or <b>3.14b</b> ), 200 $\mu$ l 2mM Re-Tamoxifen ( <b>3.12</b> )
<b>D – 3.14 + 10nM 3.12 + 100nM Tamoxifen</b>	9.5 ml media+0.5% BSA 100nM Tamoxifen, 0.5ml Tc-Tamoxifen ( <b>3.14a</b> or <b>3.14b</b> ), 10 $\mu$ l 20 $\mu$ M Re- Re-Tamoxifen ( <b>3.12</b> )

### 3.5.2 Results and Discussion

From **Figure 3.10** it can be seen that the minor Tc-Tamoxifen analogue (**3.14a**) was able to bind the MFC-7 cells with increasing affinity as the incubation time was increased, with a percent uptake of  $10.15 \pm 1.5\%$  at the fifteen minute time point and  $83.81 \pm 13.17\%$  at the 4 hour mark (group **A**). With the addition of 10 nM **3.12a** (group **B**), no significant difference was seen when compared with treatment group **A**. To determine non specific binding of **3.14a**, a blocking study using a high concentration of **3.12a** (group C, 10  $\mu$ M) was completed. From group **C** it can be seen that the cold Re-Tamoxifen analogue (**3.12a**) is able to significantly block the uptake of **3.14a** at the two and four hour time points with a percent uptake of  $44.31 \pm 4.45$  and  $48.60 \pm 5.52\%$  compared with  $68.64 \pm 7.65$  and  $83.81 \pm 13.17\%$  seen in the control group, which represents a blocking of 35 and 42% of the activity respectively. The final treatment group (**D**); using a high

concentration of Tamoxifen (10 nM) showed minimal difference in uptake when compared with group **A** ( $74.30 \pm 13.17\%$  versus  $83.81 \pm 13.17\%$  at 4 hours).

The results from the uptake assay of **3.14b** show notable differences. The % uptake for group **A** (**Figure 3.11**) shows a similar uptake at the fifteen minute and one hour time points with a percent uptake of  $20.68 \pm 2.88$  and  $26.87 \pm 4.60\%$  respectively. A significant increase is seen at the two hour mark with a percent uptake of  $75.13 \pm 15.56\%$ , while at the four hour time point there is a significant decrease in uptake seen ( $35.11 \pm 3.10\%$ ). This data suggests that the kinetics of binding of **3.14b** is faster than **3.14a**.

Similar to **3.14a**, significant blocking of **3.14b** was seen with group **C** at the two and four hour time point, but unlike **3.14a** blocking was also seen at the fifteen minute time point. The percent activity blocked was found to be 53, 61 and 72% for the fifteen minute, two and four hour time points respectively.

The results suggest that **3.14a** and **3.14b** behave significantly different *in vitro*. The most notable difference is seen in the binding profiles from group **A**, with the time to achieve maximum binding and subsequent clearance being significantly different. Both compounds show specific binding, but the results from group **D** suggest, that this binding is either not to the ER or that Tamoxifen is not able to completely inhibit **3.14a** and **3.14b**.

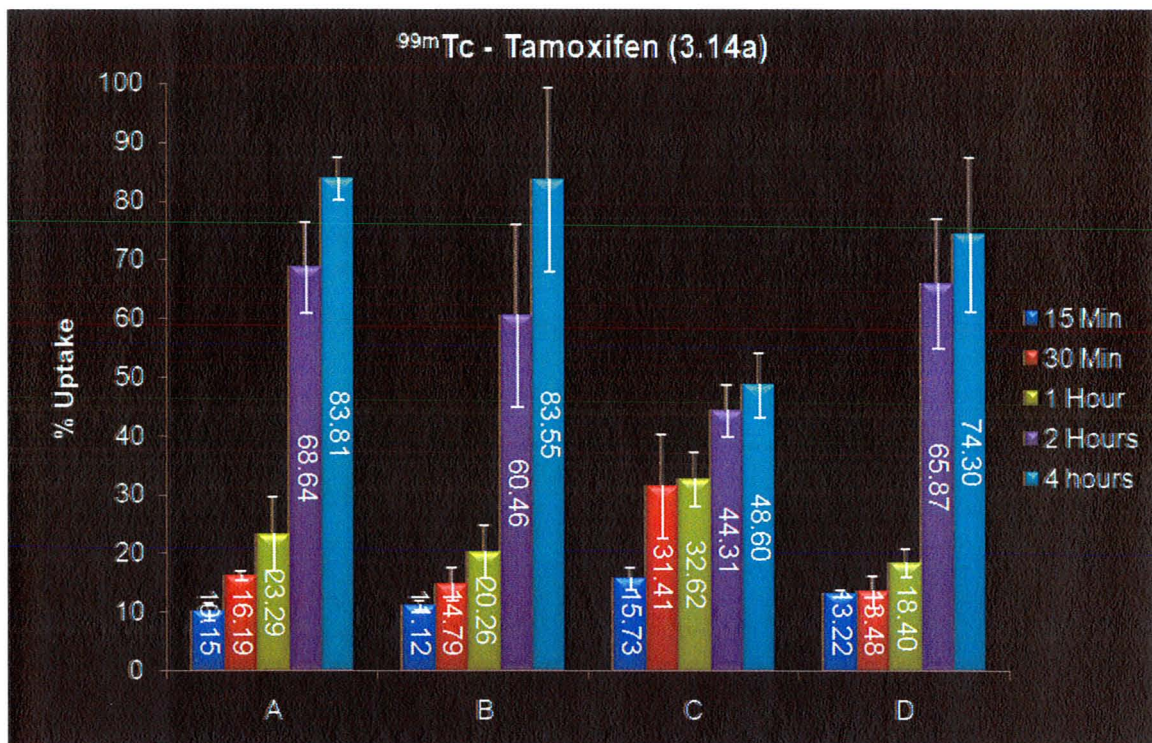


Figure 3.10: Cell Uptake Assay Results for 3.14a

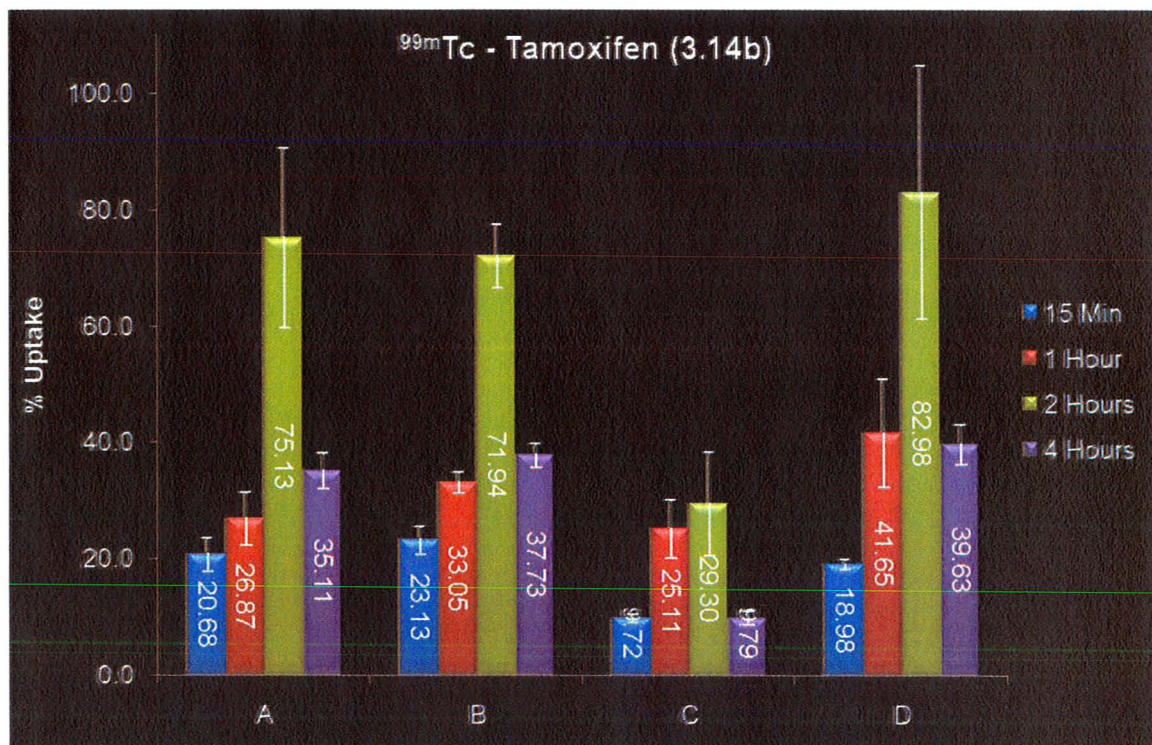
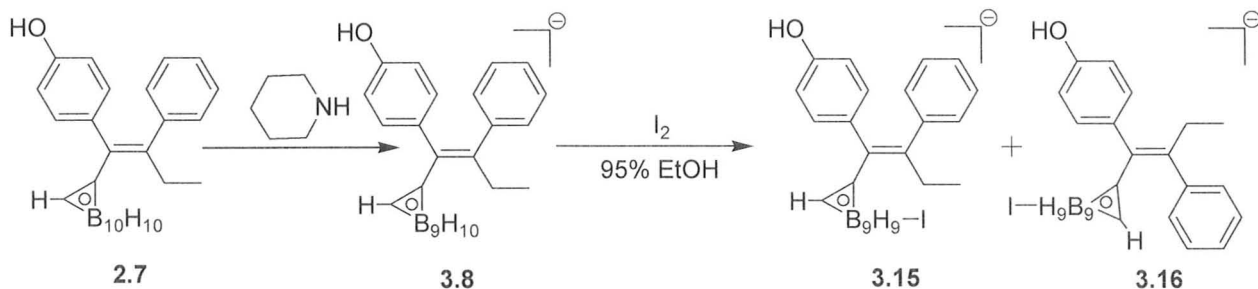


Figure 3.11: Cell Uptake Assay Results for 3.14b



### 3.6 Synthesis of Iodo-Tamoxifen

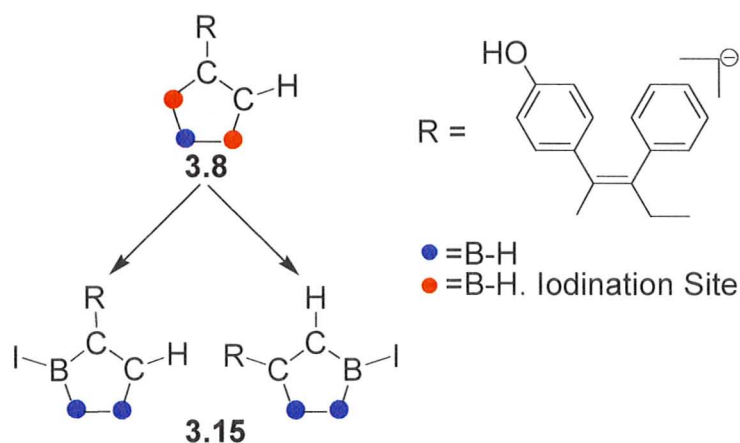
As mentioned in section 1.6, carboranes can be labeled with both technetium and iodine. To optimize the radiolabelling of **3.8** with various radioisotopes of iodine, a cold standard was first required. Iodination of the *nido* carborane cage by the addition of  $I_2$  in absolute ethanol was first investigated by Hawthorne *et al.* in 1965.<sup>19</sup> The iodination of **3.8** was achieved by adding 0.9 equivalents of  $I_2$  in a 95% ethanol solution to the *nido* carborane in the absence of light and quenching the reaction after 30 seconds to ensure no di-iodinated product was formed (**Scheme 3.8**). The expected product (**3.15**) was isolated by reversed-phase HPLC in a 38% yield.



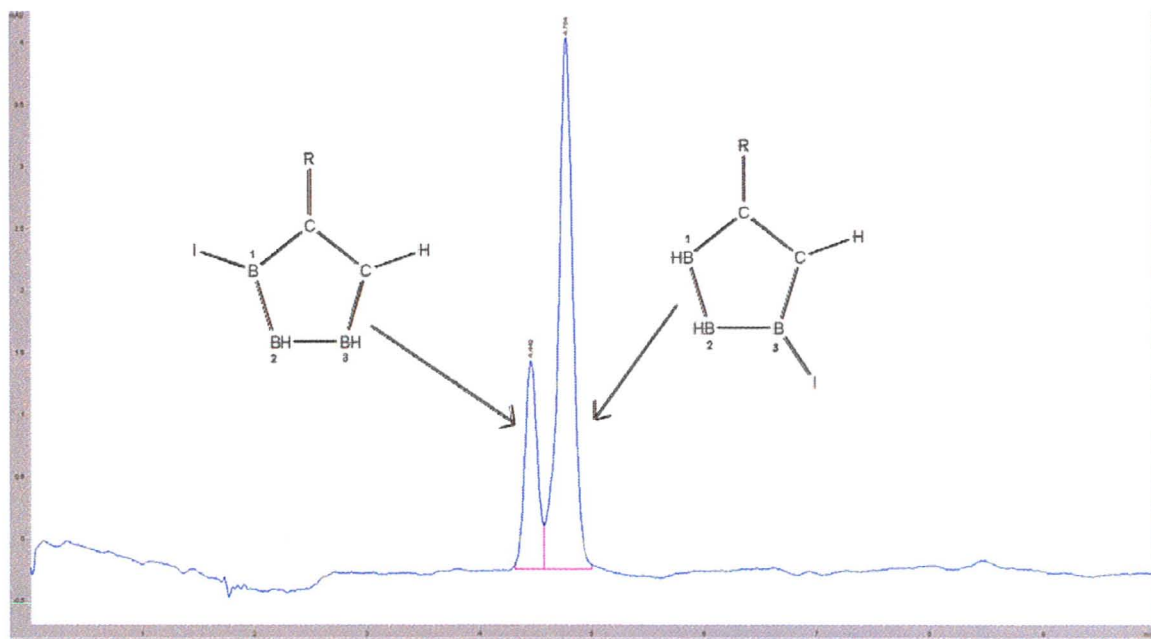
**Scheme 3.8:** Iodination of **3.8** in 95% ethanol

There are two possible positional isomers of **3.15** that can be formed because **3.8** has two possible iodination sites (**Figure 3.12**). The positional isomers can be seen in the HPLC-MS trace (**Figure 3.13**) where each peak was confirmed to be the same mass. It is interesting to note the 2:1 ratio seen in the

HPLC trace. This ratio is most likely due to the preferential formation of the iodination product on the less sterically hindered boron (B3) (**Figure 3.13**).

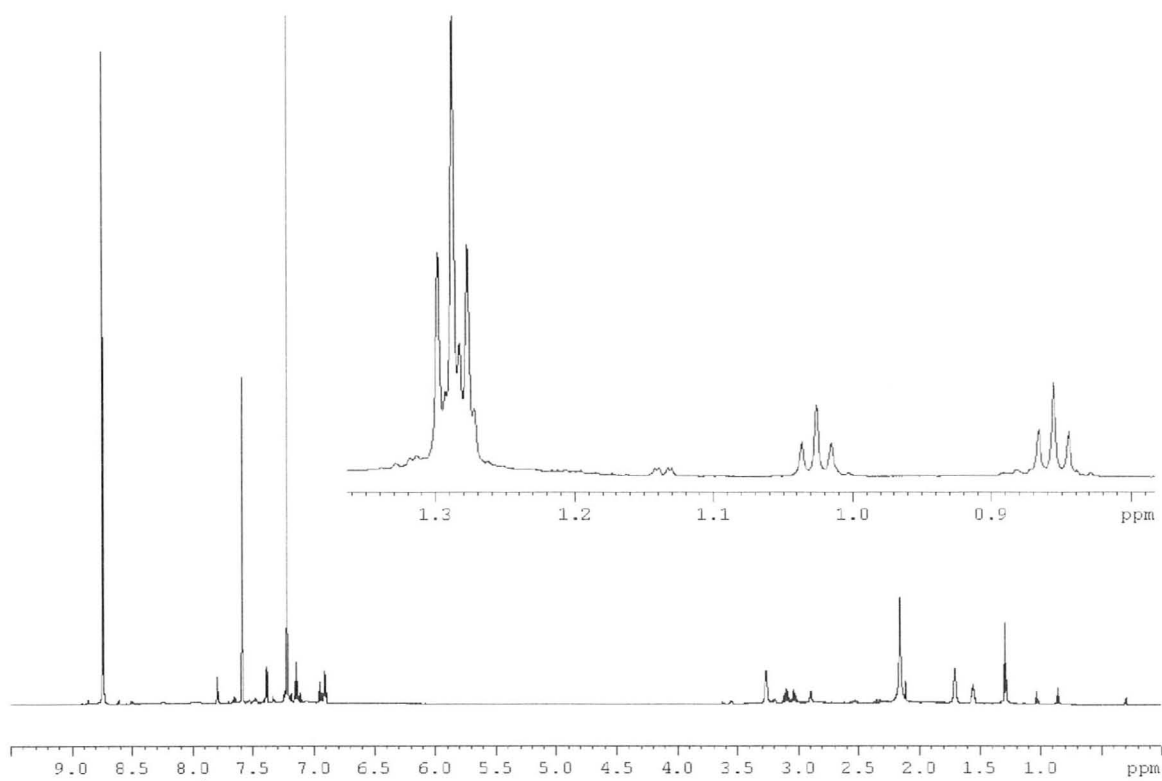


**Figure 3.12:** Representation of the top face of *nido* carborane **3.8** and **3.15** showing two possible iodination sites (the rest of the carborane has been omitted for clarity).

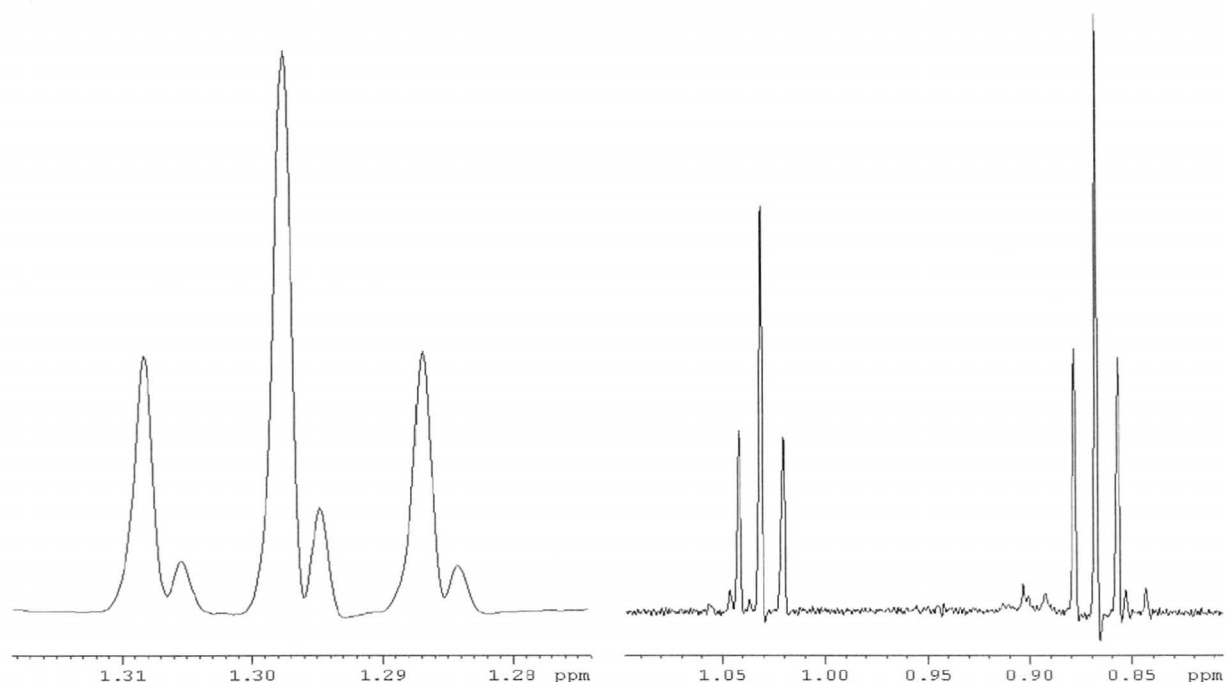


**Figure 3.13:** HPLC-ESMS (ion-trap) spectrum of **3.15** showing two distinct signals with the same mass (482 m/z) (Zorbax SB C18, 1 mL/min, 70% ACN with 15 mM ammonium acetate)

To confirm the two peaks in the HPLC trace were a result of the two different iodination sites of **3.8**, the  $^1\text{H}$  spectrum (**Figure 3.14**) was collected and analyzed in detail. The aliphatic region (**Figure 3.14**) showed significant shifts of the methyl signal (0.3 and 0.4 ppm), which is similar to the shift seen in the conversion of **2.7** to **2.8** (E and Z *closo* carborane analogues). Four triplets are clearly seen where the resolution of the two triplets at 1.3 ppm was enhanced by reprocessing the data using Gaussian multiplication (**Figure 1.15**). These two peaks most likely arose from the two Z iodinated products (see **Table 3.4**). The specific chemical shifts and most probable iodination sites are summarized in **Table 3.4**.

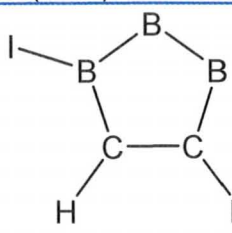
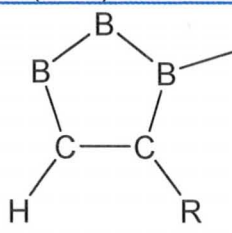
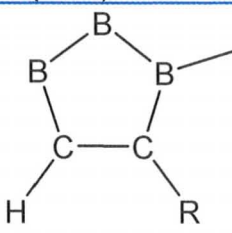
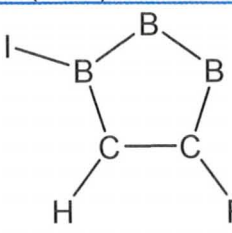


**Figure 3.14:**  $^1\text{H}$  NMR Spectrum of the products from the treatment of 3.8 with  $\text{I}_2$  (3.15 and 3.16) (Pyridine- $\text{d}_5$ , 700MHz)



**Figure 3.15:** Expansions of the aliphatic regions of the  $^1\text{H}$  NMR spectrum of ethyl groups of **3.15** / **3.16** (Pyridine- $d_5$ , 700MHz, Gaussian multiplication)

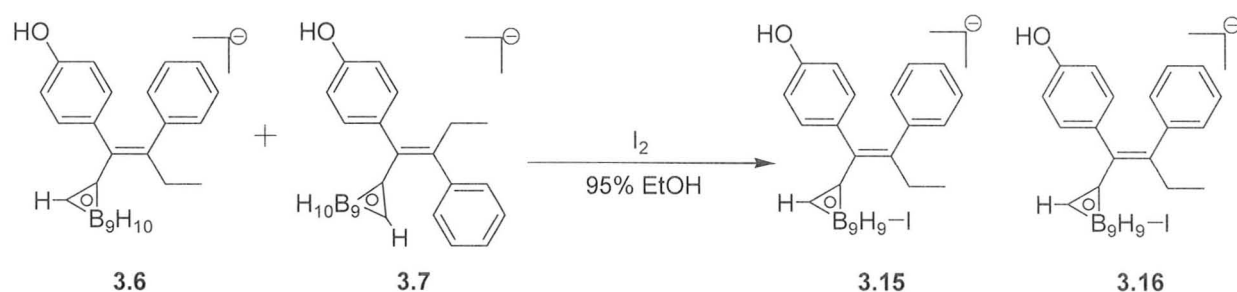
**Table 3.4:** Assignments of the E/Z Isomers of **3.15** and **3.16**

1H Shift	1.299	1.295	1.030	0.852
Isomer	Z ( <b>3.15</b> )	Z ( <b>3.15</b> )	E ( <b>3.16</b> )	E ( <b>3.16</b> )
Iodination site				

Since **3.15** undergoes E/Z isomerization under aqueous conditions, and to date the only solvents that are able to prevent this isomerization are not amenable to biological testing, it was determined that the best course of action would be to prepare the mixed E/Z mono iodinated analogues (**3.15** and **3.16**)



starting from the mixed *E/Z nido* carborane analogues (**Scheme 3.9**). The iodination reaction was repeated as describe above, although no precaution was taken to shield the reaction from light. The product was purified using semi preparative HPLC, followed by analytical HPLC to verify the purity (**Figure 3.16**). The product was characterized using multi-NMR which indicated the presence of four isomers as expected. In addition the HRMS showed the distinctive carborane isotope pattern and the IR spectrum showed a signal at  $2517\text{ cm}^{-1}$  also confirming the presence of the carborane cage.



**Scheme 3.9:** Iodination of a mixture of **3.6** and **3.7**

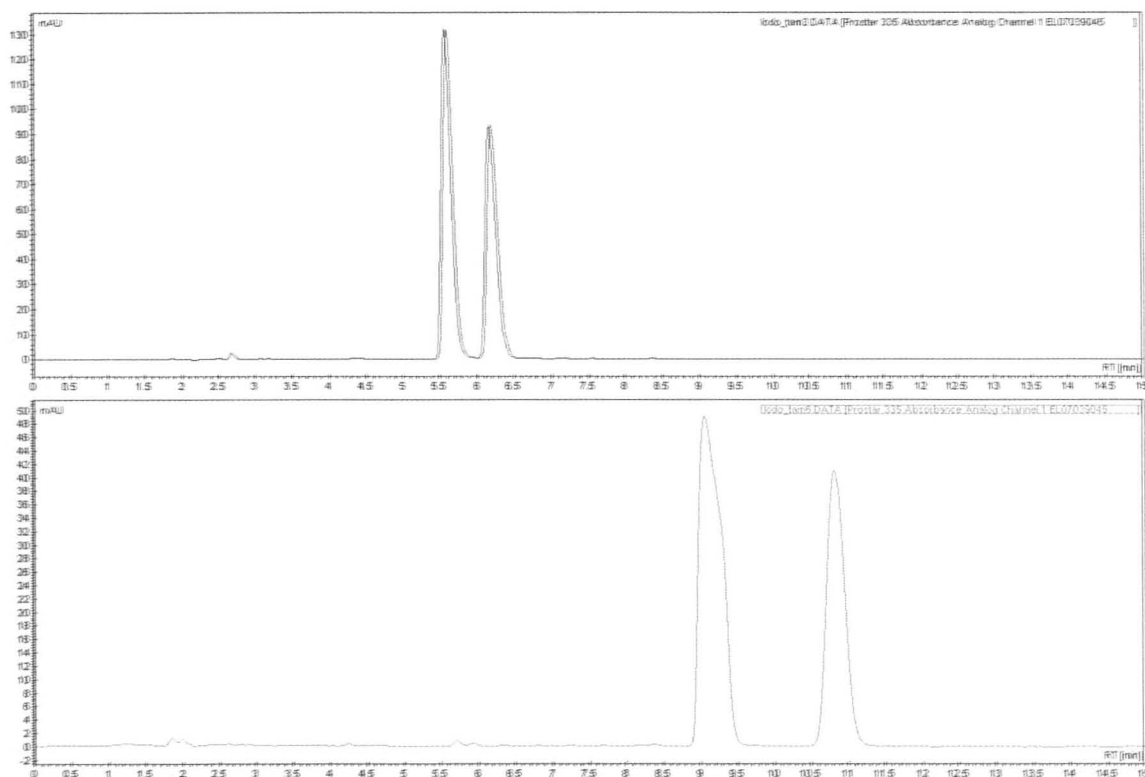


**Figure 3.16:** HPLC trace of: *nido* carboranes **3.6** and **3.7** (top) and the cold iodine standards **3.15** and **3.16** (bottom). (Zorbax SB-C18, 254nm, 1mL/min, 50% ACN (5 mM ammonium acetate). The early eluting peaks at 5.6 min (top, **3.7**) and 9.2 min (bottom, **3.16**) corresponds to the E isomer while the late eluting peaks at 6.3 min. (top, **3.6**) and 10.7 (bottom, **3.15**) correspond to the Z isomer.

An initial radiolabelling of **3.6/3.7** with iodine-125 proved successful with good correlation found between the iodo standard and the peaks seen in the gamma trace (**Figure 3.17**). The next step would be to repeat the radiolabelling experiment and isolate the two product peaks which correspond to the two peaks seen at 10 and 12.5 min in the HPLC trace (**Figure 3.17**, top). Once the pure samples of the iodinated carborane Tamoxifen analogue have been isolated they

could be evaluated for their ability to bind the ER in the same manor that was used for the Tc analogue.

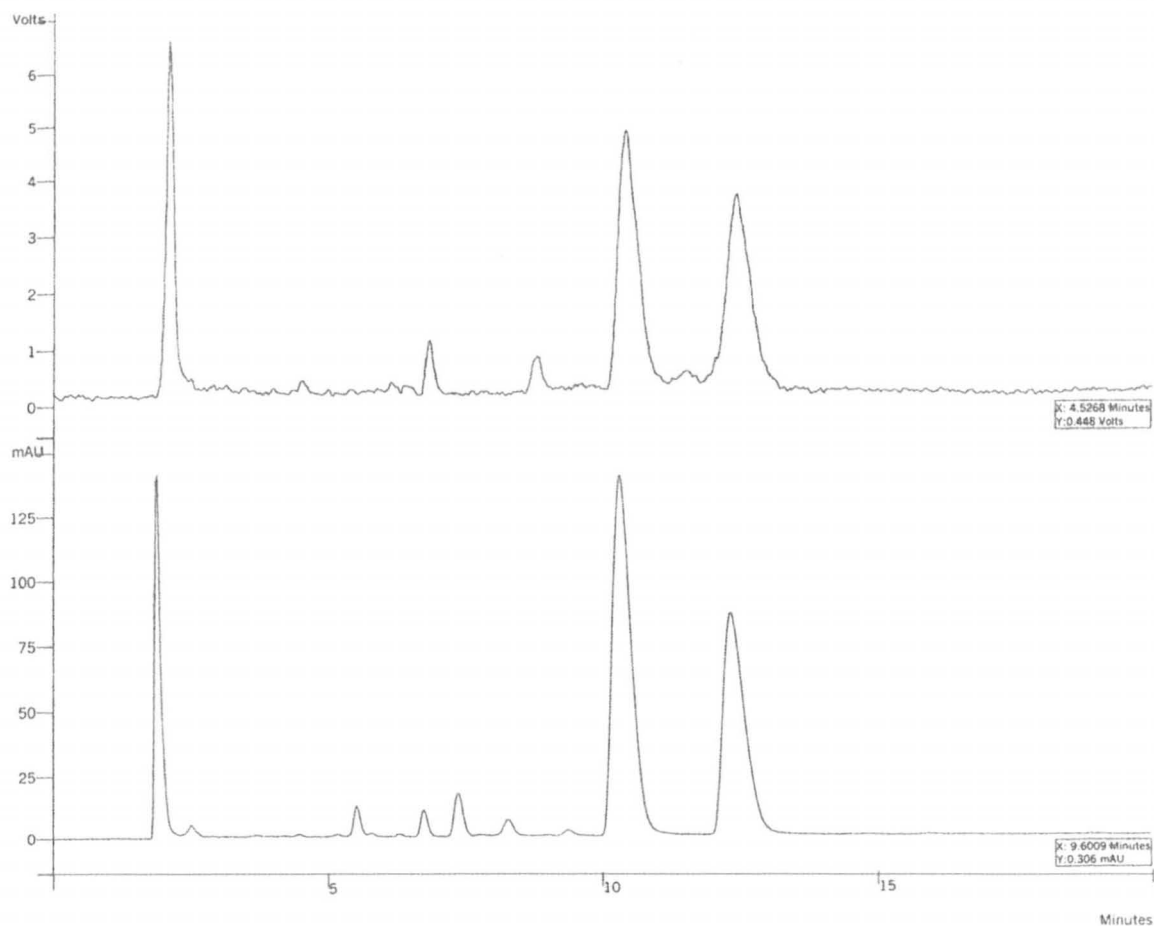


**Figure 3.17:** HPLC trace of the reaction mixture involving the labeling of **3.6/3.7** with NaI[125I] in the presence of Iodogen. (**3.16** and **3.17**, gamma, top) co-injected with the cold standard (**3.12** and **3.13**, UV, bottom). (Zorbax SB C18, 1 mL/min, 60% ACN with 0.05 mM

### 3.7 Conclusion

Labelling of the lead compound (**2.7**) with technetium and iodine was successful. The  $\text{Tc}(\text{CO})_3^+$  complex (**3.14**) was isolated in poor yield (5%), but high purity. Initial biological results of the technetium analogue (**3.14**) have shown the ability to bind MFC-7 cells, although further work is required to verify that the ER is in fact the target. Preliminary radio iodination experiments indicate incorporation of  $^{125}\text{I}$  onto the carborane and good correlation with the cold iodine standard.

### 3.8 Experimental

#### General

All reactions were carried out under argon that had been passed through drierite, using commercial grade solvents dried using a Pure Solv MD-6 solvent purification system (Innovative Technology Inc.). Chemicals were purchased from Sigma-Aldrich or SGF chemicals and used without further purification. Decaborane was purchased from Katchem. Reactions requiring microwave heating were performed using a Biotage Initiator 60 instrument. Compound **7** was prepared following literature a procedure.<sup>20</sup>  $^1\text{H}$ ,  $^{13}\text{C}$  and  $^{11}\text{B}$  NMR spectra were recorded on Bruker AV600, Bruker DRX500, or Bruker AV200 spectrometers with probe temperatures of 30, 25 and 25°C, respectively.  $^1\text{H}$  NMR chemical

shifts are reported in ppm relative to the residual proton signal of the NMR solvent. Coupling constants ( $J$ ) are reported in Hertz (Hz).  $^{13}\text{C}$  chemical shifts are reported in ppm relative to the carbon signal of the solvent while  $^{11}\text{B}$  chemical shifts are reported in ppm relative to an external standard of  $\text{BF}_3\cdot\text{Et}_2\text{O}$ . Thin layer chromatography plates (Merck F254 silica gel on aluminum plates) were visualized using 0.1%  $\text{PdCl}_2$  in 3 M  $\text{HCl}(\text{aq})$  and/or UV light. Infrared spectra were acquired using a BioRad FTS-40 FT-IR or Nicolet 510 FTIR spectrometer. High resolution mass spectra were obtained on a Waters/Micromass Q-ToF Ultima Global spectrometer. Low resolution LCMS were obtained on a Waters 2695 LC with a Quattro Ultima triple quadrupole mass spectrometer. Analytical and semi preparative HPLC were performed using a Varian Pro Star model 330 PDA detector, model 410 auto sampler, model 230 solvent delivery system and model 710 fraction collector. Analysis was conducted using Agilent Zorbax SB-C18 (4.6x250 mm (5  $\mu$ ), 9.8x250 mm (5  $\mu$ ) and 21x250 mm (7  $\mu$ )) columns.

### **Cell Lines and Tissue Culture**

MCF-7 human breast adenocarcinoma cells lines were obtained from ATCC (Manassas, VA), and were cultured in DMEM without Phenol red (CA12001-630; VWR International, Mississauga ON) supplemented with 10% charcoal-stripped fetal bovine serum (CA95039-622; VWR International), 1% L-Glutamine (25030-081; Invitrogen, Mississauga ON) and 1%

antibiotic/antimycotic (AB/AM) (15240-062; Invitrogen). All cells were maintained at 37°C in 5% CO<sub>2</sub>.

### Cell Uptake Assays

6-well plates were seeded with  $1 \times 10^5$  MCF-7 cells/well 48 hours prior to the start of the experiment with 2 mL of media per well. After incubation the media from wells was removed and washed twice with 2 mL PBS+0.5 % BSA. 500  $\mu$ l of incubation solution (group **A**, **B**, **C** or **D**) was added to each well and incubate for appropriate amount of time. After incubation, the incubation solution was aspirated and the cells were washed twice by adding 1 mL PBS+0.5% BSA to each well and rocking gently in succession. To release the cells from the growth surface 500  $\mu$ l of Trypsin/EDTA was added to each well and incubated at room temperature until cells released from growth surface (repeat twice). 500ul PBS+0.5% BSA was added to wash growth surface and the cells were transferred into test tubes and counted on a gamma counter.

### Sodium Z-1-(1,2-Dicarba-*nido*-undecaborane-1-yl)-1-(4-methoxy phenyl)-2-phenyl-but-1-ene (3.8)

**2.6** (1.0 g, 2.68 mmol) was dissolved in absolute 2-propanol (IPA) and water was added to form a 60% IPA solution (total volume 400 mL). Sodium hydroxide (10.0 g, 250 mmol) was added to the solution and heated to 70°C. The reaction was monitored by TLC for the conversion of *closo* to *nido* (48

hours). The solvent was concentrated (~150 mL) under vacuum, and CO<sub>2</sub> was bubbled through the aqueous mixture to form a milky solution which was filtered to remove the white precipitate. The sample was lyophilized yielding a hygroscopic white solid (0.845 g, 85 %). TLC (1:1 dichloromethane : Methanol) R<sub>f</sub> = 0.87; <sup>1</sup>H NMR (500 MHz, CD<sub>3</sub>OD): δ 7.12 -6.60 (m, 9H, aryl), 2.73 (m, 2H, CH<sub>2</sub>), 2.24 (s, 1H, C<sub>carborane</sub>-H), 1.01 (t, <sup>3</sup>J=7.40, 3H, CH<sub>3</sub>); <sup>13</sup>C{<sup>1</sup>H} NMR (125 MHz, CD<sub>3</sub>OD): δ 13.1, 29.6, 55.4, 112.4, 125.8, 127.9, 130.5, 132.7, 137.1, 143.1, 144.7, 145.3, 158.1; <sup>11</sup>B{<sup>1</sup>H} (160 MHz, CD<sub>3</sub>OD): -8.3, -11.0, -15.2, -17.4, -19.9, -21.6, -31.9, -35.5; m/z calculated for [M]<sup>-</sup> C<sub>19</sub>H<sub>28</sub>B<sub>9</sub>O<sup>-</sup> 371.2978 HRMS TOF EI<sup>-</sup> [M]<sup>-</sup> 371.3307; FTIR (NaCl, cm<sup>-1</sup>) ν: (2517, 2974, 3566, 3632).

**Piperidinium Z-1-(1,2-Dicarba-*nido*-undecaborane-1-yl)-1-(4-phenol)-2-phenyl-but-1-ene (2.9)**

**2.7** (440 mg, 1.2 mmol) was dissolved in of piperidine (100 mL) and stirred at room temperature for 40 minutes. Excess piperidine was removed under vacuum to yield a pale yellow semi solid. The product was purified by dissolving the solid in 20% aqueous methanol and eluting through a C18 solid phase extraction cartridge to yield a sticky dark orange semi-solid (451 mg, 85 %) TLC (1:1 hexanes : dichloromethane) R<sub>f</sub> = 0.31; <sup>1</sup>H NMR (500 MHz, CD<sub>3</sub>OD): δ 7.05 - 6.41 (m, 9H, aryl), 2.64 (m, 2H, CH<sub>2</sub>), 2.14 (s, 1H, C<sub>carborane</sub>-H), 1.00 (t, <sup>3</sup>J=7.40, 3H, CH<sub>3</sub>); <sup>13</sup>C{<sup>1</sup>H} NMR (125 MHz, CD<sub>3</sub>OD): δ 13.2, 23.7, 24.8, 29.5, 46.2, 52.7, 66.8, 113.8, 125.8, 127.8, 130.4, 132.7, 135.9, 143.0, 144.5, 145.1, 155.0; <sup>11</sup>B{<sup>1</sup>H} (160 MHz, CD<sub>3</sub>OD): -7.9, -10.6, -14.8, -17.0, -19.5, -21.2, -31.4, -35.1;

m/z calculated for  $[M]^-$   $C_{18}H_{26}B_9O^-$  357.2821 HRMS TOF EI $^-$   $[M]^-$  357.2805; FTIR (NaCl,  $cm^{-1}$ )  $\nu$ : (2515, 2955, 3171, 3495).

**Sodium rac-8-(E-1-(1,2-Dicarba-*nido*-undecaborane-1-yl)-1-(4-phenol)-2-phenyl-but-1-ene) 2,2,2-tricarbonyl-2-rhenium-2,1,8-dicarba-*closo*-dodecaborate (3.12b) and Sodium rac-1-(E-1-(1,2-Dicarba-*nido*-undecaborane-1-yl)-1-(4-phenol)-2-phenyl-but-1-ene) 2,2,2-tricarbonyl-2-rhenium-2,1,8-dicarba-*closo*-dodecaborate (3.12a)**

34 mg (0.8 mmol) of NaF and 75 mg (0.2 mmol) of **2.7** was dissolved in 3 mL of 20% ethanol, sealed in a microwave vial and heated to 180°C for 10 minutes to produce compounds **3.6** and **3.7**. To this mixture 325 mg (0.8 mmol) of  $[Re(CO)_3(OH_2)_3]Br$  was added and the mixture was heated to 180°C for 15 minutes. This was again repeated with 311 mg (0.77 mmol) of  $[Re(CO)_3(OH_2)_3]Br$  and heated again to 180°C for 15 minutes. The product was purified by passing the crude reaction mixture (20% ethanol) through a C18 solid phase extraction cartridge and eluted with acetonitrile. The product was subsequently dried at reduced pressure. The product was then twice purified via semi preparative HPLC (Zorbax SB C18, 60% acetonitrile, 40% 5 mM ammonium acetate, 5 mL/min) and dried for at reduced pressure. The product subsequently dissolved in water, frozen and lyophilized to yield a white powder (2.9 mg,  $4.6 \times 10^{-3}$  mmol, 2.3 %).  $^1H$  NMR (700 MHz,  $CD_3OD$ , major isomer):  $\delta$  6.94-6.91 (t, aryl), 6.83-6.81 (t, aryl), 6.72-6.71 (d, aryl), 6.69-6.67 (dd, aryl), 6.64-6.62 (dd, aryl), 6.40-



6.6.38 (dd, aryl), 6.36-6.35 (dd, aryl), 2.83-2.79 and 2.73-2.69 (m, 2H, CH<sub>3</sub>), 1.66 (s, 1H, carborane C-H), 0.75 (t, J=7.5Hz, 3H, CH<sub>2</sub>); <sup>1</sup>H NMR (700 MHz, CD<sub>3</sub>OD, minor isomer): δ 7.24-7.21 (m, aryl), 7.19-7.17 (m, aryl), 7.13 (m, aryl), 1.75 (q, J=7.5 Hz, 2H, CH<sub>3</sub>), 1.30 (s, 1H, carborane C-H), 0.58 (t, J=7.5Hz, 3H, CH<sub>2</sub>); <sup>13</sup>C NMR (175 MHz, CD<sub>3</sub>OD, Major isomer): δ; 200.8, 155.4, 146.5, 146.1, 139.6, 138.0, 133.0, 130.5, 127.8, 125.6, 114.2, 59.2, 29.5, 28.8, 13.5; <sup>11</sup>B NMR (160 MHz, CD<sub>3</sub>OD): δ; -5.2, -8.5, -12.8, -19.5, -21.1; m/z calculated for [M]<sup>-</sup> C<sub>21</sub>H<sub>25</sub>O<sub>4</sub>B<sub>9</sub>Re: 625.2208, HRMS ES<sup>-</sup> [M]<sup>-</sup> 625.2224; FTIR (KBr, cm<sup>-1</sup>) ν: (1869, 1903, 1998, 2559, 2928).

**Sodium rac-3- (Iodo-4-*nido*-carboranyl)-(z-1-(1,2-Dicarba-*nido*-undecaborane-1-yl)-1-(4-phenol)-2-phenyl-but-1-ene) and Sodium rac-3- (Iodo-6-*nido*-carboranyl)-(z-1-(1,2-Dicarba-*nido*-undecaborane-1-yl)-1-(4-phenol)-2-phenyl-but-1-ene) (3.15)**

**Sodium rac-3- (Iodo-4-*nido*-carboranyl)-(E-1-(1,2-Dicarba-*nido*-undecaborane-1-yl)-1-(4-phenol)-2-phenyl-but-1-ene) and Sodium rac-3- (Iodo-6-*nido*-carboranyl)-(E-1-(1,2-Dicarba-*nido*-undecaborane-1-yl)-1-(4-phenol)-2-phenyl-but-1-ene) (3.16)**

22 mg (0.55 mmol) of NaF and 50 mg (0.14 mmol) of **2.7** was dissolved in 2 mL of 20% ethanol, sealed in a microwave vial and heated to 180°C for 10 minutes to produce compounds **3.6** and **3.7**. 1 mL of the *nido* carborane mixture was diluted to 5 mL with 95% ethanol and 15 mg (0.06 mmol) of I<sub>2</sub> dissolved in 5 mL of 95% ethanol was added. The reaction was manually agitated for thirty seconds and subsequently quenched with 5 mL solution of saturated sodium

metabisulfite, transforming the solution from brown to colourless with a white precipitate. The reaction mixture was filtered using a 0.22  $\mu\text{m}$  filter and the filtrate volume was reduced to 5 mL under vacuum. The product was purified using preparative HPLC (Zorbax SB C18, 21x250 mm 7 $\mu$ , 18 mL/min, 50% acetonitrile 50% 5 mM ammonium acetate). The HPLC fractions were combined, evaporated; re dissolved in water and lyophilized yielding a white powder (10.9 mg, 0.023 mmol, 38 %).  $^1\text{H}$  NMR (500 MHz,  $\text{CD}_3\text{OD}$ ):  $\delta$  7.70 -6.31 (m, 9H, aryl), 2.63-2.53 (m, 2H), 2.50-2.43 (m, 2H), 2.25 (s, 1H), 2.07 (s, 1H), 2.05-1.88 (m, 2H), 1.99 (s, 1H), 1.66 (s, 1H), 1.31-1.26 (m, 2H), 0.97-0.93 (2 x t, 6H), 0.71 (t, 3H), 0.64 (t, 3H);  $^{13}\text{C}\{^1\text{H}\}$  NMR (125 MHz,  $\text{CD}_3\text{OD}$ ):  $\delta$  12.8, 13.5, 13.8, 29.6, 30.6, 31.4, 31.5, 113.6, 114.1, 114.6, 114.9, 125.9, 126.1, 126.8, 127.6, 127.9, 128.1, 128.9, 129.4, 130.4, 130.6, 130.9, 131.3, 131.5, 132.8, 132.9, 133.0, 135.7, 136.3, 141.5, 144.5, 144.7, 145.1, 145.4, 156.2;  $^{11}\text{B}\{^1\text{H}\}$  (160 MHz,  $\text{CD}_3\text{OD}$ ): -6.8, -13.3, -14.6, -16.5, -18.7, -21.7, -25.3, -28.9, 30.3, -36.2; m/z calculated for  $[\text{M}]^-$   $\text{C}_{18}\text{H}_{25}\text{B}_9\text{O}_7^-$  482.1837 HRMS TOF EI $^-$   $[\text{M}]^-$  482.1849; FTIR (KBr,  $\text{cm}^{-1}$ )  $\nu$ : (2529, 3182).

### 3.9 References

1. Dolores Fernandez, M.; Ian Burn, J.; Sauven, P. D.; Parmar, G.; White, J. O.; Myatt, L., Activated oestrogen receptors in breast cancer and response to endocrine therapy. *European Journal of Cancer and Clinical Oncology* **1984**, 20, (1), 41-46.

2. Wittliff, J. L., Steroid-Hormone Receptors in Breast Cancer. *Cancer* **1984**, 53, 630-643.
3. Kiesewetter, D.; Kilbourn, M. R.; Landvatter, S. W.; Heiman, D. F.; Katzenellenbogen, J. A.; Welch, M. J., Preparation of Four Fluorine-18-Labeled Estrogens and Their Selective Uptakes in Target Tissues of Immature Rats. *The Journal of Nuclear Medicine* **1984**, 25, (11), 1212-1221.
4. Yang, D.; Kuang, L.; Cherif, A.; Tansey, W.; Li, C.; Lin, W. J.; Liu, C.; Kim, E. E.; Wallace, S., Synthesis of [<sup>18</sup>F]Fluoroalanine and [<sup>18</sup>F]Fluorotamoxifen for Imaging Breast Tumors. *Journal of Drug Targeting* **1993**, 1, 259-267.
5. Wiele, C. V. d.; Vos, F. D.; Sutter, J. D.; Dumont, F.; Slegers, G.; Dierckx; Thierens, H., Biodistribution and dosimetry of (iodine-123)-iodomethyl-N,N-diethyltamoxifen, an (anti)oestrogen receptor radioligand. *European Journal of Nuclear Medicine* **1999**, 26, (10), 1959-1264.
6. Muftulera, F. Z. B.; Unaka, P.; Teksoza, S.; Acara, C.; Yolculara, S.; rekli, Y. Y., <sup>131</sup>I labeling of tamoxifen and biodistribution studies in rats. *Applied Radiation and Isotopes* **2008**, 66, 178-187.
7. Hunter, D. H.; Luyt, L. G., Single Isomer Technetium-99m Tamoxifen Conjugates. *Bioconjugate Chemistry* **2000**, 11, 175-181.
8. Kruijer, P. S.; Klok, R. P.; Koedijk, C. D. M. A. w. d.; Blankenstein, M. A.; Voskuil, J. H.; Verzeijlbergen, J. F.; Ensing, G. J.; Herscheid, J. D. M., Biodistribution of <sup>131</sup>I-Labeled +Hydroxytamoxifen Derivatives in Rats with

- Dimethylbenzylkethone-Induced Mammary Carcinomas. *Nuclear Medicine and Biology* **1997**, 24, 719-722.
9. Hanson, R. N.; Franke, L. A., Preparation and Evaluation of 17{alpha}-[<sup>125</sup>I]iodovinyl-11β-Methoxyestradiol as a Highly Selective Radioligand for Tissues Containing Estrogen Receptors: Concise Communication *Journal of Nuclear Medicine* **1984**, 25, 998-1002.
  10. Bénard, F.; Ahmed, N.; Beaugregard, J. M.; Rousseau, J.; Aliaga, A.; Dubuc, C.; Croteau, E.; Lier, J. E. v., [<sup>18</sup>F]Fluorinated estradiol derivatives for oestrogen receptor imaging: impact of substituents, formulation and specific activity on the biodistribution in breast tumour-bearing mice. *European Journal of Nuclear Medicine and Molecular Imaging* **2008**, 35, 1473-1479.
  11. Beaugregard, J. M.; Croteau, E.; Ahmed, N.; Lier, J. E. v.; Bénard, F., Assessment of Human Biodistribution and Dosimetry of 4-Fluoro-11β-Methoxy-16α-<sup>18</sup>F Fluoroestradiol Using Serial Whole-Body PET/CT. *The Journal of Nuclear Medicine* **2009**, 50, 100-107.
  12. Bennink, R. J.; Tienhoven, G. v.; Rijks, L. J.; Noorduyne, A. L.; Janssen, A. G.; Sloof, G. W., In Vivo Prediction of Response to Antiestrogen Treatment in Estrogen Receptor-Positive Breast Cancer. *Response Prediction in Breast Cancer* **2004**, 45, 1-7.
  13. Macgregor, J. I.; Jordan, V. C., Basic Guide to the Mechanisms of Antiestrogen Action. *Pharmacological Reviews* **1998**, 50, 151-196.
  14. Furr, B. J. A.; Jordan, V. C., *Pharmac. Ther* **1984**, 25, 127-205.

15. Koyama, Y.; Mukai, Y.; Kuki, M., *Laser Spectroscopy of Biomolecules*. The International Society for Optical Engineering: Bellingham, 1993.
16. Kuki, M.; Koyama, Y.; Nagae, H., *J. Phys. Chem.* **1991**, 95, 7171-7180.
17. Armstrong, A. F.; Valliant, J. F., Microwave-Assisted Synthesis of Tricarbonyl Rhenacarboranes: Steric and Electronic Effects on the 1,2-1,7 Carborane Cage Isomerization. *Inorg. Chem.* **2007**, 46, 2148-2158.
18. Dickson, R. B.; Bates, S. E.; McManaway, M. E.; Lippman, M. E., Characterization of Estrogen Responsive Transforming Activity in Human Breast Cancer Cell Lines. *Cancer Research* **1986**, 46, 1707-1713.
19. Olsen, F. P.; Hawthorne, M. F., Halodicarbaundecaborate (11) Ions. *Inorganic Chemistry* **1965**, 4, (12), 1839.
20. Smyth, T. P.; Corby, B. W., Toward a Clean Alternative to Friedel-Crafts Acylation: In Situ Formation, Observation, and Reaction of an Acyl Bis(trifluoroacetyl)phosphate and Related Structures. *Journal of Organic Chemistry* **1998**, 63, 8946-8951.

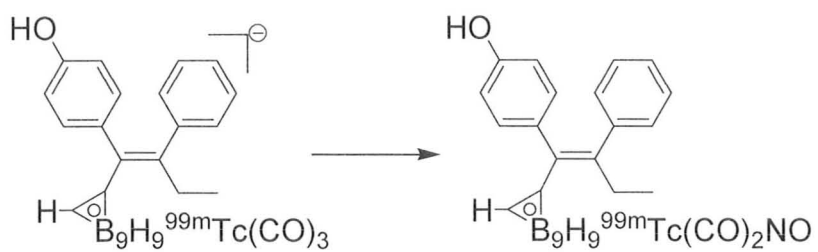
## 4.0 Future Work

### 4.1 Carborane Tamoxifen Analogue for the treatment of Estrogen Receptor Positive Breast Cancer

To determine to what extent **2.7** and **2.8** bind the estrogen receptor (ER $\alpha$  or ER $\beta$ ) a competitive *in vitro* assay with  $^3\text{H}$ -estradiol needs to be completed and the relative binding affinities (RBA) determined. Once the RBA values have been determined the next step would be to determine the ability to shrink tumours in the MCF-7 rodent model, followed by toxicity testing of **2.7** and **2.8** in two different species.

### 4.2 Carborane Tamoxifen Analogue for imaging Estrogen Receptor

To determine if compound **3.14** binds specifically, a cell uptake assay needs to be done with a compound that has the ability to block the ER (i.e. estradiol or stilbene). If **3.14** is able to bind the ER specifically, a biodistribution study in the above mentioned tumour model needs to be completed in order to quantify the uptake of **3.14** in the tumour. In addition previous work completed in this group found that negatively charged metallocarboranes had a lower affinity of the ER compared with their charge compensated analogues. A method has been established within our group to replace a CO group with a NO $^+$  moiety in order to obtain the neutral metallocarborane compound. This same technique could be used to generate a neutral analogue of **3.14** (**Scheme 4.1**)



**Scheme 4.1:** Charge Compensation of Tc Tamoxifen with NO<sup>+</sup>